Kinetics and Regulation of Mitochondrial Cation Transport Systems

Martin Jabůrek
B.S., Palacky University, 1992

A dissertation submitted to the faculty of the
Oregon Graduate Institute of Science and Technology
in partial fulfillment of the
requirements for the degree
Doctor of Philosophy
in
Biochemistry and Molecular Biology

August 1999

The dissertation "Kinetics and Regulation of Mitochondrial Cation Transport Systems" by Martin Jaburek has been examined and approved by the following Examination Committee:

Keith D. Garlid, Advisor
Professor

Gebre Woldegiorgis
Associate Professor

Peter A. Zuber
Professor

Jack H. Kaplan
Professor
Oregon Health Sciences University

DEDICATION

I would like to dedicate this thesis to my wife, Iva, my daughter, Veronika, and also to my parents, grandparents, and all the members of my large family, as an excuse for not being with them for such a long time.

ACKNOWLEDGMENTS

I would like to extend my gratitude to my major advisor, Dr. Keith Garlid. I am very fortunate to have had the opportunity to be a student in his laboratory, and I am very thankful for his support, guidance, and encouragement, without which I would not have been able to finish this degree.

I would further like to thank Dr. Gebre Woldegiorgis for the many thought-provoking and valuable discussions we had. Thanks also to Drs. Peter Zuber and Jack Kaplan for their time and for serving as members of my thesis committee.

My further thanks to Dr. Petr Paucek, who introduced me to the secrets of reconstitution; to Dr. Martin Modriansky, for being such a good roommate and for sharing the secrets of yeast expression of uncoupling proteins; to Dr. Vladimir Yarov-Yarovoy, with whom I shared a part of the mitochondrial K_{ATP} channel project; and to Dr. Hongfa Zhu, for answering many of my questions about aspects of molecular biology.

I am sincerely appreciative for the helpful assistance I received from our new students, Miroslav Varecha and Robert Bajgar, and from our excellent technicians, Craig Semrad and Yulia Yarova-Yarovaya.

I would like to acknowledge the collaborative association between our laboratory and Millennium Pharmaceuticals, Inc., who provided us with both yeast and bacterially expressed uncoupling proteins. Thanks also to Dr. Petr Jezek, of the Academy of Sciences of the Czech Republic, for valuable discussions which also contributed to the progress of my work.

I also extend my appreciation to the many other people, too many to list here, who were my teachers, gave me a valuable advice, invited me for a drink, or helped me one way or another. Among those who helped me with many "little" things are also our departmental secretaries, Nancy Christie and Terrie Hadfield. Terrie spent significant time "fixing" this thesis into library-acceptable shape. Thank you all!

TABLE OF CONTENTS

LIST OF TABLES

LIST OF FIGURES

LIST OF ABBREVIATIONS

ADP	adenosine 5′-diphosphate
ATP	adenosine 5′-triphosphate
BAT	brown adipose tissue
BSA	bovine serum albumin
CCCP	carbonyl cyanide-*p*-chlorophenylhydrazone
DTT	dithiothreitol
EDTA	ethylenediaminetetraacetic acid
EGTA	[ethylene-bis(oxyethylenenitrilo] tetraacetic acid
FA	fatty acid
FCCP	carbonyl cyanide *p*-trifluoromethoxyphenylhydrazone
GDP	guanosine 5′-diphosphate
GTP	guanosine 5′-triphosphate
HEDTA	N-hydroxyethylethylenediaminetriacetic acid
HEPES	N-(2-hydroxyethyl)piperazine-N′-(2-ethanesulfonic acid)
5-HD	5-hydroxydecanoic acid
IPTG	isopropyl-β-D-thiogalactopyranoside
KCO	potassium channel openers
mitoK_{ATP}	mitochondrial ATP-sensitive potassium channel
octyl-POE	octylpentaoxyethylene
PBFI	potassium-binding benzofuran isophtalate
SBFI	sodium-binding benzofuran isophtalate
SLS	sodium lauroylsarcosinate
SMPs	submitochondrial particles
SPQ	6-methoxy-*N*-(3-sulfopropyl)quinolinium
TEA^+	tetraethylammonium cation

TES	N-tris(hydroxymethyl)methyl-2-aminoethanesulfonic acid
TMPD	N,N,N′,N′-tetramethyl-*p*-phenylenediamine
TPP^+	tetraphenylphosphonium cation
TRIS	tris(hydroxymethyl)aminomethane
UCP	uncoupling protein
XIP	exchange inhibitory peptide

ABSTRACT

Kinetics and Regulation of Mitochondrial Cation Transport Systems

Martin Jabůrek

Supervising Professor: Keith D. Garlid

The inner mitochondrial membrane contains transport systems catalyzing influx and efflux of cations between the cytosol and mitochondrial matrix. Our laboratory studies three distinct cation cycles, and each of these cycles plays a major physiological role in the overall energy economy.

The Ca^{2+} cycle is responsible for rapid oscillations in matrix Ca^{2+}, which result in sustained activation of Ca^{2+}-sensitive dehydrogenases and regulation of ATP production. The efflux of Ca^{2+} from the mitochondrial matrix is carried by the Na^+/Ca^{2+} antiporter. We purified the Na^+/Ca^{2+} antiporter from beef heart mitochondria and reconstituted the antiporter into liposomes. The kinetics of the Na^+/Ca^{2+} exchange were consistent with its participation in rapid Ca^{2+} oscillation. The reconstitution also revealed that the antiporter was capable of both electroneutral and electrophoretic Na^+/Ca^{2+} exchange, the mode of transport depending on the availability of a pathway for charge-compensating ion transport.

The K^+ cycle maintains the integrity of the vesicular structure of the inner membrane. Influx of K^+ into the matrix is catalyzed by the mitochondrial K_{ATP} channel (mitoK_{ATP}). MitoK_{ATP} is hypothesized to be the receptor for the cardioprotective effects of K^+ channel openers (KCO) and for blocking the cardioprotection by glyburide and 5-hydroxydecanoate (5-HD). We have studied the effect of glyburide and 5-HD on isolated, respiring mitochondria. Our results show that glyburide and 5-HD are potent blockers of K^+ flux through mitoK_{ATP} only in open states, in which Mg^{2+}, ATP, and physiological (GTP) or pharmacological

(KCO) openers are present. These results are consistent with a role for mitoK_{ATP} in cardioprotection.

The H^+ cycle has been previously characterized only in brown adipose tissue mitochondria and consists of uncoupling protein (UCP1), which dissipates energy and generates heat by catalyzing back-flux of protons into the mitochondrial matrix. Recently, proteins homologous to UCP1 were discovered in many other tissues, including white fat and skeletal muscle. If the newly discovered UCP2 and UCP3 function similarly, they will enhance peripheral energy expenditure and are potential targets for the treatment of obesity. We have reconstituted bacterially expressed UCP2 and UCP3 into liposomes and shown that UCP2 and UCP3 behave similarly to UCP1, i.e., they catalyze electrophoretic flux of protons and alkylsulfonates, and proton flux exhibits an obligatory requirement for fatty acids. Proton flux is inhibited by purine nucleotides. These findings are consistent with the hypothesis that UCP2 and UCP3 behave as uncoupling proteins in the cell.

CHAPTER 1
INTRODUCTION*

1.1 The Chemiosmotic Theory and Mitochondrial Ion Transport

The chemiosmotic theory describes the mechanism by which substrate oxidation, or the absorption of light, is coupled to ATP synthesis. While some ATP synthesis is catalyzed by soluble enzyme systems, the largest proportion is associated with membrane-bound enzyme complexes which are restricted to a particular class of membrane. In the mammalian cell, this task is fulfilled by the inner mitochondrial membrane.

It was the insight of Peter Mitchell, who, working far in advance of experimental evidence, postulated that nature uses protonic batteries to perform work. He recognized that biological energy conservation is a problem in membrane transport (Mitchell, 1961).

1.1.1 The postulates of chemiosmotic theory

The chemiosmotic theory consists of four postulates, each of which has been validated by experiment:

(1) The respiratory and photosynthetic electron-transfer chains should translocate protons.

(2) The ATP synthase should function as a reversible proton-translocating ATPase.

---

* Figures 1.1, 1.2, and 1.3 have been published in this or similar form as Figures 1, 8, and 9, respectively, in *Cell Physiology Source Book*, Second Edition, and are used here with permission of Academic Press (http://www.apnet.com):

Garlid, K. D. (1998) Physiology of mitochondria. In: *Cell Physiology Source Book*, 2nd Edn., pp. 111–118, Academic Press, San Diego, CA.

(3) Energy-transducing membranes should have a low effective proton conductance.

(4) Energy-transducing membranes should possess specific exchange carriers to permit metabolites to permeate, and osmotic stability to be maintained, in the presence of a high membrane potential.

The consequence of the first three postulates, as diagrammed in Fig. 1.1, is the generation of a proton-motive force (Δp), which is defined as the electrochemical proton gradient divided by the Faraday constant ($\Delta\mu_{H+}/F$):

$$\Delta p = \Delta\Psi - Z\Delta pH$$

where Z is equal to 59 mV at 25°C, and $\Delta\Psi$ is the membrane potential. Measurements of the proton-motive force have yielded values of about -200 mV in isolated rat liver mitochondria respiring in the non-phosphorylating state 4 (Mitchell and Moyle, 1969).

1.1.2 Secondary ion transport as a consequence of chemiosmotic theory

The fourth postulate demonstrates that, from its very beginning, the chemiosmotic theory encompassed more than the mechanism of biological energy conservation. Mitchell recognized that the postulated protonic batteries would generate transmembrane forces that would have serious consequences for mitochondrial physiology within the cell. Thus, the high membrane potential required to drive ATP synthesis would cause cations, particularly potassium, to leak through the coupling membrane. Accompanied by anions and water, such leaks would subject the subcellular organelle to uncontrolled swelling and eventual lysis. Because the operating $\Delta\Psi$ is so high, cation uptake must be balanced by extrusion of ions against the electrical gradient. In recognition of this physiological necessity, Mitchell postulated the existence of ion exchange carriers for anions and cations (Mitchell, 1961, 1966).

It is noteworthy that the proposal for electroneutral exchange carriers was made at a time when there was no experimental evidence for the existence of ion-exchange carriers in any membrane. Rather, they were postulated to exist out of physiological necessity.

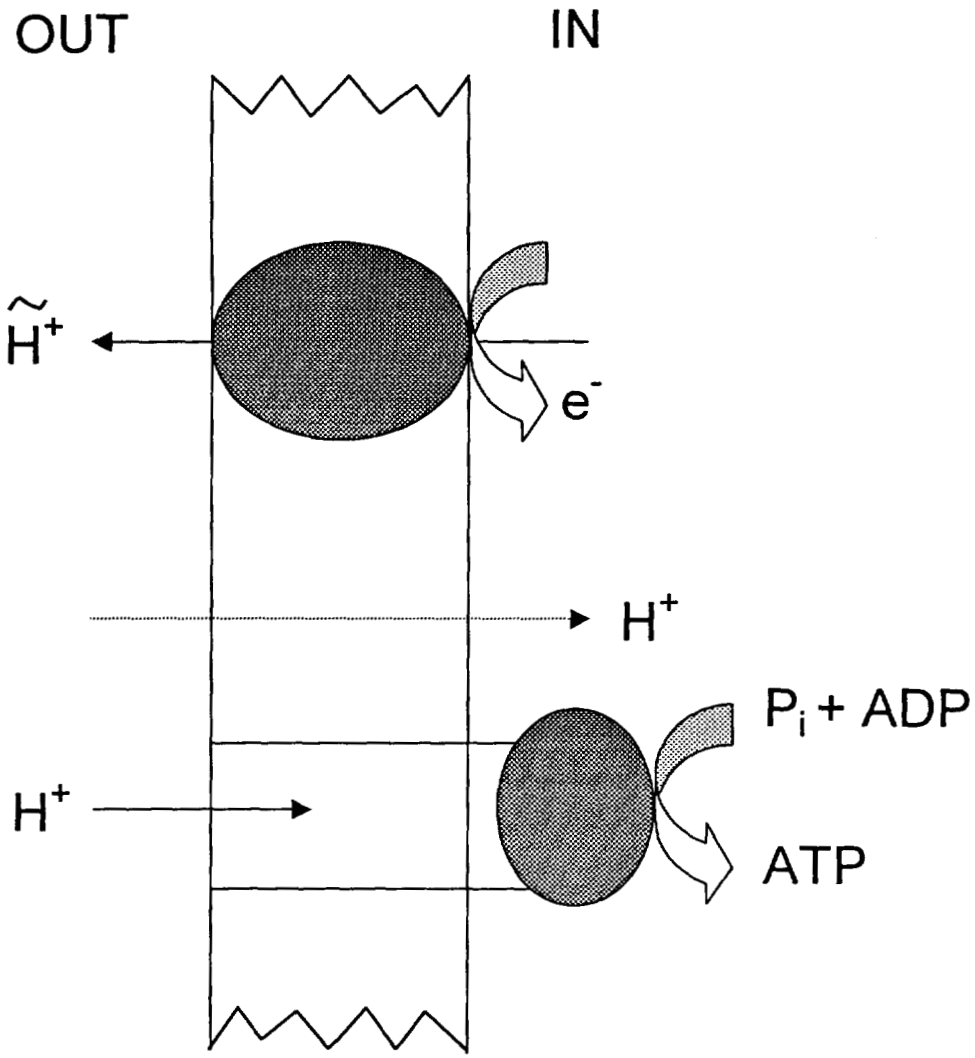

Figure 1.1 Chemiosmotic energy coupling of electron transport to ATP synthesis. The vectorial enzymes of electron transport and ATP synthesis are coupled indirectly via the proton-motive force. Efficient transfer of proton-motive energy from the redox chain to the ATP synthase is dependent upon the low permeability of the inner membrane to protons (Garlid, 1998).

Mitchell also introduced a new and useful terminology to distinguish different modes of ion transport. Transport of an ion by itself was called uniport; ion transport in exchange with another ion was called antiport; and co-transport of two or more ions was called symport.

1.2 The Volume-Regulating Potassium Cycle of Mitochondria

Maintenance of mitochondrial integrity necessitates that net K^+ flux remains near zero in the face of rapid fluxes through independent pathways. The mitochondrial K^+ cycle consists of electrophoretic K^+ uptake and electroneutral K^+ efflux across the inner membrane. The redox energy consumed by this cycle is the energy cost of regulating matrix volume (Garlid, 1980). Two transporters have been identified that catalyze K^+ transport (Fig. 1.2), and both are highly regulated. Potassium efflux is mediated by the K^+/H^+ antiporter, whose existence was predicted by Mitchell (1961) and first demonstrated by Garlid nearly 20 years later (Garlid, 1978). The K^+/H^+ antiporter, identified as an 82-kDa inner mitochondrial membrane protein (Martin et al., 1984), was subsequently purified and reconstituted (Kakar et al., 1989; Jezek et al., 1990a; Li et al., 1990). Potassium influx is mediated by the mitochondrial K_{ATP} channel. K_{ATP} channels were first identified in the plasma membrane of cardiac myocytes (Noma, 1983), while ATP-regulated mitochondrial K^+ channels were discovered in 1991 by Inoue et al. (1991), who reported evidence from patch clamp studies of fused mitoplasts. A year later, Garlid's laboratory reported reconstitution of a highly purified mitoK_{ATP} (Paucek et al., 1992).

1.2.1 Physiological roles of mitochondrial K^+ cycle

1.2.1.1 Matrix volume is determined by net potassium flux. When K^+ influx and efflux are out of balance, the resulting net K^+ flux is accompanied by electroneutral flux of anions and osmotically obligated water (Garlid, 1988). Because matrix $[K^+]$ is about 180 mM, net K^+ transport will have negligible effect on the matrix concentration of K^+, but will have a profound effect in matrix volume. Any departure from zero net K^+ flux will cause a change in matrix volume. The

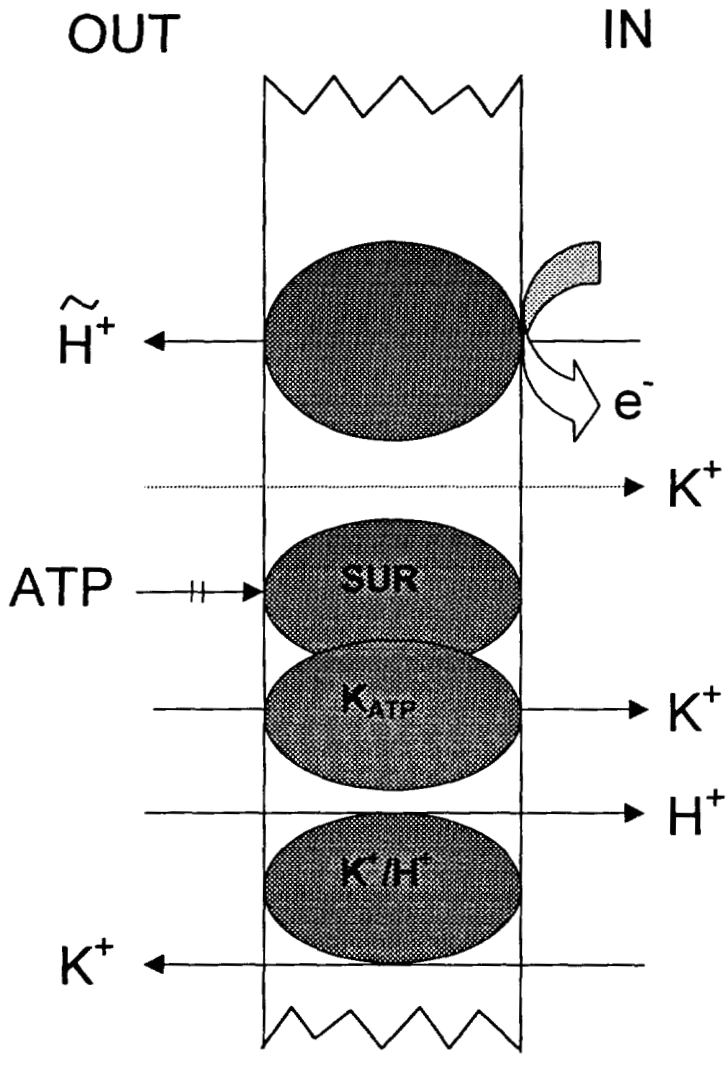

Figure 1.2 The mitochondrial K^+ cycle. Electrogenic proton ejection drives significant K^+ uptake by diffusive leak. In addition, the inner membrane contains a K_{ATP} channel, which is highly regulated by nucleotides, CoA esters, and pharmacological agents. The K_{ATP} channel was proposed to consist of two subunits, a K^+-specific channel and a sulfonylurea receptor (SUR). Net K^+ flux is regulated to zero in the matrix volume steady state by compensatory K^+ efflux provided by the electroneutral K^+/H^+ antiporter, which is regulated by matrix $[Mg^{2+}]$ and $[H^+]$ and is exquisitely sensitive to changes in matrix volume (Garlid, 1998).

importance of regulating K^+ flux to zero in the steady state is illustrated by noting that uncompensated K^+ uptake, amounting to as little as 10% of H^+ pumping, would double matrix volume within 1–2 min (Garlid, 1979). The K^+/H^+ antiporter, inhibited by matrix Mg^{2+} as well as by matrix protons, provides compensatory K^+ efflux to maintain matrix volume (Garlid, 1988).

1.2.1.2 Matrix volume regulates electron transport. Nicholls and coworkers have demonstrated that the rate of oxidation of fatty acids is strictly controlled by matrix volume in brown adipose tissue mitochondria, where fatty acids are the fuel for thermogenesis (Nicholls et al., 1972). A thorough characterization of this phenomenon by Halestrap (1989) has led to the following conclusions: (i) Increased matrix volume over the narrow range thought to occur *in vivo*, greatly stimulates activity of the respiratory chain in both heart and liver mitochondria. β-Oxidation of fatty acids is particularly sensitive to matrix volume. (ii) The site of activation has been localized to membrane enzymes that direct electrons to ubiquinone. (iii) Matrix volume changes (10–30%) have been observed *in vivo* during respiratory stimulation secondary to hormonal activation of liver (Halestrap, 1989). (iv) The molecular mechanism of volume activation is not yet known, but may involve a stretch receptor.

1.2.2 Mitochondrial K_{ATP} channels

The discovery of mitoK_{ATP} has profound new implications for the physiological role of the mitochondrial K^+ cycle, because the existence of a highly selective regulated K^+ influx pathway now permits volume regulation. MitoK_{ATP} is not voltage-gated, the flux-voltage dependence being consistent with a channel containing a single energy well near the center of the membrane. MitoK_{ATP} activity has also been demonstrated in intact mitochondria (Beavis et al., 1993; Szewczyk et al., 1993).

1.2.2.1 MitoK_{ATP} is regulated by nucleotides and long-chain acyl-CoA esters. MitoK_{ATP} is subject to complex regulation by metabolites, as indicated by the following summary of $K_{1/2}$ values for inhibitors and openers obtained with mitoK_{ATP} reconstituted in liposomes (Paucek et al., 1992, 1996; Garlid et al., 1996b).

$K_{1/2}$ values of inhibition of K^+ flux	
ATP	22–30 μM
ADP	160–200 μM
Palmitoyl CoA	0.25 μM
Glyburide	65 nM
Free Mg^{2+}	80 μM in 0.5 mM ATP
Free Ca^{2+}	150 μM in 0.5 mM ATP

$K_{1/2}$ values of activation of inhibited K^+ flux			
Activator	In the presence of 0.5 mM ATP	In the presence of 0.5 mM ADP	In the presence of 0.5 mM palmitoyl CoA
GTP	3–7 μM	0.12 μM	230 μM
GDP	140 μM	3 μM	not available

ATP and ADP are mutually competitive inhibitors of mitoK_{ATP}. The inhibition exhibits an absolute requirement for divalent cations: ATP or palmitoyl CoA have no effect in the absence of Mg^{2+}, while Mg^{2+} has no effect in the absence of ATP or palmitoyl CoA. Mg^{2+} also lowers the affinity for glyburide inhibition. Since neither glyburide nor palmitoyl CoA are Mg^{2+} chelators, these findings indicate that Mg^{2+} interacts independently with mitoK_{ATP} and not as a MgATP complex.

Guanine nucleotides are competitive with ATP. GTP appears to react with a high-affinity (0.2 μM) and a low-affinity (15–20 μM) site, whereas GDP appears to react with two low-affinity sites (20 μM). ATP is unable to inhibit in the presence of physiological GTP concentrations. On the other hand, the $K_{1/2}$ for GTP activation of palmitoyl CoA inhibition is in the physiological range. Garlid (1996) proposed that the open/closed state of the channel is determined *in vivo* by the relative occupancy of the sites by GTP or long-chain acyl-CoA esters.

1.2.2.2 MitoK_{ATP} is an intracellular receptor for K^+ channel openers.

K^+ channel openers (KCO) activate ATP-inhibited K_{ATP} channels of plasma membranes and are clinically important drugs (Quast and Cook, 1989). These drugs

were also found to act on mitochondrial K_{ATP} channels in their therapeutic range (Garlid et al., 1996b). Recognition of mitoK_{ATP} as an intracellular receptor for KCO adds a new dimension to KCO pharmacology. A particularly exciting development in KCO pharmacology was the discovery by Grover (Grover et al., 1989; Grover, 1994) that KCO is cardioprotective during experimental ischemia. Working in collaboration, Grover and Garlid (Garlid et al., 1997; Grover, 1997) reported biophysical and pharmacological evidence that KCO cardioprotection in myocytes is mediated by mitoK_{ATP} and not by sarcolemmal cellK_{ATP} channels. Liu et al. (1998) provided independent support of this observation by finding that diazoxide targets mitochondrial but not sarcolemmal K_{ATP}. The same laboratory also reported evidence that the activity of mitoK_{ATP} can be regulated by protein kinase C in intact heart cells, and this regulation provides a direct mechanistic link between the signal transduction of ischemic preconditioning and pharmacological cardioprotection targeted at ATP-dependent K^+ channels (Sato et al., 1998).

1.2.2.3 Is mitoKATP a heteromultimeric complex? Recent breakthroughs by the Bryans and colleagues (Aguilar-Bryan et al., 1995; Inagaki et al., 1995; Thomas et al., 1995) have shown that the cellK_{ATP} consists of two separate proteins, a sulfonylurea receptor (SUR) and an inward rectifying K^+ channel (KIR). Because each of the metabolic and pharmacological ligands that modify cellK_{ATP} also modify mitoK_{ATP}, these preliminary studies led Garlid and co-workers (Garlid et al., 1996b) to hypothesize that mitoK_{ATP} is also a heteromultimer consisting of an inward rectifying K^+ channel, mitoKIR, and a sulfonylurea receptor, mitoSUR. Although this hypothesis is still under active investigation, significant progress towards identifying these proteins has already been reported by several laboratories (Paucek et al., 1997; Suzuki et al., 1997; Szewczyk et al., 1997). Recently, using a SUR ligand, fluorescent BODIPY-FL glyburide, a mitochondrial 63-kDa protein was identified that supports the heteromultimeric structure of mitoKATP as consisting of a 55-kDa K^+ channel and a 63-kDa receptor (mitoSUR) (Paucek et al., 1999).

The data in Chapter 3 provide support for a ligand-induced conformational change of mitoSUR and are consistent with the role of mitoK_{ATP} in cardioprotection.

1.3 The Calcium Cycle of Mitochondria

The inner mitochondrial membrane contains at least three transporters for regulation of mitochondrial [Ca^{2+}]. The Ca^{2+} channel is characterized by high-capacity, electrophoretic Ca^{2+} uptake. Free mitochondrial [Ca^{2+}] would exceed cytosol levels *in vivo* by 10^6 if mitochondrial Ca^{2+} were at equilibrium with respect to Ca^{2+} uniport at 180 mV, but instead mitochondrial and cytosolic Ca^{2+} levels are comparable. Clearly, a Ca^{2+} efflux mechanism is required for removal of Ca^{2+} in the face of a high $\Delta\Psi$. The Ca^{2+} efflux mechanism consists of two transporters. The inward Na^+ gradient drives Ca^{2+} efflux via the Na^+/Ca^{2+} antiporter, with the Na^+ being removed by the electroneutral Na^+/H^+ antiporter. The energy expenditure of this futile Ca^{2+} cycle (Fig. 1.3) is the cost of regulating mitochondrial metabolism to meet the energetic needs of the cell. In addition, the inner mitochondrial membrane contains a Ca^{2+}-activated, nonselective, permeability-increasing pore, which is closed in tightly coupled mitochondria (Gunter and Gunter, 1994).

Considerable work has been done on purifying the mitochondrial Ca^{2+} uniporter, and several candidates have been identified (Gunter and Pfeifer, 1990; Saris et al., 1993; Mironova et al., 1994). The mitochondrial Na^+/H^+ antiporter was identified as a 59-kDa protein and was partially purified and reconstituted (Garlid et al., 1991). Polyclonal antibodies raised against this protein were found to be potent inhibitors of Na^+ flux (Shariat-Madar and Garlid, 1993). The identification, purification, and reconstitution of the mitochondrial Na^+/Ca^{2+} antiporter has also been reported (Li et al., 1992). Both Na^+/H^+ and Na^+/Ca^{2+} exchange activities from beef heart mitochondria were first observed by reconstitution of detergent-extracted mitochondrial inner membrane proteins which had undergone DEAE-cellulose chromatography fractionations. The Na^+/Ca^{2+} antiporter activity correlated with a 110-kDa protein in a reconstituted system. Transport through a reconstituted Na^+/Ca^{2+} antiporter was inhibited by polyclonal antibodies raised against the 110-kDa protein (Li et al., 1992).

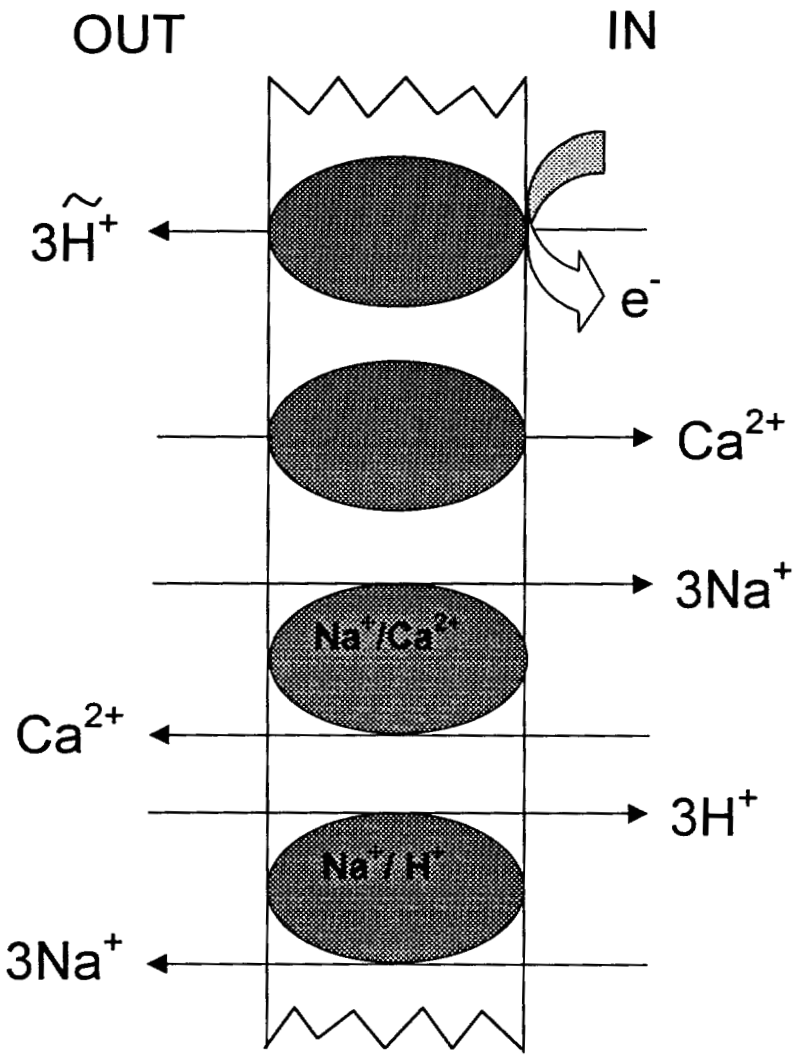

Figure 1.3 Mitochondrial Ca^{2+} cycle. Ca^{2+} enters the matrix via the electrophoretic Ca^{2+} channel and is ejected by the electrophoretic Na^+/Ca^{2+} antiporter, utilizing three ejected protons per Ca^{2+} taken up. The Na^+ is then expelled by the electroneutral Na^+/H^+ antiporter (Garlid, 1998).

1.3.1 Physiological roles of mitochondrial Ca^{2+}

1.3.1.1 Ca^{2+} is a secondary messenger. While mitochondria increase their rate of ADP phosphorylation many fold in response to either increased ADP and P_i concentrations or to decreased ATP concentrations, it has become evident that this substrate-product feedback control is not the primary metabolic control mechanism (Gunter, 1994). Changes within the cell that require a modification of the metabolic rate are generally signaled to the cell through hormones, neurotransmitters, or growth factors (so-called primary messengers), while the agent of these changes within the cell is most likely to be a common secondary messenger. Of the known secondary messengers, it appears that only Ca^{2+} is transferred into the mitochondrial matrix (Denton and McCormack, 1990).

1.3.1.2 Ca^{2+} regulates the tricarboxylic cycle. Intramitochondrial Ca^{2+} has been reported to be capable of increasing the rate of oxidative phosphorylation through activation of a series of steps in metabolic pathways, including dehydrogenases coupled to the tricarboxylic acid cycle, electron transport, phosphorylation at the F_1F_0ATPase, and adenine nucleotide transport (Hansford, 1985, 1991; Denton and McCormack, 1990; Gunter et al., 1994). Three dehydrogenases of the Krebs cycle are Ca^{2+}-regulated enzymes: NAD^+-isocitrate-, 2-oxoglutarate-, and pyruvate-dehydrogenase (ICDH, OGDH and PDG). In the case of ICDH and OGDH, the affinity for the substrate has been shown to be increased, independently, by both Ca^{2+} and ADP/ATP ratio (Denton et al., 1978; McCormack and Denton, 1979). This implies complex regulation, which includes, together with the relay signalling from extracellular agonists, a feedback control by the end-product of aerobic metabolism (Rutter and Denton, 1988). In the case of PDH, the action of Ca^{2+} is not on the enzyme itself, but on a phosphatase which relieves an inhibitory phosphorylation of PDH by a kinase associated with the multi-subunit complex (Denton et al., 1972). The reported range of Ca^{2+} affinity of the three dehodrogenases is different for each enzyme, and also depends on ADP/ATP ratio (Rutter and Denton, 1988, 1989). Thus, the mitochondrial Ca^{2+} transport mechanisms, which control mitochondrial Ca^{2+} concentration, control the rate of ATP production, and play a major physiological role in cellular bioenergetics.

1.3.1.3 Mitochondria are tuned to cytosolic Ca^{2+} oscillations. Matrix [Ca^{2+}] increases and rapidly oscillates upon cell stimulation with the agonist coupled to IP_3 generation. The IP_3-induced Ca^{2+} oscillations have been observed by several laboratories in a variety of tissues (Rizzuto et al., 1994; Hajnóczky et al., 1995; Sparagna et al., 1995; Jou et al., 1996; Rutter et al., 1996). Frequency-modulated oscillations of cytosolic Ca^{2+} are believed to be important in signal transduction, but it has been difficult to correlate these oscillations directly with the activity of Ca^{2+}-regulated targets. Recent major progress by Hajnóczky et al. (1995) studied the control of Ca^{2+}-sensitive mitochondrial dehydrogenases by simultaneously monitoring mitochondrial Ca^{2+} and the redox state of flavoproteins and pyrimidine nucleotides. Rutter et al. (1996) compared mitochondrial Ca^{2+} with the activity of the Ca^{2+}-sensitive matrix enzyme, pyruvate dehydrogenase, using the Ca^{2+} sensitive photoprotein, aequorin, incorporated into mitochondria. These studies concluded that mitochondria are tuned to oscillating cytosolic Ca^{2+} signals, but not the steady-state increases in matrix Ca^{2+}, and the frequency of Ca^{2+} oscillations can control the Ca^{2+}-sensitive mitochondrial dehydrogenases over the full range of their activities.

1.3.2 Na^+-Dependent Ca^{2+} Efflux

A Na^+-dependent transport mechanism is thought to dominate the Ca^{2+} efflux of mitochondria from heart, brain, skeletal muscle, parotid gland, adrenal cortex, brown fat, and other excitable cells (Crompton et al., 1977, 1978; Murphy and Fiskum, 1988).

1.3.2.1 Kinetics and regulation of Na^+ dependent Ca^{2+} efflux. In intact mitochondria, the Na^+-dependent Ca^{2+} efflux mechanism transports Sr^{2+} (Crompton et al., 1976) but not Mn^{2+} (Gavin et al., 1990, 1991) as a substitute for Ca^{2+}, while Li^+ can substitute for Na^+ (Crompton et al., 1976). This mechanism can be inhibited by a wide variety of inhibitors including Mg^{2+} (Wingrove and Gunter, 1986), Mn^{2+} (Gavin et al., 1990, 1991), trifluoroperazine (Hayat and Crompton, 1985), diltiazem (Chiesi et al., 1987; Rizzuto et al., 1987), verapamil (Wolkowicz et al., 1983), clonazepam (Chiesi et al., 1987), amiloride (Jurkowitz et al., 1983; Sordahl et al., 1984; Schellenberg et al., 1985), and tetraphenylphosphonium

(Wingrove and Gunter, 1986). Transport via this mechanism is activated by spermine and spermidine (Nicchitta and Williamson, 1984) and stimulated in brain mitochondria by ethanol (Rottenberg and Marbach, 1991).

Studies on the purified reconstituted Na^+/Ca^{2+} antiporter revealed a new finding that this protein catalyzes Na^+/Li^+ exchange in the absence of Ca^{2+} (Li et al., 1992). Further characterization of the reconstituted Na^+/Ca^{2+} antiporter is described in Chapter 2.

1.3.2.2 Na^+:Ca^{2+} stoichiometry. Prior to 1994, a most researchers thought of the Na^+-dependent Ca^{2+} efflux mechanism as a passive electroneutral $Ca^{2+}/2Na^+$ antiporter. This conclusion, based on transport kinetic studies (Crompton et al., 1977; Wingrove and Gunter, 1986), received particularly strong support from the results of Brand (1985) and the reconstitution studies of Li et al. (1992).

However, Baysal et al. (1991) found that the Ca^{2+} efflux was increased by addition of nigericin, which decreased ΔpH and increased $\Delta\Psi$. This suggested an electrophoretic component for this transport. Baysal et al. (1994) also determined that the Na^+-dependent mechanism has more energy available to it than can be explained by the mechanism functioning as an electroneutral antiporter.

The earlier results of Brand (1985) were reevaluated by Jung and co-workers (Jung et al., 1995), who found Brand's approach conceptually sound, but raised questions concerning some of the assumptions and approximations used. The conclusion of this study was that the stoichiometry of this transporter was at least $3Na^+$ ions per Ca^{2+} ion. These results thus reopened the issue of stoichiometry and energy supply for the mechanism and suggested that the Na^+-dependent Ca^{2+} efflux mechanism may function under some conditions as a $Ca^{2+}/3Na^+$ antiporter. It was also suggested that the antiporter may be able to promote either electroneutral or electrophoretic exchange as a function of its regulatory state, but this remains to be demonstrated (Brierley et al., 1994).

Our results, summarized in Chapter 2, obtained with a purified reconstituted Na^+/Ca^{2+} antiporter, provide additional kinetic data and further support the proposed variability in the stoichiometry of this transport protein.

1.4 The Mitochondrial Proton Cycle

When inner mitochondrial membrane permeability to H^+ ions is increased, electron transport is uncoupled from oxidative phosphorylation. Redox energy is rapidly burned off as heat, because protons leak back into the matrix and no energy is conserved to make ATP.

1.4.1 General physiology of UCP1

Nature has designed a protein expressly for the purpose of uncoupling. Uncoupling protein-1 (UCP1), cloned in 1985 (Bouillaud et al., 1985, 1986; Jacobson et al., 1985; Ridley et al., 1986) and called UCP until 1997, is an inner mitochondrial membrane protein (Cinti et al., 1989) expressed exclusively in the brown adipose tissue (Cannon et al., 1982; Cadrin et al., 1985; Klaus et al., 1991). UCP1 short-circuits the insulating inner membrane, thereby causing mitochondria to produce heat instead of ATP (Cannon and Nedergaard, 1985).

In rodents, brown adipose tissue (BAT) contributes to both the maintenance of body temperature in a cold environment through nonshivering thermogenesis and the control of body weight through the regulatory part of diet-induced thermogenesis (Rothwell and Stock, 1979; Himms-Hagen, 1990). It has been shown that during cold acclimation the capacity of brown adipocytes to produce heat is determined by the UCP1 content of their mitochondria (Heaton et al., 1978; Hansen and Knudsen, 1986; Rafael et al., 1986).

1.4.2 Physiological regulation of UCP1-mediated uncoupling

The expression of UCP1 is regulated at the transcriptional level (Ricquier et al., 1991), and its control has been extensively studied (Silva et al., 1997). Norepinephrine is a strong physiological activator of UCP1 expression (Mory et al., 1984; Ricquier et al., 1986) and activation of the β1-, β2-, β3- and α1-adrenergic receptors (Ricquier et al., 1986; Muzzin et al., 1989; Rehnmark et al., 1990). Inhibition of the α2-adrenergic receptor (Savontaus et al., 1997) has been shown to increase the expression of UCP1. The thyroid hormone tri-iodothyronine

(T3) has been reported to act as a permissive factor for the full induction of UCP1 gene expression by norepinephrine (Bianco and Silva, 1988; Silva, 1988).

The kinetic regulation of UCP1-mediated uncoupling is still an unresolved problem. After norepinephrine activation of specific receptors on the plasma membrane, levels of cAMP increase and protein kinases are activated. This leads to a release of fatty acids from cellular stores and increased uncoupling. Uncoupling via UCP1 requires fatty acids and is inhibited by cytosolic ATP, which binds to the protein without hydrolysis (LaNoue et al., 1986). However, results from kinetic studies (Jezek et al., 1994), EPR probes (Jezek and Freisleben, 1994) and site-directed mutagenesis (Murdza-Inglis et al., 1994) indicate that fatty acids do not affect nucleotide binding or inhibition. Normal cytosol [ATP] should therefore prevent thermogenesis no matter how much fatty acid is released from cellular stores after stimulation. These findings raise again the long-standing question of how UCP1 is regulated in the cell (Nedergaard and Cannon, 1992).

Several types of regulation have been proposed: (i) *Cytosol pH.* This has been most thoroughly studied by Klingenberg and coworkers (Lin and Klingenberg, 1982; Huang and Klingenberg, 1995). The K_D for ATP binding increases strongly with pH above 7. This is due to three dissociations, one at the terminal phosphate and two at the protein binding site. The latter includes Glu/Asp and His residues, each of which must be protonated to bind ATP. Thus, as pH increases above 7.2, both sites lose protons, and binding will decrease despite greater availability of tetravalent ATP. (ii) *Cytosol Mg^{2+}.* Free ATP binds to UCP1, so increased cytosol [Mg^{2+}] will also reduce binding and inhibition. (iii) *ATP redistribution.* Observations by LaNoue et al. (1986) led to the proposal that ATP may redistribute from the cytosol to the mitochondrial matrix upon activation of the brown fat cell, resulting in reduced cytosolic [ATP]. (iv) *Cytosolic agonist.* Nedergaard and Cannon (1992) raised the possibility that a partial agonist may bind to UCP1, displacing ATP without inhibiting transport.

The most important clue to physiological regulation of UCP1 may be the one pointed out by LaNoue (LaNoue et al., 1986): brown fat cells consist largely of fat droplets and mitochondria; cytosol volume is vanishingly small. This means that pH,

[Mg^{2+}], and [ATP] can be perturbed more significantly by a signal arising from norepinephrine-induced stimulation.

1.4.3 Mechanisms of UCP1 transport

Any mechanism needs to account for the following experimental observations: (i) UCP1 mediates electrophoretic proton transport. (ii) Proton transport requires the presence of free fatty acids (Nicholls, 1979; Jezek et al., 1994; Winkler and Klingenberg, 1994). (iii) UCP1 mediates transport of halides, alkyl-sulfonates, and a variety of other monovalent anions (Jezek and Garlid, 1990; Jezek et al., 1990b). (iv) Both anion and proton transport are allosterically inhibited upon binding of a purine nucleotide to UCP1 (Lin and Klingenberg, 1982; Jezek and Garlid, 1990; Jezek et al., 1990b; Winkler and Klingenberg, 1994).

An early hypothesis by Nicholls (1974) and Klingenberg (1990) explained UCP1 transport by proposing that it is an anion carrier for which OH^- is the preferred substrate, with Cl^- competing with OH^-. Fatty acids activate the carrier allosterically by an unspecified mechanism without affecting Cl^- transport. This hypothesis became untenable in the face of new data provided by Jezek et al. (1994), which supported a mechanism in wich the transport pathway for anions is identical with fatty acid binding site and distinct from the nucleotide binding site.

Although the mechanism of transport of UCP1 is still a matter of controversy, there are two main hypotheses explaining this mechanism. The fatty acid-buffering model, introduced by Winkler and Klingenberg (1994), suggested that free fatty acids bind UCP1, and their carboxyl groups serve as H^+ donors. In this model, fatty acids are not translocated through the membrane. The second model, introduced by Skulachev and Garlid, proposes that deprotonated fatty acid anions are transported by UCP1, and the protonated form traverses (flip-flops) the phospholipid bilayer of the membrane (Skulachev, 1991; Garlid et al., 1996b). In both models, protonation/deprotonation of fatty acid carboxyl groups participate in H^+ transport.

These two hypotheses are reviewed in greater detail in Chapter 4, which also discusses how the two main mechanisms of transport relate to newly discovered uncoupling proteins.

1.4.4 Emergence of a new uncoupling protein family

Several observations led to the hypothesis that there could exist uncoupling proteins in tissues other than BAT. First, adult humans, who possess very little active BAT (Cunningham et al., 1985; Lean et al., 1986), produce heat in their skeletal muscle in response to glucose or catecholamine administration (Astrup et al., 1985, 1986, 1989; Simonsen et al., 1993). Second, mitochondrial H^+ leaks have been observed in tissues devoid of UCP (Brand, 1990; Nobes et al., 1990; Harper et al., 1993); they may account for up to 50% of the oxygen consumption of some tissues (Brand et al., 1994; Rolfe and Brand, 1996) and up to 30% of whole body metabolic rate in the rat (Rolfe and Brand, 1997). It was suggested that the H^+ leak was related to resting metabolic rate (Porter and Brand, 1993; Rolfe and Brand, 1997). Supporting these previous observations, several groups independently cloned novel UCPs, i.e., UCP2 (Fleury et al., 1997; Gimeno et al., 1997) and UCP3 (Boss et al., 1997; Vidal-Puig et al., 1997) (Fig. 1.4). UCP2, which has amino acid identity of 55% to UCP1, maps to regions of human chromosome 11 and mouse chromosome 7 that have been linked to hyperinsulinemia and obesity. UCP2 is expressed in most tissues studied in humans and rodents. UCP2 mRNA is not regulated by norepinephrine, but rather by the adipocyte hormone, leptin, which may upregulate UCP2 in tissues that express the leptin receptor (Zhou et al., 1997). UCP3 is 57% identical with UCP1 and 73% identical with UCP2. It is expressed only in BAT and glycolytic skeletal muscle (Boss et al., 1997). A short form of UCP3 was also found. It is missing the C-terminus (amino acids 276–312), which is a crucial part of the nucleotide binding domain in UCP1 (Boss et al., 1997). Thus, UCP1, which was thought to be a protein unique to BAT, is in fact a member of an emerging family of uncoupling proteins expressed in humans and animals, and even in plants (Vercesi et al., 1995; Jezek et al., 1996; Laloi et al., 1997).

1.4.5 Proposed physiological roles and regulation of the new UCP2

The physiological functions of UCP2 and UCP3 have been deduced primarily from their striking homology to UCP1, which is the terminal effector of the catabolic cascade of fatty acid-mediated, nonshivering thermogenesis. Except for the

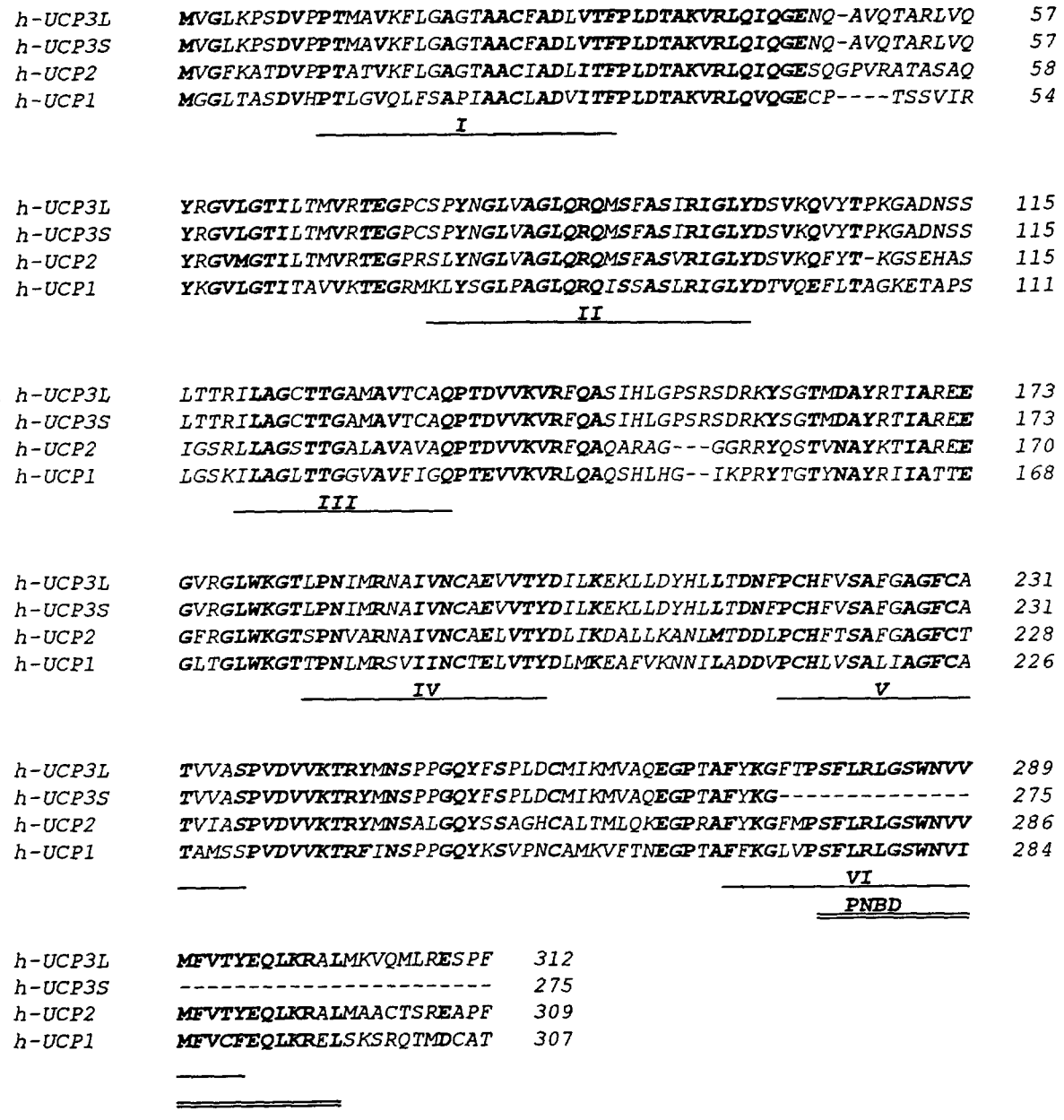

Figure 1.4 Amino acid sequence alignments of human UCP3L, UCP3S, UCP2 and UCP1. The sequences are presented in single letter code. Identical or similar amino acids are highlighted. Gaps introduced into the alignments are illustrated with a dash. Potential transmembrane α-helixes are underlined and numbered in roman numerals (I–VI). The potential purine-nucleotide binding domain (PNBD) is underlined twice (according to Boss et al., 1998).

studies summarized in Chapter 5, the transport mechanisms and regulation of the new UCPs are unknown, and their physiological roles are hypothetical.

1.4.5.1 Possible role of UCP2 in the maintenance of low levels of oxygen and oxygen radicals. Under resting conditions, energy consumption is low and the availability of ADP for phosphorylating respiration decreases, which may result in an increase in intracellular levels of O_2 and one-electron O_2 reductants. These conditions could enhance the formation of reactive oxygen species (ROS), such as superoxide ions, hydrogen peroxide, or the hydroxyl radical, which then cause oxidative damage within the cell. It has been proposed by Skulachev that nonphosphorylating (uncoupled or noncoupled) mitochondrial respiration allows the maintenance of low levels of both O_2 and ROS when phosphorylating respiration fails due to a lack of ADP. An increase in the H^+ leak of the mitochondrial membrane in State 4 would thus stimulate O_2 consumption and decrease the formation of ROS (Skulachev, 1996). Experimental support for the role of UCP2 in the control of cellular processes involving free radicals generated by mitochondria was provided by Negre-Salvayre et al. (1997).

1.4.5.2 Possible role of UCP2 in the control of insulin secretion. Glucose-induced insulin secretion by pancreatic islet cells has been shown to require mitochondria (Soejima et al., 1996) and to involve an increase in the cellular ATP/ADP ratio (Nilsson et al., 1996). UCP2 is expressed in pancreatic islets (Zhou et al., 1997) and might, by decreasing the cellular ATP levels, blunt glucose-induced insulin secretion. Leptin, which decreases the insulin response to glucose and other fuels (Koyama et al., 1997), was found to increase UCP2 mRNA expression in pancreatic islets (Zhou et al., 1997). It can be hypothesized that a high level of UCP2 could decrease insulin secretion.

1.4.5.3 UCP2 and UCP3 as obesity gene candidates. Because UCP2 and UCP3 may be involved in energy dissipation, they might participate in weight regulation. Mutations in their genes could play a role in the development of obesity and/or noninsulin-dependent diabetes. But even if no defects in the UCP2 and UCP3 genes can be associated with human obesity, these proteins could still represent good targets for drugs aimed at increasing energy expenditure. The maintenance of skeletal

muscle UCP3 expression during food restriction and refeeding might prevent the observed increase in food efficiency and might abet weight loss or inhibit weight gain (Boss et al., 1998).

CHAPTER 2

ELECTRONEUTRAL AND ELECTROPHORETIC Na^+/Ca^{2+} EXCHANGE MEDIATED BY THE RECONSTITUTED BEEF HEART MITOCHONDRIAL Na^+/Ca^{2+} ANTIPORTER

2.1 Introduction

The Ca^{2+} cycle of cardiac mitochondria is responsible for rapid oscillations in matrix Ca^{2+}, which result in sustained activation of Ca^{2+}-sensitive matrix dehydrogenases in response to cellular demands for increased ATP production (Rizzuto et al., 1992, 1994; Hajnóczky et al., 1995; Sparagna et al., 1995; Jou et al., 1996; Rutter et al., 1996). The Na^+/Ca^{2+} antiporter carries out the efflux side of this important cycle, and Cox and Matlib (1993) have shown directly that the cardiac mitochondrial Na^+/Ca^{2+} antiporter plays a central role in regulating turnover of the tricarboxylic acid cycle and the rate of oxidative phosphorylation.

We showed previously that the purified beef heart mitochondrial Na^+/Ca^{2+} antiporter catalyzes Na^+ and Ca^{2+} flux following its reconstitution into liposomes. The exchange that we observed was obligatorily electroneutral, consistent with Brand's conclusion (Brand, 1985) that the antiporter catalyzes electroneutral exchange in a Na^+:Ca^{2+} ratio of 2:1. Subsequently, however, Jung et al. (1995) made the important discovery that the cardiac Na^+/Ca^{2+} antiporter is electrophoretic. We have re-investigated this problem with the surprising result that the exchanger catalyzes 2:1 electroneutral exchange in the absence of counterion movement in liposomes and 3:1 electrophoretic exchange when a counterion transport pathway is provided. It is evident that electrophoretic coupling (Jung et al., 1995) is the physiologically important mode in mitochondria respiring *in vivo*.

The kinetics of Na^+/Ca^{2+} exchange are consistent with its participation in mitochondrial Ca^{2+} oscillation. In particular, exchange is strongly inhibited at alkaline pH, an effect mediated by a sharp increase in the K_m for Ca^{2+}. We found that BSA increased the V_{max} of Na^+/Ca^{2+} exchange by 3 to 4-fold. By exclusion, this effect appears to be due to protein–protein interaction, raising the intriguing possibility that the exchanger is subject to autoregulation by an intrinsic peptide, as has been demonstrated for plasma membrane Na^+/Ca^{2+} antiporters (Li et al., 1991; Kleiboeker et al., 1992; Chin et al., 1993).

2.2 Materials and Methods

2.2.1 Materials

SBFI and Calcium Green were obtained from Molecular Probes and Fura-2 from Calbiochem. Octylpentaoxylene was obtained from Bachem. Other chemicals and reagents were from Sigma. Beef heart mitochondria were prepared by differential centrifugation (Garlid et al., 1991).

2.2.2 Purification and reconstitution of the Na^+/Ca^{2+} antiporter

The protocols for purifying and reconstituting the Na^+/Ca^{2+} antiporter have been described in detail (Li et al., 1992; Garlid et al., 1995). Briefly, beef heart submitochondrial particles were prepared and treated to remove the F_1 subunit of ATPase and other adherent proteins (McEnery et al., 1989). Proteins (100 mg) were extracted for 1 h in buffer containing 3% Triton X-100, then centrifuged, and the supernatant collected for purification. The solubilized protein was loaded onto a 20-ml DEAE-cellulose column and washed with 80 ml of loading buffer containing 1% Triton X-100. The second bed volume was further purified on a 5-ml DEAE-cellulose column, with Na^+/Ca^{2+} exchange activity being found in the second bed volume. This fraction is reconstitutively active and contains two dominant protein bands on SDS-PAGE at 110 kDa and 70 kDa (Li et al., 1992).

The purified protein fraction was added to a 10:1 mixture of L-α-lecithin (Avanti) and cardiolipin in 10% octylpentaoxyethylene. The buffer composition at

this stage defines the *internal medium*, the composition of which is described in detail in the figure legends. This mixture was loaded onto a 2-ml Bio-Beads SM-2 column (Bio-Rad) to remove detergent and form proteoliposomes. After incubation for 90 min at 0–4°C, the column was centrifuged at 400 × *g* for 2 min to collect the proteoliposomes. To remove extravesicular probe, 200-μl aliquots of the proteoliposome suspension were passed twice through 4-ml Sephadex G-25-300 columns. The final stock vesicle suspension (nominally 50 mg lipid/ml) was stored on ice during the experiment. Protein content, measured by the Amido Black method (Kaplan and Pedersen, 1985), was normally 50–70 ng protein per mg of lipid. Intraliposomal volume of each preparation was estimated from the volume of distribution of entrapped probe and was normally found to be 1 μl per mg of starting lipid (Garlid et al., 1995).

2.2.3 Fluorescence measurements

We used Fura-2 (500 μM) and Calcium Green (100 μM) to measure internal Ca^{2+} concentration and SBFI (250 μM) to measure internal Na^+ concentration. Proteoliposomes were added to 2 ml of assay medium at a final concentration of 0.5 mg of lipid per ml of assay medium, and probe fluorescence was measured on an SLM-Aminco 8000c spectrophotometer (Li et al., 1992; Garlid et al., 1995). Excitation and emission wavelengths corresponded to those described by Molecular Probes.

2.2.4 Determination of free Ca^{2+}

Internal and external media were buffered with high concentrations of EGTA and/or HEDTA. The pH shift at pH 7.3, caused by additions of $CaCl_2$ to the medium, was compensated by immediate addition of an amount of TEA-OH determined by pH electrode to neutralize the effect of the added Ca^{2+}. Free [Ca^{2+}] was estimated using the software Chelator, which was kindly provided by Dr. T. J. M. Schoenmakers. The Chelator software accounts for the effect of medium pH, temperature, and ionic strength in the calculation of apparent dissociation constants for CaEGTA or CaHEDTA (Blinks et al., 1982; Schoenmakers et al., 1992).

2.2.5 Fluorescent probe calibration

Fluorescence emission, **F**, by the probe increases with increasing free concentrations of the cationic ligand, $[M]_{free}$. The initial concentration, $[M^o]_{free}$, may be zero or non-zero by experimental design. The following general relationship holds for any value of $[M]_{free}$:

$$F - F_1 = \{\Delta[M]_{free}/K_d'\}\ \{F_{max} - F\} \quad (1)$$

where $\Delta[M]_f \equiv [M]_{free} - [M^o]_{free}$, F_1 is the fluorescence when $\Delta[M]_f = 0$, and F_{max} is the fluorescence at saturating cation concentration. The apparent probe dissociation constant, K_d', is related to the true dissociation constant, K_d, as follows:

$$K_d' = K_d + [M^o]_{free} \quad (2)$$

or,

$$K_d' = K_d^* \{F_{max} - F_0\}/\{F_{max} - F_1\} \quad (3)$$

where F_o is the fluorescence in the absence of ligand. Thus, K_d can be obtained from Equation 2 if $[M^o]_{free}$ is known or from Equation 3 if it is not.

Calibrations of intraliposomal probe were performed on each preparation. The cation, Na^+ or Ca^{2+}, was added stepwise to the external medium in the presence of ionophore to equilibrate the cation with the intraliposomal space (Garlid et al., 1991). Monensin was used for Na^+ in calibrating SBFI, and ionomycin was used for Ca^{2+} in calibrating Fura-2 and Calcium Green-2. Data were fitted to a linearized form of Equation 1, yielding the parameters F_{max} and K_d', and K_d was evaluated according to Equations 2 or 3. Calibrations routinely yielded values of K_d in good agreement with the literature. For Na^+ flux measurements, calibration parameters were applied to each experimental run to convert SBFI fluorescence intensity to $[Na^+]$, from which the initial rates were obtained by linear regression.

For Ca^{2+} flux, the desired quantity is total intraliposomal Ca^{2+} concentration, $[Ca^{2+}]_{total}$. For this purpose, we devised a simple and accurate approximation to Equation 1 that yields $[Ca^{2+}]_{total}$ directly:

$$F - F_1 = \alpha\ \Delta[Ca^{2+}]_{total} \quad (4)$$

where α is the proportionality constant, given by

$$\text{Lim}\ \alpha\ \{\text{as}\ \Delta[Ca^{2+}]_{free} \rightarrow 0\} = (K_E/K_d')\ \{(F_{max} - F_1)/[HEDTA]_F\} \quad (5)$$

where $[HEDTA]_F$ is free intraliposomal HEDTA concentration, and K_E is the apparent dissociation constant of CaHEDTA, as determined by the Chelator program.

This approximation is justified on theoretical grounds. Because HEDTA was present in excess, and because initial rates were measured within the first 20 s after initiation of Ca^{2+} flux, $\Delta[Ca^{2+}]_{total}$ was $\leq$ 100 μM and $\Delta[Ca^{2+}]_{free}$ was $\leq$ 20 nM, satisfying the condition in Equation 5. Experimental validation of Equations 4 and 5 are provided by the calibration curves in Fig. 2.1. Fluorescence is linear with $\Delta[Ca^{2+}]_{total}$ for both Fura-2 and Calcium Green-2, as predicted. Furthermore, the measured values of α yield calculated K_d values, using Equation 5, of 167 nM for Fura-2 and 820 nM for Calcium Green, in reasonable agreement with published values (Grynkiewicz et al., 1985) and those given by Molecular Probes.

Accordingly, it is justifiable to use the following expression for Ca^{2+} flux into the liposomes:

$$d[Ca^{2+}]_{total}/dt = (1/\alpha)\ dF/dt \qquad (6)$$

where α is determined by calibration. The primary advantages of Equation 6 are that it bypasses ambiguities in estimating K_d and K_E and yields the desired Ca^{2+} flux directly.

2.3 Results

2.3.1 Stoichiometries of electroneutral and electrophoretic Na^+/Ca^{2+} exchange

Figs. 2.2 and 2.3 summarize data relating to the stoichiometries of the two modes of exchange. Fig. 2.2 contains the $[Ca^{2+}]$-dependence of *electroneutral* Ca^{2+} uptake and Na^+ efflux. The two curves are from parallel reconstitutions that were identical except that one preparation contained SBFI and the other contained Fura-2. Na^+/Ca^{2+} exchange is electroneutral in this experiment, because no counterion was available to support charge movement through the antiporter, and the liposomes are highly impermeable to ions. Proton flux, the only significant diffusive flux under these conditions, amounted to less than 10% of the observed Ca^{2+} flux. In three independent experiments, the K_m for Ca^{2+} was 2.10 $\pm$ 0.16 μM in the Ca^{2+}

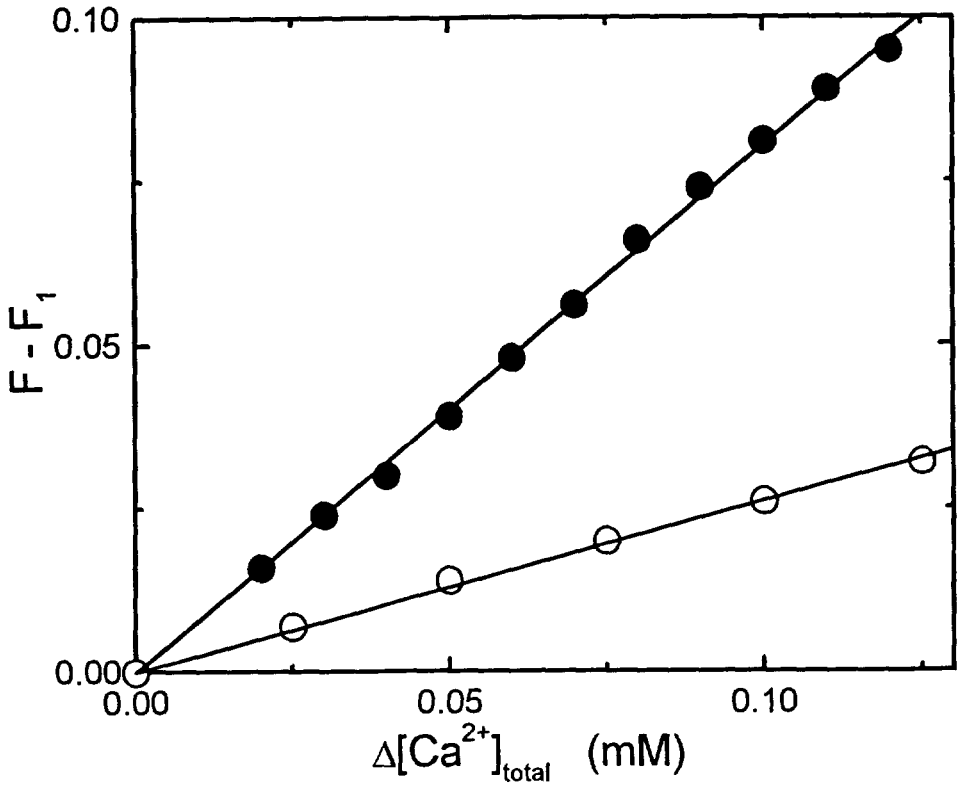

Figure 2.1 Dependence of Fura-2 and Calcium Green™-2 fluorescence on total Ca^{2+}. The Ca^{2+}-dependent increase in fluorescent intensity ($F - F_1$) is plotted versus $\Delta[Ca^{2+}]_{total}$, as defined in Section 2.2. Calcium was equilibrated in the presence of 250 nM ionomycin, and 2 min were allowed for equilibration after each addition. Linear regression of the data gave values of $\alpha = 0.805$ mM^{-1} for Fura-2 (•) and 0.265 mM^{-1} for Calcium Green™-2 (○). Internal and external media contained 125 mM TEA-Cl, 25 mM NaCl, and 25 mM TEA-TES, pH 7.30. At the start of the Fura-2 experiment, vesicles contained 500 μM Fura-2, 10 mM TEA-HEDTA, and no Ca^{2+}. The following values were used for the calculations in the text: $K_E = 1.66$ μM, $[HEDTA]_F = 10$ mM, and $(F_{max} - F_1) = 0.81$. At the start of the Calcium Green-2 experiment, vesicles contained 100 μM Calcium Green-2, 5 mM TEA-HEDTA, and 1.9 mM Ca^{2+}; $K_E = 1.66$ μM, $[HEDTA]_F = 3.1$ mM, and $(F_{max} - F_1) = 0.91$.

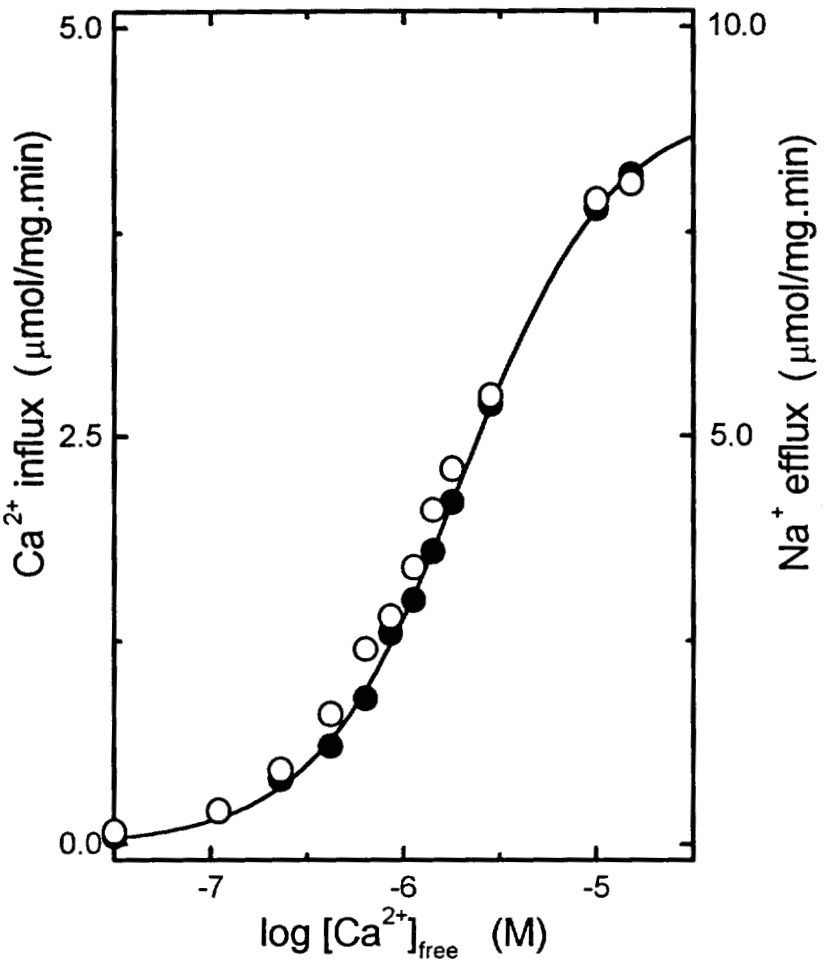

Figure 2.2 Electroneutral Na^+/Ca^{2+} exchange and its dependence on $[Ca^{2+}]$. Initial rates of Ca^{2+} influx (•) and Na^+ efflux (○), measured in proteoliposomes reconstituted with the purified Na^+/Ca^{2+} antiporter, are plotted versus external free $[Ca^{2+}]$. Fura-2 and SBFI were loaded separately into two preparations of proteoliposomes. Internal medium contained 125 mM TEA-Cl, 25 mM NaCl, and 10 mM TEA-HEDTA. External medium contained 5 mM TEA-EGTA, 5 mM TEA-HEDTA, and 150 mM TEA-Cl. Both media contained 25 mM TEA-TES, pH 7.30. $CaCl_2$ and TEA-OH were added to external medium in order to vary free $[Ca^{2+}]$ without changing pH, as described in Section 2.2.

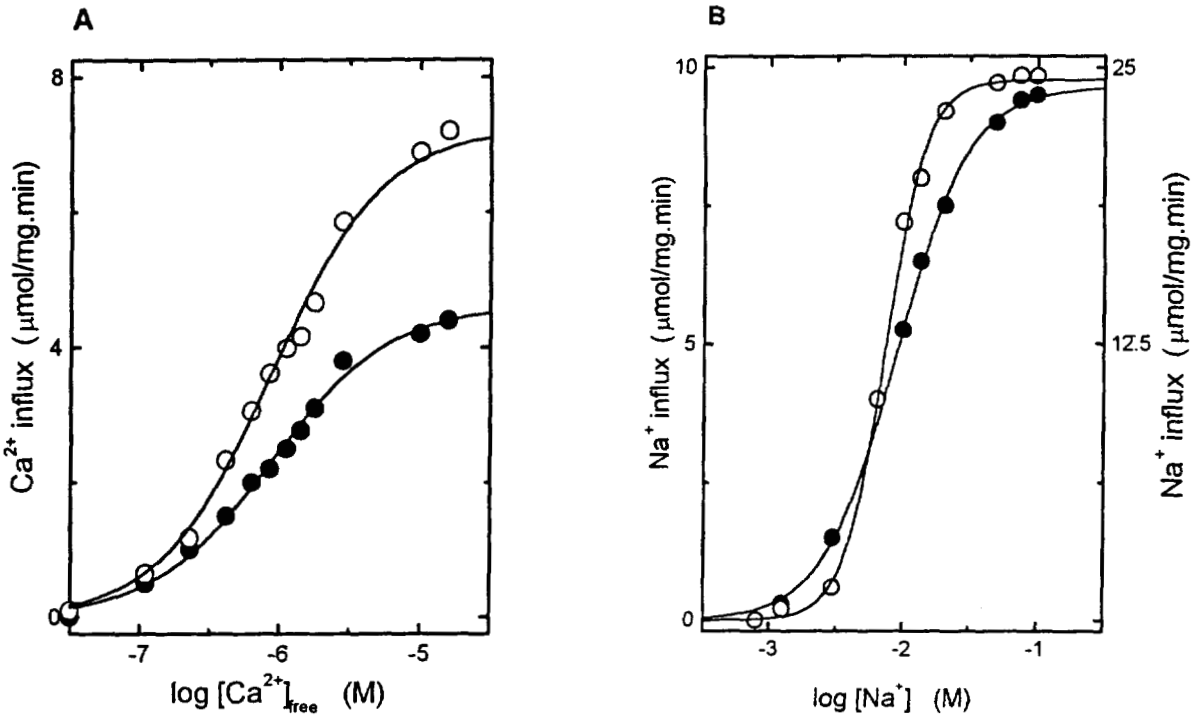

Figure 2.3 Electroneutral and electrophoretic Na^+/Ca^{2+} exchange by the reconstituted Na^+/Ca^{2+} antiporter. ***PANEL A*** contains the $[Ca^{2+}]$-dependence of Ca^{2+} influx in the presence (○) or absence (•) of 25 nM valinomycin in medium containing 150 mM K^+. Valinomycin increased V_{max} without affecting Hill slope or K_m for Ca^{2+}. Ca^{2+} uptake on the antiporter was driven by a Na^+ gradient. Internal medium contained 500 μM Fura-2, 100 mM TEA-Cl, 50 mM NaCl, 10 mM TEA-HEDTA, and 25 mM TEA-TES, pH 7.3. External medium contained 5 mM TEA-EGTA, 5 mM TEA-HEDTA, 150 mM KCl, and 25 mM TEA-TES, pH 7.3. ***PANEL B*** contains the $[Na^+]$-dependence of Na^+ influx in the presence (○) or absence (•) of 25 nM valinomycin in medium containing 150 mM K^+. Valinomycin increased V_{max} and Hill slope without affecting the K_m for Na^+. Na^+ uptake on the antiporter was driven by a Ca^{2+} gradient; internal $[Ca^{2+}]_{free}$ was 5 μM. Internal medium contained 250 μM SBFI, 50 mM TEA-Cl, and 100 mM KCl. External medium contained 150 mM Cl^- as the Na^+ or TEA^+ salt, as indicated on the abscissa. Both media contained 5 mM TEA-EGTA, 5 mM TEA-HEDTA, and 25 mM TEA-TES, pH 7.30.

influx experiment and 1.98 ± 0.06 μM in the Na^+ efflux experiment. The Hill slopes for both Ca^{2+} influx and Na^+ efflux were about 0.9. The ratio (Na^+:Ca^{2+}) of the V_{max} values was 1.9, indicating a 2:1 exchange in the electroneutral mode.

Fig. 2.3A demonstrates the effects of a permeant counterion on Ca^{2+} influx via the Na^+/Ca^{2+} antiporter. The two experiments shown were carried out in the presence or absence of valinomycin in identical media, containing 150 mM $[K^+]_o$. In a large number of experiments of this type, valinomycin always increased the V_{max} for Ca^{2+} influx by 50–150%. The K_m for Ca^{2+} was 0.9 μM and was unaffected by $\Delta\Psi$. This lower value (compare with 2 μM in Fig. 2.2) was due to the presence of K^+ in the medium (as discussed below).

Fig. 2.3B demonstrates the effects of a permeant counterion on Na^+ influx via the Na^+/Ca^{2+} antiporter. The two experiments shown were carried out in the presence or absence of valinomycin in identical media, with the vesicles containing 100 mM $[K^+]_o$ and 10 μM free Ca^{2+}. Valinomycin always increased the V_{max} for Na^+ influx by 150–250%. The K_m for Na^+ was 8.2 ± 1.4 mM (n = 4) and was unaffected by valinomycin. The most striking effect of valinomycin was on the Hill slopes for Na^+ influx. These were 1.8 ± 0.2 (n = 4) in the absence of valinomycin, indicative of 2:1 Na^+/Ca^{2+} exchange in the electroneutral mode, and 2.8 ± 0.2 (n = 3) in the presence of valinomycin, indicative of 3:1 Na^+/Ca^{2+} exchange in the electrophoretic mode of transport.

2.3.2 Further evidence for 3:1 Na^+/Ca^{2+} stoichiometry in the electrophoretic mode of Na^+/Ca^{2+} exchange

We also exploited the dependence of Na^+/Ca^{2+} exchange on $\Delta\Psi$ to determine the stoichiometry of the Na^+/Ca^{2+} antiporter. As shown in Fig. 2.4, Ca^{2+} influx increases linearly with increasing $\Delta\Psi$ over the range measured. The Na^+/Ca^{2+} stoichiometry, n, is contained in the total driving force for Na^+/Ca^{2+} exchange, $\Delta\tilde{\mu}_{Na/Ca}$:

$$\Delta\tilde{\mu}_{Na/Ca} = n\,\Delta\tilde{\mu}_{Na+} - \Delta\tilde{\mu}_{Ca2+} \qquad (7)$$

where

$$\Delta\tilde{\mu}_M = RT \ln([M]_{in} / [M]_{out}) + zF\Delta\Psi \qquad (8)$$

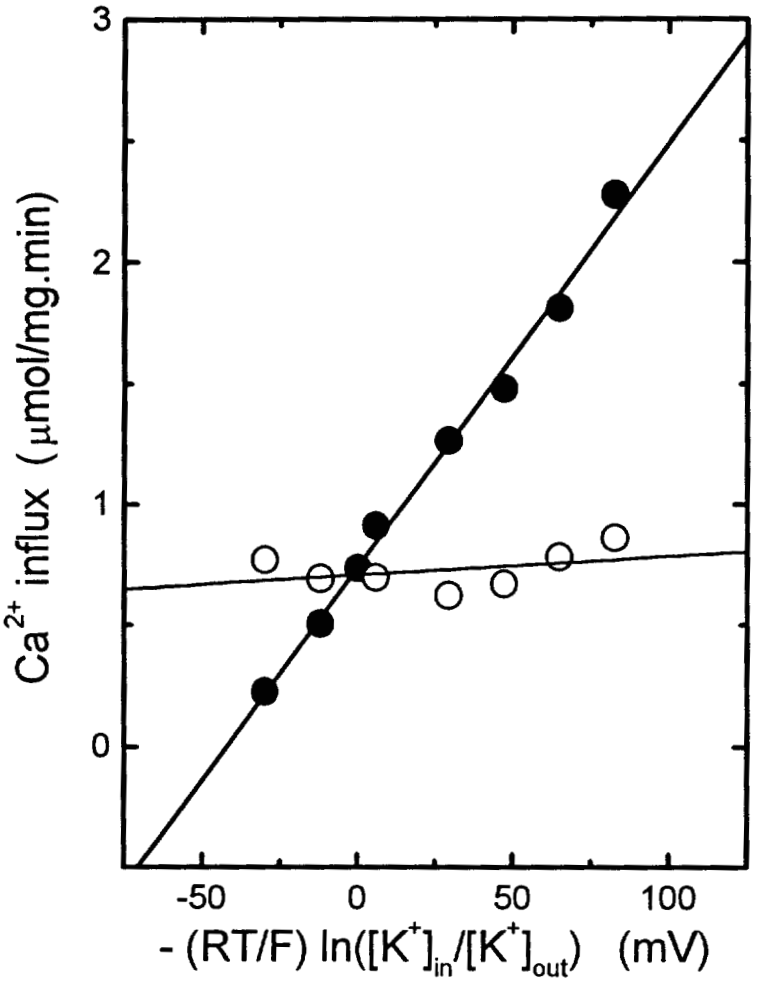

Figure 2.4 Membrane potential dependence of Ca^{2+} flux and the stoichiometry of Na^+/Ca^{2+} exchange. Ca^{2+} influx data are plotted versus $\Delta\Psi$ in the presence (•) or absence (○) of 25 nM valinomycin. Internal medium contained 100 μM Calcium Green™-2, 1 μM free [Ca^{2+}] and 5 mM K^+. External medium contained 5 μM free [Ca^{2+}] and 125 mM TEA-Cl, which was replaced by KCl to achieve the indicated $\Delta\Psi$ values. Both media contained 25 mM Na^+, 5 mM TEA-HEDTA, and 25 mM TEA-TES, pH 7.3. Transport rates where determined from fluorescence traces within 10 s after the transport was initiated by addition of proteoliposomes to the assay medium. Each point represents an average from three determinations.

is the electrochemical potential of cation **M**, z is its charge, R is the gas constant, T is absolute temperature, and F is the Faraday constant. At gradients causing zero Ca^{2+} flux (x-intercept), the overall driving force is also zero, and

$$n\,\Delta\tilde{\mu}_{Na+} = \Delta\tilde{\mu}_{Ca2+} \qquad (9)$$

The stoichiometry can thus be calculated from the known Na^+ and Ca^{2+} concentrations and the steady-state value of $\Delta\Psi$ at the intercept, $\Delta\Psi_o$.

The experiment of Fig. 2.4 was carried out in the absence of a Na^+ gradient, and linear regression of the dependence of Ca^{2+} influx on $\Delta\Psi$ yielded a value for $\Delta\Psi_0$ of -42.8 mV. The stoichiometry was then calculated as

$$n = 2 + (RT/F\Delta\Psi_0)\,(\ln [Ca^{2+}]_{in}/\,[Ca^{2+}]_{out}) = 2.97$$

A similar response to $\Delta\Psi$ was observed when both Na^+ and Ca^{2+} gradients were present (not shown). Linear regression yielded a value for $\Delta\Psi_o$ of -212.6 mV, leading to a stoichiometry of $n = 2.81$.

2.3.3 Electroneutral Na^+/Li^+ and Na^+/K^+ exchange in the absence of calcium

To our surprise, we observed that the purified reconstituted Na^+/Ca^{2+} antiporter catalyzed electroneutral Na^+/Li^+ and Na^+/K^+ exchange in the absence of Ca^{2+}, as shown in Fig. 2.5. The V_{max} was about the same as the V_{max} for Na^+ flux during electroneutral Na^+/Ca^{2+} exchange (see Fig. 2.2). The K_m for K^+ was 20 $\pm$ 3 mM (n = 3), and the K_m for Li^+ was 27 $\pm$ 4 mM (n = 3). Na^+/Li^+ and Na^+/K^+ exchange were each inhibited by diltiazem and TPP^+, and the $K_{1/2}$ values for inhibition were approximately the same as those for inhibition of Na^+/Ca^{2+} exchange (not shown).

It is important to emphasize that these experiments were carried out in the absence of Ca^{2+}. In the presence of Ca^{2+}, Na^+ did not induce K^+ flux, K^+ was not competent to induce Ca^{2+} counter-flux, and Ca^{2+} did not induce K^+ counter-flux (data not shown).

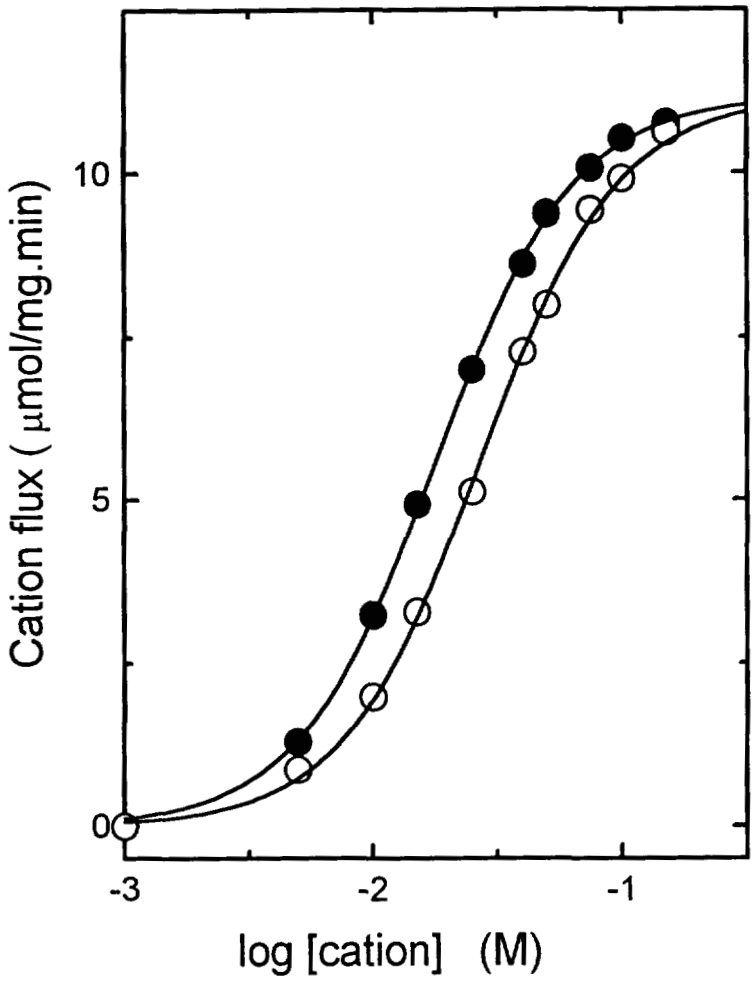

Figure 2.5 Na^+/Li^+ and Na^+/K^+ exchange via the Na^+/Ca^{2+} antiporter in Ca^{2+}-free media. Initial rates of Na^+ efflux are plotted versus medium $[K^+]$ (•) and medium $[Li^+]$ (○). Proteoliposomes contained 125 mM TEA-Cl, 25 mM NaCl and 250 μM SBFI. External medium contained 150 mM TEA-Cl, substituted with LiCl or KCl to achieve the indicated cation concentrations. Both media contained 1 mM TEA-EGTA and 25 mM TEA-TES, pH 7.30.

2.3.4 Regulation of the Na^+/Ca^{2+} antiporter by K^+

K^+ stimulates both Na^+/Ca^{2+} and Ca^{2+}/Ca^{2+} exchange via the Na^+/Ca^{2+} antiporter in intact mitochondria (Crompton et al., 1980; Hayat and Crompton, 1982). As summarized in Table 2.1, K^+ caused an increase in the apparent affinity of the carrier for Ca^{2+} without affecting the V_{max} for Ca^{2+} uptake. The K_m for Ca^{2+} was decreased from 2 μM in the presence of 2.5 mM [K^+] to 0.9 μM in the presence of 100 mM K^+. This effect was only observed when K^+ was present on the same side of the membrane as Ca^{2+}; *trans* K^+ had no effect on the K_m for Ca^{2+}.

2.3.5 Regulation of the Na^+/Ca^{2+} antiporter by pH

Baysal et al. (Baysal et al., 1991) showed, in intact beef heart mitochondria, that the Na^+/Ca^{2+} antiporter is regulated by matrix pH and exhibits maximal activity at pH 7.4–7.6. We investigated the effects of pH on Na^+-dependent Ca^{2+} uptake via the reconstituted Na^+/Ca^{2+} antiporter and observed maximum activity at pH 7.0 (Fig. 2.6). Ca^{2+} flux was strongly inhibited at alkaline pH. This result, which supports the conclusion that pH is a powerful modulator of mitochondrial Na^+/Ca^{2+} exchange (Baysal et al., 1991), does not indicate the target of this effect. This was elucidated in further experiments that examined the effect of pH on the V_{max} and K_m for Na^+/Ca^{2+} exchange. As shown in Fig. 2.7, the effect of varying pH is mediated entirely via changes in the K_m for Ca^{2+}. In three independent experiments, the K_m was shifted from 0.55 $\pm$ 0.16 μM at pH 7.0 to 42 $\pm$ 14 μM at pH 6.5, and to approximately 1.0 $\pm$ 0.4 mM at pH 7.8.

2.3.6 Regulation of Na^+/Ca^{2+} exchange by diltiazem and TPP^+

Diltiazem inhibits Na^+/Ca^{2+} exchange in beef heart mitochondria with $K_{1/2}$ = 7 μM (Vaghy et al., 1982), and TPP^+ inhibits Na^+/Ca^{2+} exchange in rat liver mitochondria with $K_{1/2}$ = 0.2 μM (Wingrove and Gunter, 1986). These agents also inhibited Na^+/Ca^{2+} exchange in the reconstituted system, as shown in Fig. 2.8. The $K_{1/2}$ for diltiazem was 10 $\pm$ 3 μM, and the $K_{1/2}$ for TPP^+ was 0.6 $\pm$ 0.2 μM.

TABLE 2.1

Effects of Internal and External K^+ on K_m for Ca^{2+} Influx

	$[K^+]_i$ = 2.5 mM	$[K+]_i$ = 100 mM
$[K^+]_o$ = 2.5 mM	1.98 ± 0.12 μM	1.97 ± 0.16 μM
$[K^+]_o$ = 100 mM	0.94 ± 0.15 μM	0.91 ± 0.11 μM

Shown are K_m values for Ca^{2+} observed when Ca^{2+} influx was measured under conditions varying with respect to intra- and extra-vesicular $[K^+]$. KCl was substituted for TEA-Cl to obtain the indicated concentrations. Parallel proteoliposome preparations were made for measurements differing with respect to internal $[K^+]$. Internal and external media were otherwise as described in the legend to Fig. 2, with $[Ca^{2+}]_o$ being varied. Data are expressed as the mean obtained in three independent experiments.

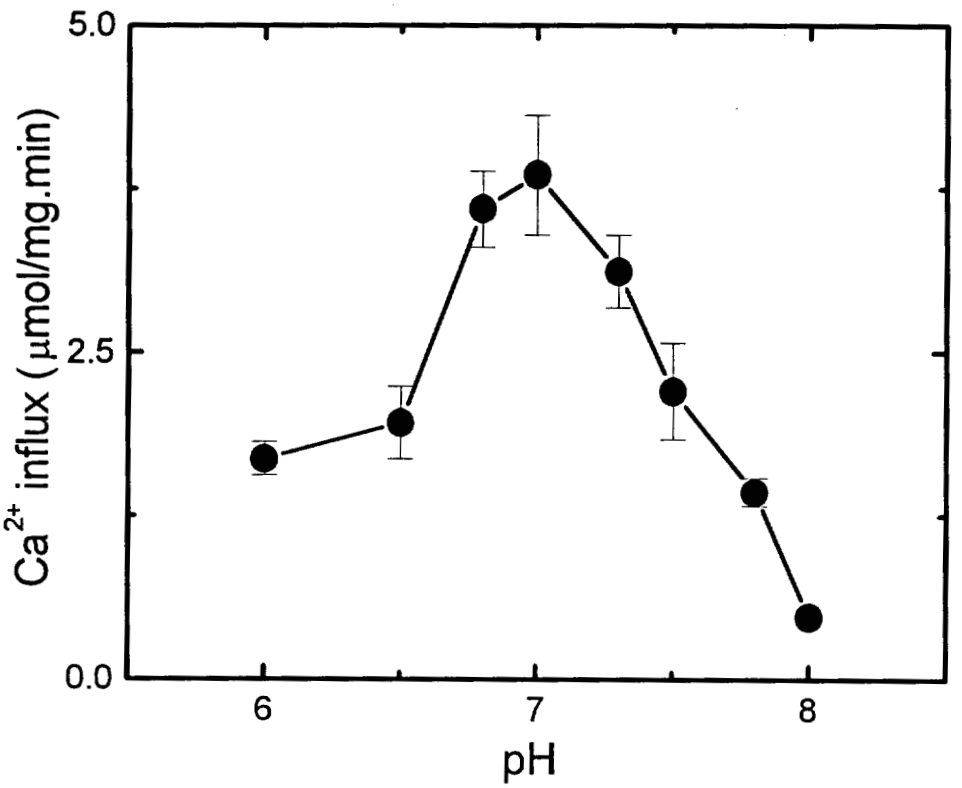

Figure 2.6 Regulation of the Na^+/Ca^{2+} antiporter by pH. Initial Ca^{2+} uptake rates were measured in proteoliposomes at different media pH values. Proteoliposomes were loaded with 500 μM Fura-2 and 50 mM NaCl. Rates at each pH were measured in triplicate, and the error bars reflect the means $\pm$ standard error of the estimate. 2 μM free Ca^{2+} was present in external medium. Internal and external media were otherwise as described in the legend to Fig. 2.2.

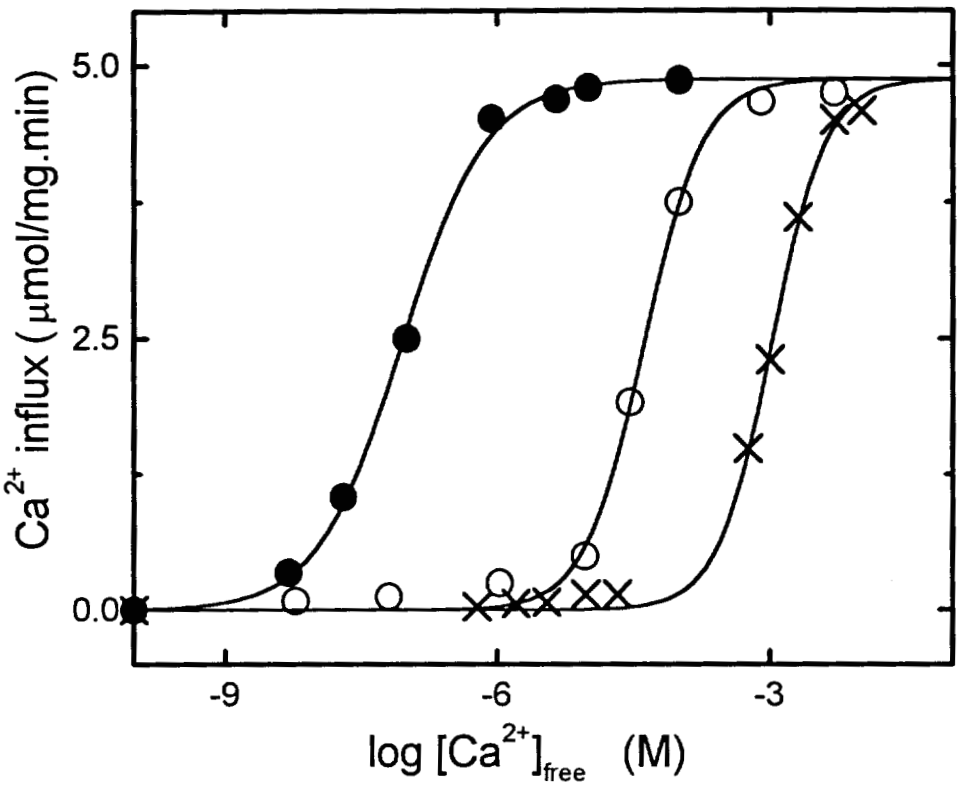

Figure 2.7 The effect of pH on the kinetics of Na^+/Ca^{2+} exchange. Initial rates of Ca^{2+} uptake into proteoliposomes were measured as medium $[Ca^{2+}]$ was varied at three different values of medium pH. Internal and external media were as described in the legend to Fig. 2.2. The estimated K_m values are given in the text. The curves are plotted with Hill coefficients of 1. Medium pH was 7.0 (•), 6.5 (○), or 7.8 (×).

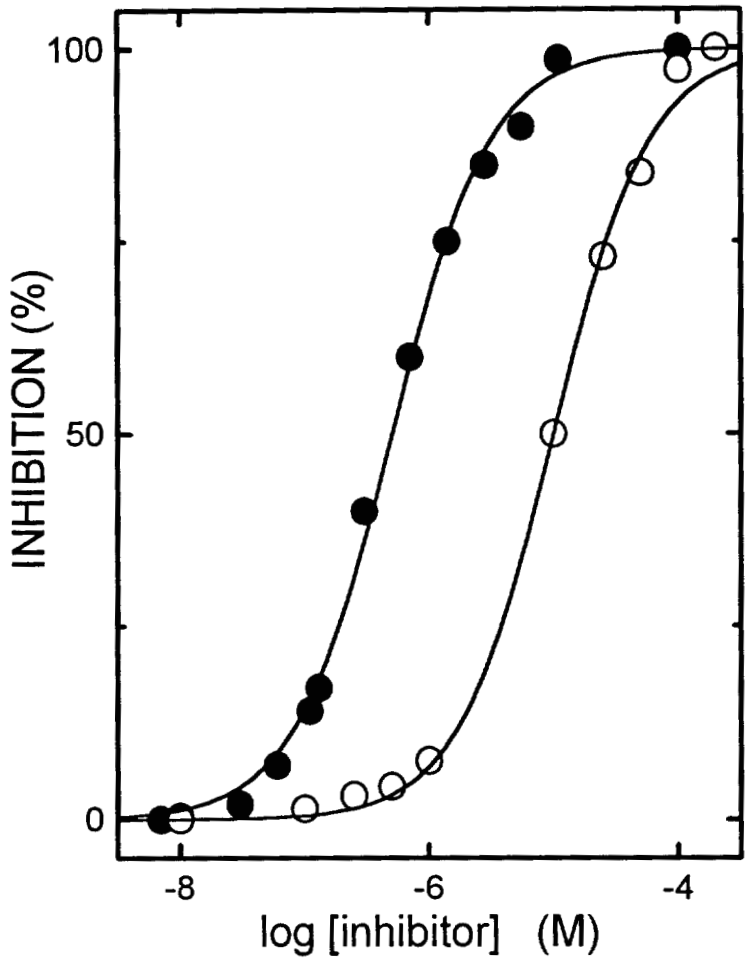

Figure 2.8 Inhibition of Na/Ca^{2+} exchange by TPP^+ and diltiazem. Percent inhibition of initial rates of Ca^{2+}-induced Na^+ efflux is plotted versus medium [TPP^+] (•) or [diltiazem] (○). Proteoliposomes were reconstituted with purified Na^+/Ca^{2+} antiporter and loaded with 250 μM SBFI. 5 μM free Ca^{2+} was present in external medium. Internal medium contained 125 mM TEA-Cl and 25 mM NaCl. External medium contained 150 mM TEA-Cl. Both media contained 5 mM TEA-EGTA, 5 mM TEA-HEDTA, and 25 mM TEA-TES, pH 7.30.

Complete inhibition of the cardiac mitochondrial Na^+/Ca^{2+} antiporter by TPP^+ has not previously been reported. The data in Fig. 2.8 are measurements of Ca^{2+}-dependent Na^+ efflux. Nearly identical results were obtained when Na^+-dependent Ca^{2+} efflux, K+-dependent Na+ efflux, or Li+-dependent Na+ efflux were measured.

2.3.7 Regulation of Na^+/Ca^{2+} exchange by bovine serum albumin

During the development of a protocol to help preserve the purified Na^+/Ca^{2+} antiporter for longer periods of time, we found that BSA stimulated Na^+/Ca^{2+} exchange when added to the assay medium. Fig. 2.9A contains representative traces from proteoliposomes incubated with BSA for 2 min, followed by the addition of 5 μM free Ca^{2+} to initiate Na^+/Ca^{2+} exchange. Electroneutral Ca^{2+} uptake on the exchanger was about 2-fold higher in the presence of BSA (*trace c* of Fig. 2.9A), as compared with control (*trace b* of Fig. 2.9A). Electrophoretic Ca^{2+} uptake was also stimulated about 2-fold by BSA (data not shown); thus the effects of BSA and $\Delta\Psi$ are additive.

BSA is a potent activator of Na^+/Ca^{2+} exchange, as illustrated by the dose–response curves in Fig. 2.9B. The apparent K_m for this effect was about 250 nM (16 μg/ml), and maximal stimulation was 3-fold in this experiment and up to 4-fold in other experiments. Removal of endogenous fatty acids, which are very low in this preparation, did not appear to be responsible for this effect, because fatty acids had no effect on Na^+/Ca^{2+} exchange. Moreover, BSA removal of a heavy metal inhibitor can be excluded, because a high concentration of HEDTA was present on both sides of the membrane. It is worth noting that there was no decay of Na^+/Ca^{2+} exchange activity during these incubations, and the BSA stimulation was unchanged when BSA and control runs were compared at the beginning and end of a 4-h experiment.

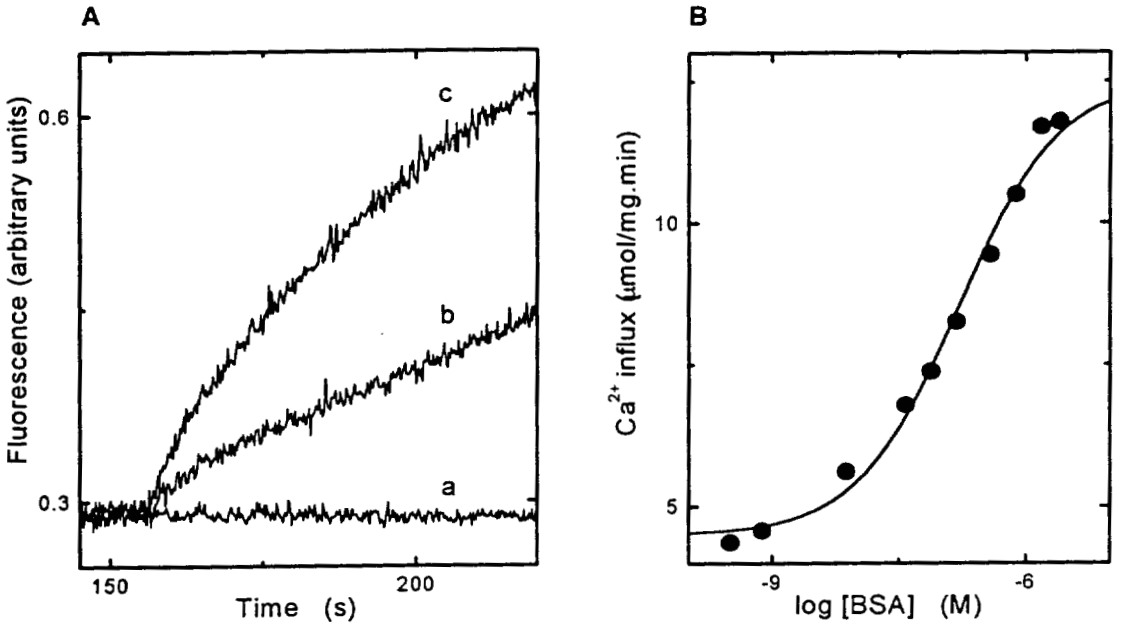

Figure 2.9 Stimulation of Na^+/Ca^{2+} exchange by BSA. Ca^{2+} uptake was initiated by adding 5 μM free Ca^{2+} after proteoliposomes were preincubated for 2 min in assay medium containing indicated [BSA]. Internal and external media were otherwise as described in the legend to Fig. 2.2. ***PANEL A:*** Fura-2 fluorescence intensity is plotted versus time. *Trace a*, no Ca^{2+}; *trace b*, 5 μM free Ca^{2+}; *trace c*, 5 μM free Ca^{2+} and 1 μM (64 μg/ml) BSA. ***PANEL B:*** Ca^{2+} influx is plotted versus [BSA].

2.4 Discussion

Understanding the kinetics and regulation of the mitochondrial Na^+/Ca^{2+} antiporter is essential for assessing its role in regulating mitochondrial metabolism and for comparing its structure-function with other members of this expanding gene family. Reconstitution is a particularly useful technique for these purposes, because it provides reliable estimates of kinetic parameters that are difficult to obtain in isolated mitochondria. Reconstitution is also capable of revealing new properties that could not readily be obtained in the complex setting of intact mitochondria.

2.4.1 Stoichiometry of the mitochondrial Na^+/Ca^{2+} antiporter

The Na^+/Ca^{2+} antiporter is able to catalyze both electroneutral and electrophoretic exchange. Electroneutrality is required to explain spontaneous exchange in the absence of a permeant counterion and is further supported by the kinetic data. In three parallel experiments, the ratio of Na^+:Ca^{2+} V_{max} values was 1.8–1.95, and the Na^+ dependence of Na^+ uptake exhibited a Hill slope close to 2. We conclude that the antiporter catalyzes 2:1 Na^+/Ca^{2+} exchange in the electroneutral mode.

Valinomycin stimulated Na^+/Ca^{2+} exchange in the presence of a K^+ gradient (Fig. 2.3), and the Hill slope for Ca^{2+}-dependent Na^+ flux increased to 2.8. A thermodynamic analysis of the $\Delta\Psi$ dependence of Ca^{2+} flux (Fig. 2.4) yielded Na^+/Ca^{2+} stoichiometry values of 2.8–3.0. We conclude that the antiporter catalyzes electrophoretic 3:1 Na^+/Ca^{2+} exchange in the presence of permeant counterion. These results support findings in intact mitochondria, which suggested three independent binding sites for Na^+ (Hayat and Crompton, 1982) and confirm findings of electrophoretic Na^+/Ca^{2+} exchange in intact mitochondria by Jung et al. (1995).

2.4.2 Ion selectivity of the mitochondrial Na^+/Ca^{2+} antiporter

The surprising new result that this carrier mediates Na^+/K^+ and Na^+/Li^+ exchange in the absence of Ca^{2+} would be difficult to discern in mitochondria due to the multiplicity of transport pathways for alkali cations. Li^+ can

induce Ca^{2+} efflux from mitochondria (Crompton et al., 1978), but there was no previous indication of Na^+/Li^+ exchange in the absence of Ca^{2+}.

K^+ could not substitute for Na^+ in inducing Ca^{2+} transport, nor did Ca^{2+} induce K^+ transport. Nevertheless, the Na^+/Ca^{2+} antiporter catalyzed Na^+/K^+ exchange. This is reminiscent of the K^+/H^+ antiporter, in which cation/cation exchange proceeds normally when K^+/H^+ exchange is fully inhibited by DCCD (Garlid et al., 1986; Kakar et al., 1989). The cation exchange pathway in both carriers is non-selective for alkali cations. If the Na^+/Ca^{2+} antiporter contains separate pathways for alkali cations and Ca^{2+}, it follows that Na^+ and Li^+, but not K^+, induce a conformational change that permits Ca^{2+} movement across the protein. K^+ is also transported by the electrophoretic Na^+/Ca^{2+} exchanger of the bovine rod outer segment, which exchanges 1 K^+ and 1 Ca^{2+} for 4 Na^+ (Schnetkamp and Szerencsei, 1991).

2.4.3 Kinetics and regulation of the mitochondrial Na^+/Ca^{2+} antiporter

Studies on mitochondria have indicated a K_m for Ca^{2+} between 2 and 13 μM Ca^{2+} (Crompton et al., 1976; Coll et al., 1982; Hansford and Castro, 1982). In the reconstituted system, we estimate the physiologically relevant K_m to be 0.9 μM in the presence of K^+ (Table 2.1). The effect of K^+, which has also been observed in intact mitochondria (Crompton et al., 1980), is mediated by an increase in the apparent affinity for Ca^{2+}. The K_m for Ca^{2+} is profoundly affected by pH with a profile in general agreement with the one observed in isolated mitochondria (Baysal et al., 1991). As with all such measurements, the K_m values for Ca^{2+} depend strongly on the estimate of free $[Ca^{2+}]$. We note that the Chelator program (Schoenmakers et al., 1992) yields values of free $[Ca^{2+}]$ that are two and three times higher than those estimated by Grynkiewicz et al. (1985) and McCormack et al. (1989), respectively.

The K_m for Na^+ was 8 mM when proteoliposomes contained 10 μM free Ca^{2+}, in agreement with values obtained in isolated mitochondria, which vary between 2.6 and 12 mM (Cox and Matlib, 1993; Hayat and Crompton, 1982; Crompton et al., 1978; Crompton et al., 1976). Cytosolic $[Na^+]$ has been estimated between 5.7 and 10 mM in heart (Lee and Fozzard, 1975; Van Echteld et al., 1991).

The Na^+/Ca^{2+} antiporter is sensitive to a variety of pharmacological agents, including trifluoperazine (Hayat and Crompton, 1985), diltiazem (Vaghy et al., 1982) and amiloride (Jurkowitz et al., 1983). Our studies show that diltiazem and tetraphenylphosphonium cation inhibit the antiporter with potencies similar to those observed in isolated mitochondria (Vaghy et al., 1982; Wingrove and Gunter, 1986).

2.4.4 Regulation of Na^+/Ca^{2+} exchange by BSA

BSA stimulated Na^+/Ca^{2+} exchange, primarily by increasing V_{max}. The effect appears to be due to protein–protein interaction and we suggest that BSA may be mimicking an endogenous regulator. Plasma membrane Na^+/Ca^{2+} antiporters from a variety of tissues contain an intrinsic *exchange inhibitory peptide* (XIP) (Li et al., 1991; Kleiboeker et al., 1992; Chin et al., 1993) which has been suggested to react with another region of the exchanger to produce an inactive conformation or with neighboring lipid to produce an active conformation (Shannon et al., 1994). In view of these results, we are investigating the possibility that BSA is masking an intrinsic autoregulatory inhibitor peptide of the mitochondrial carrier.

2.4.5 The role of the Na^+/Ca^{2+} antiporter in regulating matrix Ca^{2+}

It was proposed some years ago that mitochondrial Ca^{2+} cycling is responsible for the energetic response to signals calling for increased work and, hence, ATP production (Denton and McCormack, 1985; Hansford, 1985). These concepts have now been extended by studies, beginning with Rizzuto et al. (1992), showing that matrix $[Ca^{2+}]$ increases rapidly and *transiently* upon stimulation with agonists coupled to IP3 generation. The phenomenon of rapid Ca^{2+} oscillations has been observed by several laboratories in a variety of tissues (Rizzuto et al., 1994; Hajnóczky et al., 1995; Sparagna et al., 1995; Rutter et al., 1996; Jou et al., 1996). It was also demonstrated that Ca^{2+} oscillations, and not steady-state increases in matrix Ca^{2+}, are responsible for sustained activation of Ca^{2+}-sensitive dehydrogenases (Hajnóczky et al., 1995; Rutter et al., 1996).

These new findings impose new requirements on regulation of the Na^+/Ca^{2+} antiporter, because it must exchange slowly during the Ca^{2+} uptake phase and rapidly

during the ejection phase. Inhibition of Na^+/Ca^{2+} exchange during Ca^{2+} uptake can be understood in the following way: Rapid Ca^{2+} uptake will transiently alkalinize the matrix and lower $\Delta\Psi$. As shown here, both effects will severely inhibit Ca^{2+} efflux on the exchanger, causing increased amplitude of the Ca^{2+} spike. pH and $\Delta\Psi$ will soon be restored toward normal values by uptake of phosphoric acid on its carrier, thereby reactivating the Na^+/Ca^{2+} antiporter as the cytosolic Ca^{2+} spike begins to decay. It is not clear that these effects are sufficient to account for the observed decay phase of matrix Ca^{2+}, which is extremely rapid. Thus, further regulation, such as exists for the plasma membrane Na^+/Ca^{2+} exchanger in the form of XIP, may be required for the support of rapid Ca^{2+} oscillations in mitochondria.

CHAPTER 3

STATE-DEPENDENT INHIBITION OF THE MITOCHONDRIAL K_{ATP} CHANNEL BY GLYBURIDE AND 5-HYDROXYDECANOATE*

3.1 Introduction

During steady-state respiration, K^+ influx into mitochondria is balanced by K^+ efflux on the K^+/H^+ antiporter, and steady-state volume is maintained. Opening the mitochondrial K_{ATP} channel (mitoK_{ATP}) will increase K^+ influx into mitochondria and shift matrix volume to a higher steady state. The energetic costs of this futile cycle are small, between 100 and 150 nmol H^+/mg protein · min at 25°C, and we have concluded that the sole function of mitoK_{ATP} is to regulate matrix volume (Garlid, 1996). It has been suggested that matrix expansion secondary to mitoK_{ATP} opening plays an important role in cell-signaling pathways calling for activation of electron transport and stimulation of fatty acid oxidation (Halestrap, 1994).

A pharmacological role for mitoK_{ATP} in cardiac ischemia seems clearer. During prolonged cardiac ischemia, myocyte ATP levels fall, and the heart does not survive reperfusion. Either pretreatment with K^+ channel openers (KCO) or preconditioning with a brief period of ischemia protects the heart: during subsequent ischemia, ATP loss is reduced, and the heart recovers to nearly normal function upon reperfusion (Grover, 1994). Importantly, cardioprotection by either KCO or preconditioning is blocked by glyburide and 5-HD. This set of agents—KCO,

---

* This material has been published in this or similar form in the *Journal of Biological Chemistry* and is used here with permission of the American Society for Biochemistry and Molecular Biology:

Jabůrek, M., Yarov-Yarovoy, V., Paucek, P., and Garlid, K. D. (1998) State-dependent inhibition of the mitochondrial K_{ATP} channel by glyburide and 5-hydroxydecanoate. *J. Biol. Chem.* **273,** 13578–13582.

glyburide, and 5-HD—identifies the receptor as a K_{ATP} channel, and pharmacological studies indicate that mitoK_{ATP} is the receptor for these effects (Garlid et al., 1997).

A major problem with this hypothesis has been that glyburide appears to be ineffective as a specific inhibitor of K^+ flux in intact, respiring mitochondria (Beavis et al., 1993). Non-specific inhibition of K^+ flux does occur (Beavis et al., 1993); however, we have attributed this effect, which occurs at high doses of glyburide, to low-affinity reactions with key energy-transducing enzymes (Debeer et al., 1974; Somogyi et al., 1995; McGuinness and Cherrington, 1990). The effect of these non-specific actions is to reduce $\Delta\Psi$, the driving force for K^+ uptake, and has nothing to do with mitoK_{ATP}. We have now verified this conclusion in experiments that examine the effects of glyburide on both respiration and respiration-driven cation uptake into mitochondria.

Failure to inhibit mitoK_{ATP} seemed to be a property of both glyburide and 5-HD. We recognized, however, that these drugs had only been studied under conditions when no other ligands of mitoK_{ATP} were present, a condition that never occurs *in vivo*. We now report that glyburide and 5-HD are potent blockers of K^+ flux through mitoK_{ATP} in open states in which Mg^{2+}, ATP, and physiological (GTP) or pharmacological (KCO) openers are present. In intact rat heart mitochondria, $K_{1/2}$ values for glyburide and 5-HD are about 1 μM and 50 μM, respectively. We infer that susceptibility to glyburide and 5-HD requires a ligand-induced conformational change in the mitochondrial sulfonylurea receptor (mitoSUR). These results are consistent with a role for mitoK_{ATP} in cardioprotection (Garlid et al., 1997; Grover, 1997).

3.2 Experimental Procedures

3.2.1 Preparations

Rat liver mitochondria were prepared according to Pedersen et al. (1978), and rat heart mitochondria were prepared by the Glass-Teflon® homogenization procedure according to Matlib et al. (1984). The final mitochondrial pellet was washed and resuspended at 50 mg/ml (liver) or 20 mg/ml (heart) in 0.22 M

mannitol, 0.07 M sucrose, and potassium salts of 5 mM TES and 0.5 mM EGTA. Mitochondria were kept on ice at pH 7.2 during the experiments. MitoK_{ATP} was purified and reconstituted as described previously (Paucek et al., 1996).

3.2.2 Assay of ion transport in intact mitochondria

K^+ or TEA^+ uptake was assayed by following swelling, which accompanies net salt transport, using previously established light-scattering techniques (Beavis et al., 1985; Garlid and Beavis, 1985). Reciprocal absorbance (A^{-1}) at 520 nm varies linearly with matrix volume within three well-defined regions, separated by transitions at 115 and 68 mosmolal (Beavis et al., 1985). β is a dimensionless parameter that normalizes A^{-1} for mitochondrial protein concentration, P (mg/ml),

$$\beta \equiv P/P_s\,(A^{-1} - a), \tag{1}$$

where a is a machine constant (0.25 for our apparatus), and P_s equals 1 mg/ml.

To obtain initial rates ($d\beta/dt$), it is necessary to avoid the sharp discontinuities in the relationship between β and matrix volume. For ion flux measurements, we normally begin measurements at 115 mosmolal, where the outer membrane begins to break (Garlid and Beavis, 1985). This technique is particularly important for light scattering of rat heart mitochondria, which is only weakly sensitive to volume changes in the isosmotic domain. Thus, kinetic curves in 250 mosmolal salts exhibit an artifactual "lag" during salt uptake as volume goes through the first transition point (Garlid and Beavis, 1985).

115 mosmolal assay media contained either K^+ or TEA^+ salts of chloride (45 mM), acetate (25 mM), EGTA (0.1 mM), and TES (5 mM), pH 7.4. Media also contained $MgCl_2$ (0.1 mM), rotenone (5 μg/mg), and cytochrome c (10 μM). Respiratory substrates were either succinate (3 mM) or ascorbate (2.5 mM) plus TMPD (0.25 mM). Mitochondria were assayed at a concentration of 0.1 mg of protein/ml at 25°C.

3.2.3 Measurement of respiration

Respiration was measured with a Yellow Springs oxygen electrode assembly in a hypotonic assay medium identical to the one used for measurement of

K^+ uptake, or in an isotonic assay medium consisting of K^+ salts of chloride (120 mM), succinate (10 mM), phosphate (5 mM), TES (5 mM), and $MgCl_2$ (0.1 mM), pH 7.4, supplemented with rotenone (2 μg/mg of protein). Mitochondria were assayed at 1 mg of protein/ml at 25°C.

3.2.4 Assay of K^+ flux in liposomes

$MitoK_{ATP}$ was partially purified from rat liver mitochondria and reconstituted into proteoliposomes loaded with PBFI according to previously published protocols (Garlid et al., 1996b). *Internal medium* contained TEA^+ salts of sulfate (100 mM), EGTA (1 mM), and HEPES (25 mM), at pH 6.8. 15 μl of stock proteoliposomes (50 mg of phospholipids/ml) were added to 2 ml of *external medium* containing 150 mM KCl and TEA^+ salts of EGTA (1 mM) and HEPES (25 mM), at pH 7.4. Temperature was maintained at 25°C during assays. Electrophoretic K^+ flux was initiated by the addition of 1 μM FCCP to provide charge compensation and measured from changes in PBFI fluorescence (Paucek et al., 1996).

3.2.5 Chemicals and reagents

PBFI was obtained from Molecular Probes; HEPES was obtained from Calbiochem; 5-HD was obtained from RBI; and other drugs and chemicals were obtained from Sigma. The Tris salt of ATP was titrated to pH 7.2 with Tris base.

3.3 Results

3.3.1 Specific and non-specific cation flux in respiring heart mitochondria

Respiring mitochondria take up K^+ by non-specific and specific mechanisms, i.e., *via* diffusion and *via* $mitoK_{ATP}$. We used TEA^+ to distinguish between these two parallel mechanisms, as demonstrated by the four traces in Fig. 3.1A. K^+ flux (*trace a*) is greater than TEA^+ flux (*trace b*). Addition of ATP inhibits K^+ flux (*trace c*) but not TEA^+ flux (*trace d*). These results, which are routinely observed in rat heart (Fig. 3.1) and liver (Beavis et al., 1993)

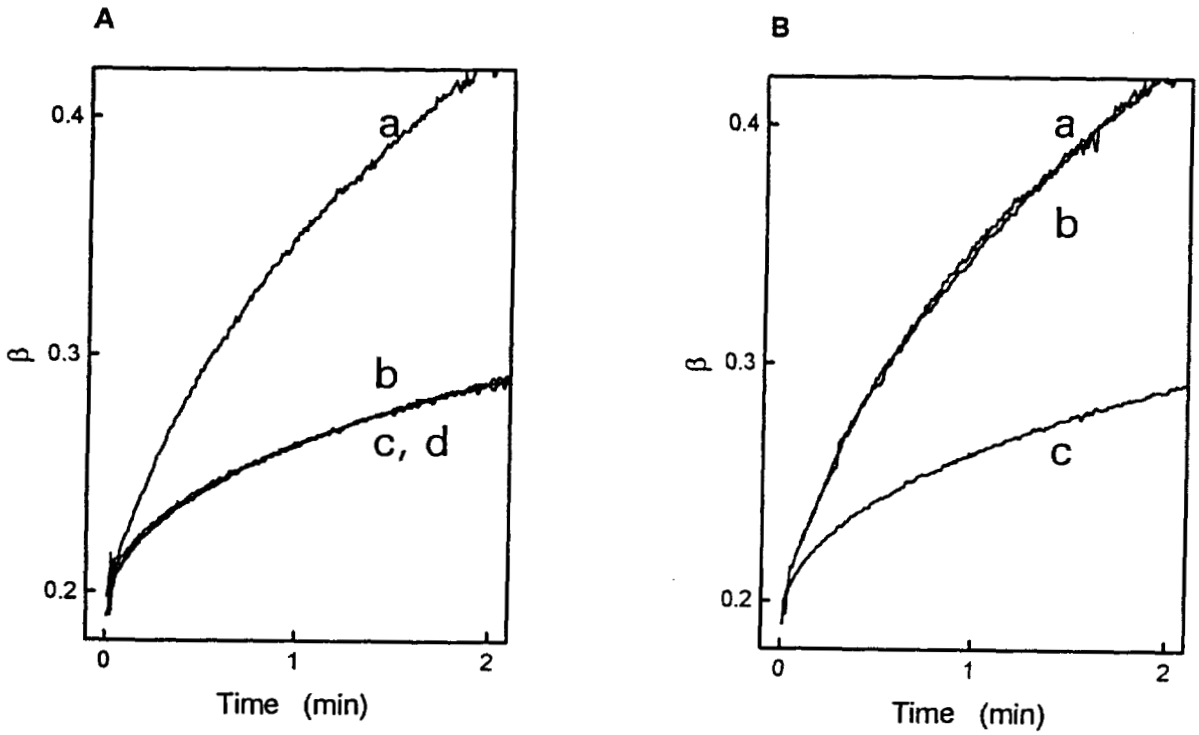

Figure 3.1 ATP-dependent K^+ uptake by mitochondria. Light-scattering traces from rat heart mitochondria respiring on ascorbate/TMPD in K^+ or TEA^+ medium, as described in Section 3.2. **(A)** $MitoK_{ATP}$ is K^+ selective: *trace a*, K^+ influx in the absence of ATP; *trace b*, K^+ influx in the presence of 0.2 mM ATP; *trace c*, TEA^+ influx in the absence of ATP; *trace d*, TEA^+ influx in the presence of 0.2 mM ATP. **(B)** Failure of glyburide to inhibit K^+ influx: *trace a*, K^+ influx in the absence of ATP; *trace b*, K^+ influx in the presence of 10 μM glyburide; *trace c*, K^+ influx in the presence of 0.2 mM ATP.

mitochondria, permit the following conclusions: (a) TEA^+ is transported solely by diffusive leak (Garlid et al., 1989) and is not transported by mitoK_{ATP}; and (b) in the presence of ATP, K^+ is transported solely by diffusion, and its flux equals that of TEA^+. Thus, TEA^+ flux may be used as a control for the component of K^+ flux due to leak.

The traces in Fig. 3.1B show that 10 μM glyburide does not inhibit K^+ flux under these conditions, despite the fact that mitoK_{ATP} is evidently open. 100 μM 5-HD was similarly ineffective (data not shown). To summarize a large body of experiments, these agents did not inhibit K^+ flux at these doses in rat liver or heart mitochondria respiring on succinate or TMPD/ascorbate. This failure of glyburide and 5-HD to inhibit is the central problem addressed by this paper.

3.3.2 Non-specific effects of glyburide on K^+ flux in mitochondria

In massive doses, glyburide does inhibit K^+ flux, as previously reported by us (Beavis et al., 1993) and by Belyaeva et al. (1993) and Szewczyk et al. (1996). We concluded, however, that this effect was secondary to inhibition of respiration (Beavis et al., 1993). Cation uptake into respiring mitochondria is exquisitely sensitive to $\Delta\Psi$ (Garlid et al., 1989), and it is essential to differentiate between non-specific inhibition due to reduced driving force and specific inhibition of mitoK_{ATP}. Accordingly, we examined the effect of glyburide on uncoupled respiration, on respiration-driven K^+ and TEA^+ uptake, and on respiration-driven K^+ uptake in the presence of valinomycin.

The dose–response curves in Fig. 3.2 confirm that glyburide inhibits succinate utilization during uncoupled respiration. In hypotonic assay medium supplemented with acetate and cytochrome c, the $K_{1/2}$ values for inhibition were 5.7 $\pm$ 2.7 μM (n = 3) in rat heart mitochondria and 157 $\pm$ 27 (n = 3) in rat liver mitochondria. In isotonic assay medium without acetate, the $K_{1/2}$ values for inhibition were 5.3 $\pm$ 0.5 μM (n = 2) in rat heart mitochondria and 70 $\pm$ 2 μM (n = 2) in rat liver mitochondria (not shown).

A more direct demonstration of the non-specific effect of glyburide on K^+ uptake was obtained in protocols measuring respiration-dependent cation uptake. As

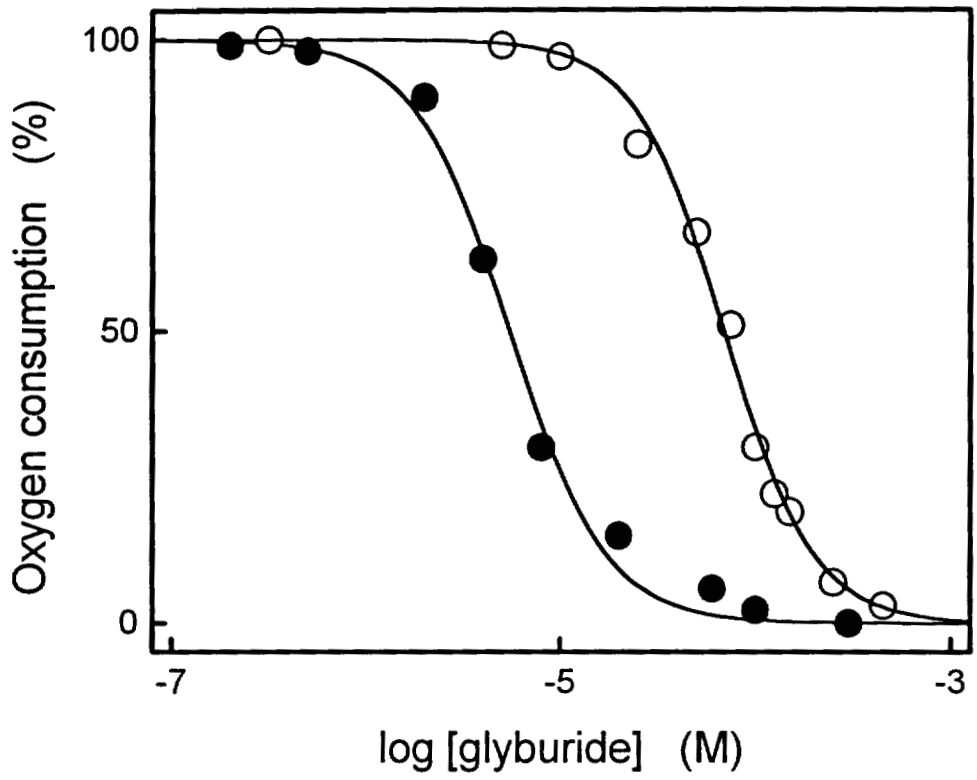

Figure 3.2 Glyburide inhibits respiration of rat liver and rat heart mitochondria. Oxygen consumption of rat heart (•) and rat liver (○) mitochondia (1 mg of protein/ml) respiring on succinate is plotted versus medium glyburide concentration. Mitochondria were uncoupled by addition of 0.25 μM CCCP.

shown in Fig. 3.3, cation uptake was inhibited by glyburide as a function of dose. In rat heart mitochondria (Fig. 3.3A), the $K_{1/2}$ values were 6.4 ± 1.1 μM (n = 3) when succinate was used as substrate and 470 ± 35 μM (n = 2) when ascorbate/TMPD was used as substrate. In rat liver mitochondria (Fig. 3.3B), the $K_{1/2}$ values were 63 ± 13 μM (n = 3) when succinate was used as respiratory substrate and 476 ± 34 μM (n = 3) when ascorbate/TMPD was used as substrate. Inhibition was nonselective—K^+ flux and TEA^+ flux were inhibited at the same doses—and the $K_{1/2}$ values were essentially the same as $K_{1/2}$ values for respiratory inhibition (Fig. 3.2). These findings demonstrate that inhibition of cation flux was due to reduction in driving force and not due to inhibition of mitoK$_{ATP}$. Similar results were obtained for valinomycin-induced swelling in potassium medium (data not shown).

We conclude that the only inhibition mediated by glyburide under these conditions is non-specific, secondary to inhibition of respiration and a reduction of the driving force for cation uptake.

3.3.3 Non-specific effects of 5-HD on K^+ flux in mitochondria

An identical series of experiments was carried out using 5-HD. 5-HD had no effect on K^+ flux under these conditions. In contrast to glyburide, 5-HD did not inhibit uncoupled respiration or cation uptake in either rat liver or heart mitochondria up to 500 μM (data not shown).

3.3.4 Open states in which glyburide and 5-HD specifically inhibit rat heart mitoK$_{ATP}$

Under the conditions of Fig. 3.1, mitoK$_{ATP}$ is open because no inhibitory ligands are present. *In vivo*, mitoK$_{ATP}$ would be opened by pharmacological agents (KCOs), such as diazoxide or cromakalim (Garlid et al., 1996b), or physiological ligands, such as GTP (Paucek et al., 1996). Moreover, ATP and Mg^{2+} would also be present *in vivo*. When mitochondria were studied under these more physiological conditions, glyburide and 5-HD were potent, specific inhibitors of K^+ flux, as illustrated by the traces in Fig. 3.4. Control K^+ flux (*trace a,* Fig. 3.4) was inhibited in the presence of ATP and Mg^{2+} (*trace b,* Fig. 3.4) and

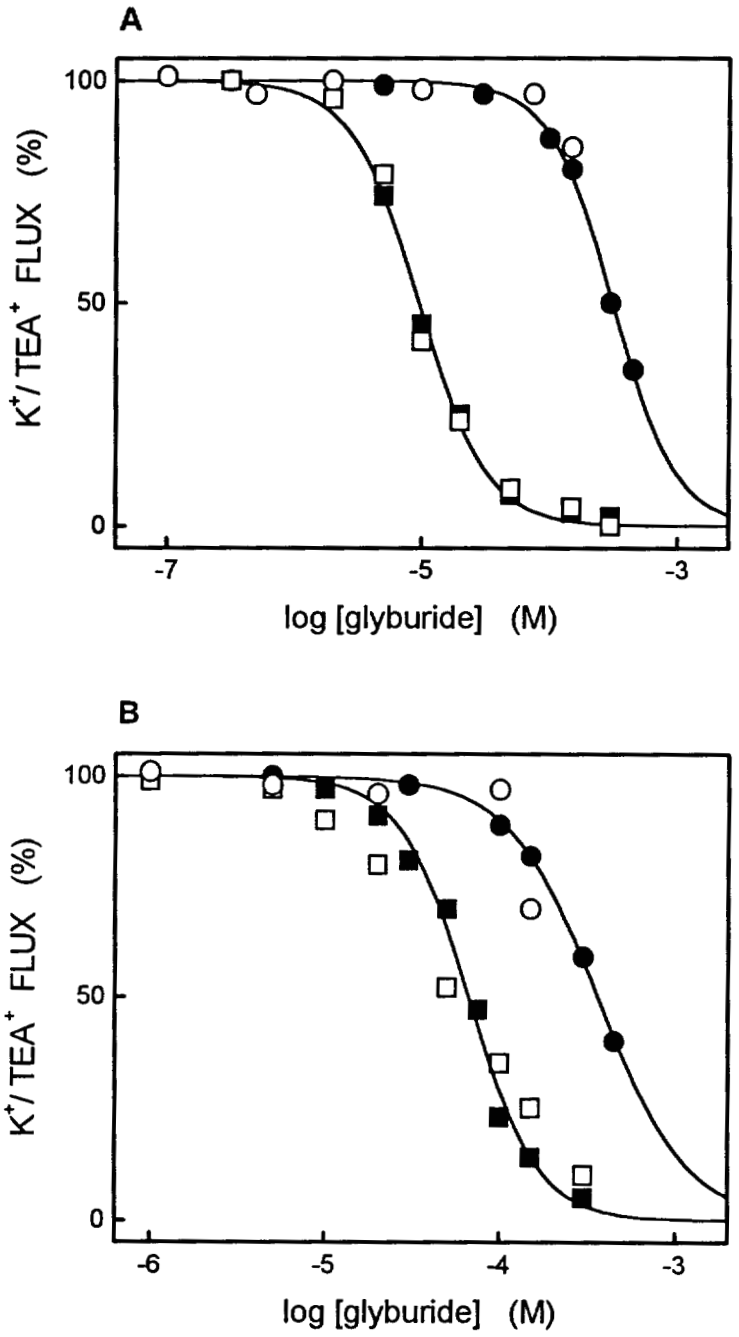

Figure 3.3 Glyburide non-specifically inhibits cation flux into mitochondria. Dose–response curves for glyburide inhibition of respiration-driven mitochondrial swelling in K^+ (○,□) and TEA^+ (•,■) media. K^+ and TEA^+ were inhibited identically in both succinate (□,■) and ascorbate/TMPD (○,•). **(A)** Rat heart mitochondria. **(B)** Rat liver mitochondria.

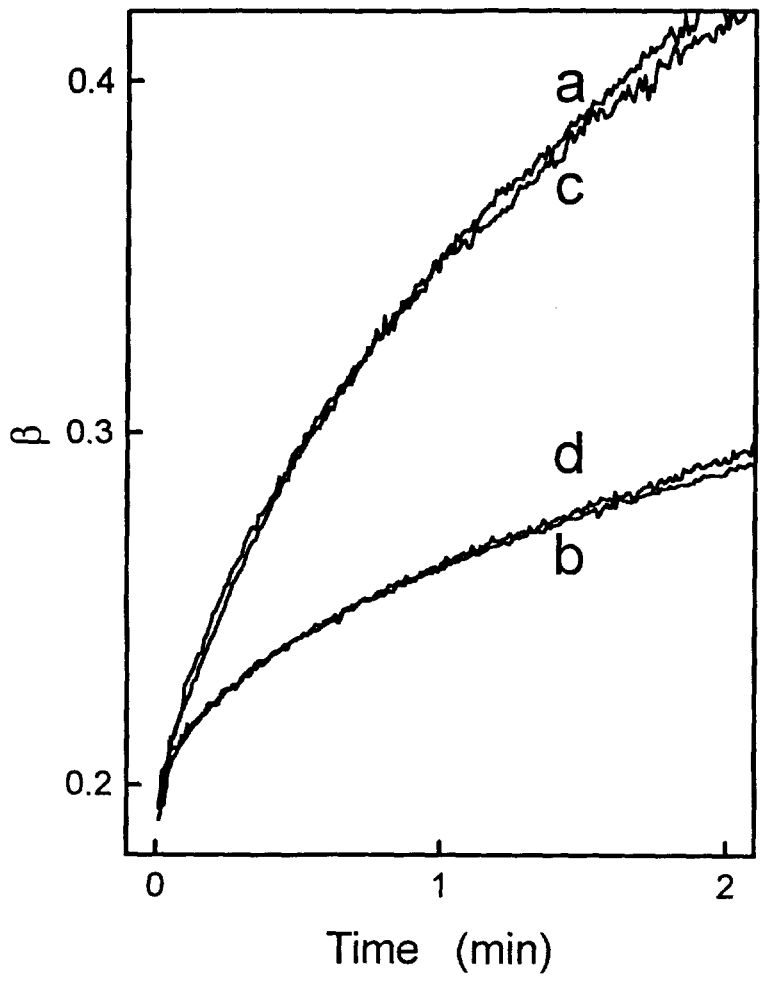

Figure 3.4 Glyburide inhibits the pharmacological open state of mitoK$_{ATP}$. Light-scattering traces from rat heart mitochondria respiring on ascorbate/TMPD in K^+ medium. *Trace a*, K^+ influx in the absence of ATP; *trace b*, K^+ influx in the presence of 0.2 mM ATP; *trace c*, reversal of inhibition by 10 μM diazoxide in the presence of 0.2 mM ATP; *trace d*, re-inhibition by 10 μM glyburide in the presence of 10 μM diazoxide and 0.2 mM ATP.

then restored to control values by diazoxide (*trace c,* Fig. 3.4). This pharmacologically induced K^+ flux was strongly inhibited by 10 μM glyburide to the level associated with ATP inhibition (*trace d,* Fig. 3.4). Note that this glyburide dose had no effect on respiration in ascorbate/TMPD and no effect on TEA^+ flux (see Fig. 3.3A). Therefore, the effect is specific for K^+ flux through mitoK_{ATP}.

Figs. 3.5A and B contain the concentration dependencies of specific glyburide and 5-HD inhibition of K^+ flux. The opening effect of 10 μM diazoxide was reversed by glyburide with $K_{1/2}$ = 1.1 μM (closed circles in Fig. 3.5A), and by 5-HD with $K_{1/2}$ = 45 μM (closed circles in Fig. 3.5B). The opening effect of 50 μM GTP was reversed by glyburide with $K_{1/2}$ = 6 μM (open circles in Fig. 3.5A), and by 5-HD with $K_{1/2}$ = 58 μM (open circles in Fig. 3.5B).

Three additional ligands were required for specific glyburide inhibition of mitoK_{ATP}: Mg^{2+}, ATP, and either GTP or a KCO. No single one of these, nor any combination of two, was effective.

3.3.5 Open states in which glyburide and 5-HD specifically inhibit rat liver mitoK_{ATP}

An identical series of experiments was carried out with rat liver mitochondria, and the results were qualitatively identical to the results with rat heart mitochondria. We were also able to compare the effect of substrates on glyburide potency in liver mitochondria, because the margin of safety for non-specific inhibition during respiration on succinate is much wider in liver than in heart mitochondria (compare Figs. 3.3A and B). The results are summarized in Table 3.1. The $K_{1/2}$ for glyburide inhibition was 3.4 μM when either succinate or ascorbate/TMPD was the respiratory substrate. 5-HD also inhibited cromakalim-opened mitoK_{ATP} in liver mitochondria respiring on either succinate or ascorbate/TMPD with equal potency ($K_{1/2}$ = 73 μM).

3.3.6 Specific inhibition of reconstituted mitoK_{ATP} by glyburide and 5-HD

Table 3.1 also summarizes the effects of glyburide and 5-HD on reconstituted mitoK_{ATP} purified from rat liver mitochondria. In the presence of Mg^{2+},

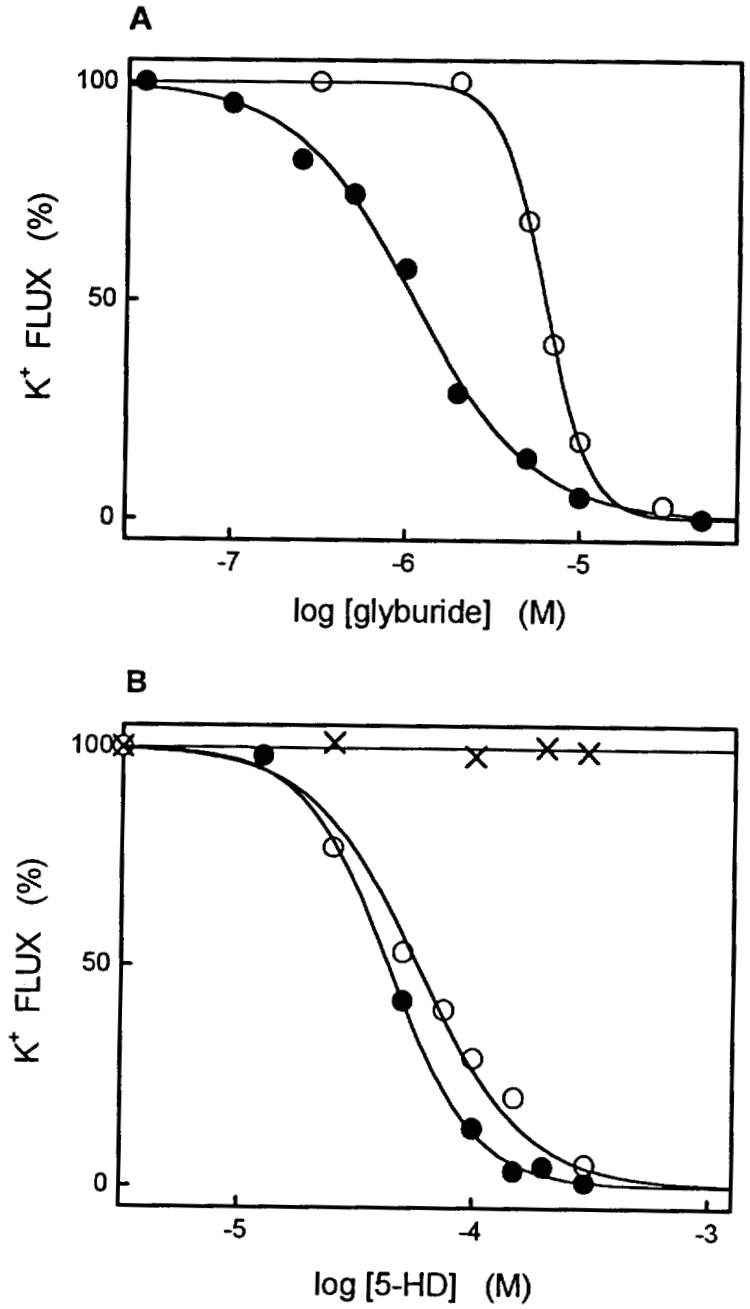

Figure 3.5 Specific inhibition of K^+ influx in rat heart mitochondria by glyburide and 5-HD. K^+ influx, estimated from the light-scattering assay, was measured in mitochondria respiring on ascorbate/TMPD in K^+ medium containing 0.1 mM Mg^{2+}. **(A)** Inhibition by glyburide. Dose–response curves were generated in the presence of a pharmacological opener (•), containing 0.2 mM ATP plus 10 μM diazoxide, and in the presence of a physiological opener (○), containing 0.2 mM ATP plus 50 μM GTP. **(B)** Inhibition by 5-HD. Dose–response curves were generated in the presence of a pharmacological opener (•), containing 0.2 mM ATP plus 10 μM diazoxide, and in the presence of a physiological opener (○), containing 0.2 mM ATP plus 50 μM GTP. In the absence of ATP (X), 5-HD failed to inhibit. Rates of ATP-dependent K^+ influx were determined from light-scattering traces similar to those shown in Fig. 3.4.

TABLE 3.1

Specific Inhibition of MitoK$_{ATP}$ by Glyburide and 5-HD

Experimental Preparation	$K_{1/2}$ - glyburide	$K_{1/2}$ - 5HD
Rat heart mitochondria		
- no ATP	no effect	no effect
- ATP + 10 μM diazoxide	1.1 $\pm$ 0.2 μM	45 $\pm$ 5 μM
- ATP + 50 μM GTP	6 $\pm$ 1 μM	58 $\pm$ 5 μM
Rat liver mitochondria		
- no ATP	no effect	no effect
- ATP + 10 μM cromakalim	3.4 $\pm$ 0.3 μM	73 $\pm$ 3 μM
Reconstituted mitoK$_{ATP}$		
- no ATP	250 $\pm$ 15 nM	no effect
- ATP + 10 μM cromakalim	90 $\pm$ 6 nM	85 $\pm$ 5 μM
- ATP + 20 μM GTP	80 $\pm$ 5 nM	N.D.

The table compares the mean values of half-maximal inhibition ($\pm$ S.D., n = 3) by glyburide and 5-HD in three different preparations. Intact mitochondria were respiring on succinate or ascorbate/TMPD in K^+ medium, and K^+ influx was estimated from the light-scattering assay. Assay media for mitochondria contained varying doses of glyburide or 5-HD and 0.1 mM Mg^{2+}. When added, ATP was 0.2 mM. K^+ flux through reconstituted rat liver mitoK$_{ATP}$ was determined from fluorescence of PBFI. Assay media for liposomes contained varying doses of glyburide or 5-HD and 0.5 mM Mg^{2+}. When added, ATP was 0.5 mM.

ATP, and cromakalim, both glyburide and 5-HD inhibited mitoK$_{ATP}$. Glyburide inhibited with $K_{1/2}$ = 90 nM, and 5-HD inhibited with $K_{1/2}$ = 85 μM. In the absence of ATP, 5-HD had no effect, but glyburide inhibited K^+ flux with $K_{1/2}$ = 250 nM. The latter result is consistent with our previous results on reconstituted mitoK$_{ATP}$ in the presence of Mg^{2+} (Paucek et al., 1992). Glyburide was also a potent inhibitor ($K_{1/2}$ = 80 nM) of the reconstituted mitoK$_{ATP}$ in the presence of Mg^{2+}, ATP, and GTP (Table 3.1).

3.4 Discussion

There is growing evidence for the hypothesis that mitoK$_{ATP}$ is the receptor for the cardioprotective actions of K^+ channel openers and the cardio-damaging actions of glyburide and 5-HD (Garlid et al., 1997; Grover, 1997). Glyburide is a prototypical sulfonylurea inhibitor that acts on all K$_{ATP}$ channels and blocks the protective effects of both KCOs and cardiac preconditioning (Grover et al., 1989; Gross and Auchampach, 1992). 5-HD, which is structurally unrelated to glyburide, has been characterized as an ischemia-selective inhibitor of K$_{ATP}$ channels (McCullough et al., 1991; Schultz et al., 1997). Like glyburide, 5-HD selectively blocks the protective effects of both KCOs (McCullough et al., 1991) and cardiac preconditioning (Auchampach et al., 1992; Hide and Thiemermann, 1996). There have been no previous studies of the effects of 5-HD on mitochondria. The hypothesis that mitoK$_{ATP}$ is involved in cardiac protection has been clouded by the lack of a crucial piece of evidence: a convincing demonstration that glyburide and 5-HD inhibit ATP-dependent K^+ uptake in intact mitochondria.

MitoK$_{ATP}$ activity can readily be elicited in respiring mitochondria, as demonstrated by the data in Fig. 3.1. We showed previously that glyburide inhibits K^+ flux under these conditions; however, inhibition required high doses that inhibit respiration in the presence of succinate, and we concluded that this inhibition was non-specific (Beavis et al., 1993). Belyaeva et al. (1993) concluded to the contrary that mitoK$_{ATP}$ was specifically inhibited by 150 μM glyburide. To resolve this disagreement, we carried out a thorough study of the non-specific effects of

glyburide, as reported in Section 3.3. We found that glyburide is a potent inhibitor of uncoupled respiration in both liver and heart mitochondria when succinate was used as the respiratory substrate (Fig. 3.2). Over the same dose range, glyburide also inhibited diffusive K^+ and TEA^+ fluxes (Fig. 3.3). TEA^+ is transported solely by leak pathways; accordingly, glyburide inhibited K^+ and TEA^+ fluxes by depression of $\Delta\Psi$ and not by inhibition of mitoK_{ATP}. Thus, glyburide inhibition of K^+ flux under these conditions is non-specific.

Respiration using ascorbate/TMPD is relatively insensitive to inhibition by glyburide and 5-HD, and the flux experiments using these substrates (Fig. 3.3) permit a further conclusion: Glyburide and 5-HD, *at any dose*, are completely ineffective under the conditions that have routinely been used to study inhibition of K^+ flux through mitoK_{ATP}, namely respiration on succinate with rotenone.

These findings presented a serious obstacle to studies of the pharmacological regulation of mitoK_{ATP} in mitochondria. We finally recognized, however, that the conditions routinely used—namely, in the absence of other ligands of mitoK_{ATP}—are far from those present *in vivo*. In a living cell, the open channel would never be exposed to glyburide under such conditions. Rather, the channel would be exposed to ATP and Mg^{2+} and then opened by GTP or a K^+ channel opener (Paucek et al., 1996; Garlid et al., 1996b). Indeed, when the *in vitro* experiments were adjusted to mimic these *in vivo* conditions, we found glyburide and 5-HD to be potent, specific blockers of K^+ flux in the open states induced by physiological or pharmacological ligands (Figs. 3.4, 3.5, Table 3.1). We emphasize that three components were required to achieve inhibition by either of these drugs: Mg^{2+}, ATP, and a physiological or pharmacological opener. No single component nor any combination of two components was sufficient. This phenomenon was observed in both heart and liver mitochondria.

Results with reconstituted mitoK_{ATP} qualitatively reflect results in intact mitochondria (Table 3.1). With glyburide, the $K_{1/2}$ value was reduced when studied in the pharmacological open state. With 5-HD, no inhibition was observed in the absence of ATP, but 5-HD inhibited in the pharmacological open state when ATP and a KCO were present.

Some aspects of these findings raise new scientific questions: (i) What renders mitoK$_{ATP}$ susceptible to these inhibitors in one open state and not the other? In view of the fact that K^+ fluxes are identical in all open states, we conclude that the protein must be in a different state. Thus, we infer that Mg^{2+}, ATP, and an opener induce a conformation in mitoSUR that renders it susceptible to glyburide and 5-HD. (ii) Why is glyburide a potent inhibitor of reconstituted mitoK$_{ATP}$ under conditions in which it is ineffective in intact mitochondria? The logical inference is that mitochondria are regulated by a factor that is lost during reconstitution. These hypotheses are under investigation.

In conclusion, our results are consistent with the hypothesis that mitoK$_{ATP}$ is the essential drug receptor involved in ischemic cardioprotection. They also remove the previous deterrent to pharmacological studies on mitoK$_{ATP}$ in intact mitochondria.

CHAPTER 4
THE MECHANISM OF PROTON TRANSPORT MEDIATED BY MITOCHONDRIAL UNCOUPLING PROTEINS*

4.1 Introduction

Uncoupling protein 1 (UCP1) catalyzes electrophoretic proton back-flux across the inner membrane of brown adipose tissue (BAT) mitochondria, dissipating redox energy and providing heat to mammals. Knowledge of the mechanism by which UCP1 catalyzes proton conductance has achieved new importance with the discovery of new and rather ubiquitous mammalian uncoupling proteins 2 (UCP2) and 3 (UCP3), whose transport functions have so far been inferred only by virtue of their strong sequence identities with UCP1 (Boss et al., 1997; Fleury et al., 1997; Gimeno et al., 1997; Vidal-Puig et al., 1997). However, the mechanism of H^+ transport by UCP1 has remained controversial, and this disagreement inevitably raises a barrier to progress in understanding the function of all UCPs. This chapter will therefore focus on the biophysical basis of UCP1-mediated uncoupling.

4.2 The Fatty Acid Protonophore Mechanism of UCP-Mediated H^+ Flux

The fatty acid (FA) protonophore model, diagrammed in Fig. 4.1, was introduced by Skulachev (1991) and Garlid et al. (1996a). Subsequent reports have appeared both in support of the model (Kamp and Hamilton, 1993; Jezek et al., 1996,

---

* This material has been published in this or similar form in *FEBS Letters* and is used here with permission:

Garlid, K. D., Jaburek, M., and Jezek, P. (1998) The mechanism of proton transport mediated by mitochondrial uncoupling proteins. *FEBS Lett.* **438,** 1–14.

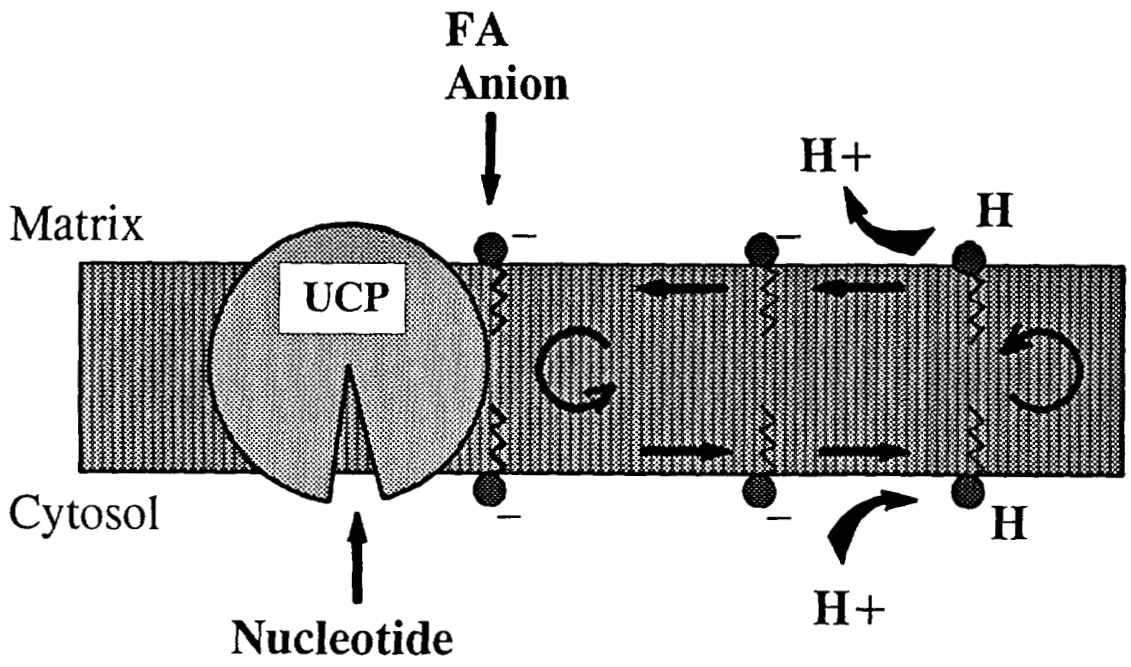

Figure 4.1 The UCP-catalyzed protonophoretic cycle. The diagram shows an inner membrane segment containing UCP1. The complete uncoupling cycle consists of the following steps:

(i) FA anion partitions in the lipid bilayer with its head group at the level of the acyl glycerol linkages and *below* the surface of the phospholipid head groups. This location is shielded from the aqueous phase, which causes the pK_a values of FA in membranes to be 3–4 units higher than their values in solution (Hamilton and Cistola, 1986). There is no significant flux of FA anion, because the bilayer energy barrier is too high (Garlid et al., 1989).

(ii) The FA anion diffuses laterally in the bilayer to reach a subsurface binding site on UCP that is shielded from the bulk aqueous phase (Jezek and Garlid, 1990).

(iii) The energy barrier to FA anion transport is lowered by a weak binding site located about halfway through the UCP transport pathway (Garlid, 1990). The electric field created by redox-linked proton ejection drives the anionic head group to the energy well. The preference of UCP for hydrophobic anions (Jezek and Garlid, 1990) indicates that the hydrophobic FA tail remains in the bilayer during transport.

(iv) The FA carboxylate group moves to the other side of the membrane by a flip-flop mechanism (Kamp and Hamilton, 1992), then diffuses laterally away from the conductance pathway.

(v) The FA is protonated, and the protonated FA rapidly flip-flops again, delivering protons electroneutrally to the mitochondrial matrix and completing the cycle.

1997a,b; Skulachev, 1998) and in opposition to the model (Bienengraeber et al., 1998; Gonzalez-Barroso et al., 1998). As shown in Fig. 4.1, UCP catalyzes flip-flop of the anionic head group of FA from the matrix leaflet to the outer leaflet of the inner membrane. Transport of the anion is driven by the high, inside-negative membrane potential ($\Delta\Psi$). After the carboxyl head group has crossed the membrane, it picks up a proton, and the protonated FA spontaneously and rapidly flip-flops back to the matrix side, where deprotonation completes the cycle. The net result of the cycle is delivery of protons with charge to the matrix. Thus, FA behave as cycling protonophores by virtue of the fact that UCP permits the anionic charge to move across the inner membrane.

A striking feature of this model is that UCP1 does not conduct protons at all. In the FA protonophore model, UCP transports anions, and proton flux occurs independently, by non-ionic diffusion. The physiological substrates of UCP1 are FA, but a wide variety of anions are transported (Jezek and Garlid, 1990) and are hypothesized to share parts of the same pathway used by FA anions, as discussed below.

The FA protonophore hypothesis arose from the discovery that alkylsulfonates are transported by UCP1 and that both the V_{max} and the apparent affinity ($1/K_m$) increase with increasing alkyl chain length (Jezek and Garlid, 1990). This of course was a major clue, because alkylsulfonates and FA are identical, except for their head groups.

The strongest evidence for the hypothesis was provided by a comparison of two close analogues: laurate and undecanesulfonate. Undecanesulfonate anion is transported by UCP1 with K_m very similar to the K_m for laurate-induced H^+ transport. Undecanesulfonate is also a competitive inhibitor of laurate-induced H^+ transport, and both anions are competitive inhibitors of Cl^- transport. These analogues differ in two important respects: undecanesulfonate does not catalyze UCP-mediated H^+ transport and cannot support nonionic diffusion across the bilayer. The latter property is due to the fact that sulfonates are very strong acids. From these facts, we deduced that undecanesulfonate transport reflects a half-cycle of the physiological transport mechanism. Inasmuch as the anionic head group of undecanesulfonate, which

resembles laurate in its kinetic properties, is transported by UCP1, there is no physicochemical basis for excluding the FA anionic head group from this pathway.

We devoted considerable effort to experiments designed to falsify the hypothesis by identifying a FA (or analogue) that induced UCP-mediated H^+ transport but could not deliver protons by non-ionic diffusion. An extensive study turned up no such exceptions (Jezek et al., 1997a,b). Moreover, absence of protonated FA flip-flop was found to correlate with inability to support UCP1-mediated H^+ transport.

4.3 The Fatty Acid Buffering Mechanism of UCP-Mediated H^+ Flux

Protons are directly transported by UCP in the buffering model of uncoupling, introduced by Winkler and Klingenberg (1994). In recognition of the requirement for FA (Jezek et al., 1994; Winkler and Klingenberg, 1994), it was postulated that FA are buffering cofactors that operate in conjunction with resident H^+-conducting amino acids, such as histidines (Winkler and Klingenberg, 1994; Bienengraeber et al., 1998).

The isolated fact that alkylsulfonates are competitive inhibitors of FA-induced H^+ transport via UCP1 (Jezek et al., 1994; Garlid et al., 1996a) is consistent with this model, because alkylsulfonates are strong acids and cannot buffer. On the other hand, the fact that the anionic charge on alkylsulfonates is *transported across the membrane* is a serious problem for the buffering model. As stated above, there is no known physicochemical mechanism that would permit alkylsulfonate anion transport and prohibit fatty acid anion transport.

In an important study, Klingenberg and coworkers (Bienengraeber et al., 1998) showed that mutation of two histidine residues in UCP1 causes loss of H^+ transport. The authors' interpretation of this result was that His^{145} and His^{147} comprise part of the proton-conducting pathway, and they extrapolated their findings to the new UCPs: because UCP2 contains neither histidine, they concluded that it does not conduct H^+ ions. Because UCP3 contains only one histidine, they concluded that it must conduct protons only weakly. It should be pointed out, however, that plant uncoupling protein (PUMP) catalyzes FA-dependent H^+ flux (Jezek et al., 1996)

and contains no histidines in this region (see Table 4.2). Moreover, preliminary evidence from our laboratories shows that UCP2 and UCP3 also catalyze FA-dependent H^+ flux (see Chapter 5).

4.4 Are Fatty Acids Required for UCP Activity?

On the basis of experiments on BAT mitochondria and liposomes, the laboratories of Klingenberg (Winkler and Klingenberg, 1994; Bienengraeber et al., 1998) and Garlid (Jezek et al., 1994; Garlid et al., 1996a) agree that FA are obligatory for UCP1 activity. This requirement has been called into question in a paper showing that a residual, GDP-sensitive uncoupling remains in the presence of BSA, leading the authors to conclude that UCP1 can conduct protons in the absence of FA (Gonzalez-Barroso et al., 1998). It must be stressed that the BSA-insensitive rate is only about 10–15% of the V_{max} in the presence of palmitate. This small degree of uncoupling is incompetent to achieve the physiological role of UCP1, so the relevance of the effect is not clear. It is also not clear that the effect is outside the range of measurement error.**

As commonly prepared, BAT mitochondria also remain partially uncoupled in the absence of nucleotides and the presence of BSA (Nicholls, 1977). This finding also led to the conclusion that mitochondria are uncoupled in the absence of fatty acids. We carried out a series of experiments that raise doubts about this interpretation. When prepared in the usual way, BAT mitochondria exhibited a high GDP-sensitive rate of uncoupling that could not be reversed by BSA, even by lengthy incubations with high BSA concentrations. On the other hand, when BSA (2–5 mg/ml) was added to the BAT tissue *during homogenization*, and maintained in the wash media during isolation, uncoupling was reduced to undetectable levels (Jezek et al., 1994). This hysteresis in the BSA effect emphasizes the fact that BSA cannot

** It is impossible to evaluate whether the BSA-insensitive rates are statistically different from zero. No state 4 respiration rates whatsoever are provided in the paper, nor are statistics provided. Instead, the effects of BSA are compared on the basis of respiratory control ratios from two different populations of mitochondria.

remove all endogenous FA once they are bound to mitochondria. We believe that three factors contribute to BSA hysteresis: (i) when present during tissue homogenization and release of FA from stores, BSA can efficiently adsorb FA; (ii) if BSA is not present at this time, mitochondria become abnormally exposed to FA that bind with high affinity to mitochondria (partition coefficients surpass 10^5, even for those FA that are readily removed by BSA (Anel et al., 1993); (iii) once FA have been allowed to partition into the inner membrane, they will be more difficult to remove—they must leave the inner membrane, cross the intermembrane space to reach the outer membrane, and then leave the outer membrane to bind to BSA. Taking these factors into account, together with the experimental phenomenon of hysteresis, we are skeptical of claims (Nicholls, 1977; Gonzalez-Barroso et al., 1998) that brief exposure to BSA in the assay medium is equivalent to complete FA removal.

The obligatory requirement of UCP1 for FA is most apparent in reconstitution experiments, in which BioBeads are employed to remove detergent and form liposomes (Winkler and Klingenberg, 1994; Garlid et al., 1996a). When *frozen* BAT mitochondria were used, we invariably observed a residual H^+ flux in proteoliposomes. This effect was eliminated by washing the thawed mitochondria with 5 mg/ml BSA prior to extraction (Garlid et al., 1996a). When *fresh* BAT mitochondria were used, Bio-Beads alone apparently removed all of the endogenous FA, because residual proton flux was nearly identical to proton leak in protein-free liposomes (Garlid et al., 1996a). From these experiments, and those of Winkler and Klingenberg (1994), it is clear that UCP1-mediated H^+ flux exhibits an absolute requirement for FA in the reconstitution system.

4.5 The Apparent K_m for Fatty Acid-Induced Uncoupling by UCP1

In the protonophore model, FA diffuse laterally within the membrane until they reach a weak binding site on UCP that serves to concentrate the FA in the conductance pathway (Garlid et al., 1996a). It is evident that FA interaction with UCP takes place in the lipid phase. We reported K_m values based on total FA, $[FA]_{Tot}$. These can readily be converted to K_m values based on membrane FA,

$[FA]_{Memb}$, through recently available partition coefficients in liposomes (Anel et al., 1993):

$$[FA]_{Memb} = \frac{K_p\,[FA]_{Tot}}{\{1 + K_p \cdot V_m/V_a\}} \quad (1)$$

where K_p is the partition coefficient and V_m/V_a is the lipid:aqueous volume ratio, taken to be 0.5×10^{-3} in these experiments (0.5 mg lipid/ml). The corresponding aqueous concentration, $[FA]_{Aq}$, is given by

$$[FA]_{Aq} = [FA]_{Memb}/K_p \quad (2)$$

Table 4.1 contains K_m data for three FA studied in liposomes containing reconstituted UCP1. The aqueous K_m values vary by a factor of 10^3, whereas membrane K_m values are remarkably similar at 10–11 mM, consistent with a common binding site on UCP1.

A recent paper (Gonzalez-Barroso et al., 1998) contains a confused discussion of the apparent affinity of UCP1 for palmitate. The authors compared *aqueous* K_m values with *total* K_m values, despite an explicit statement that the latter values include the partition coefficients (Garlid et al., 1996a). The erroneous conclusion that one set of values is more "physiological" than the other (Gonzalez-Barroso et al., 1998) arises entirely from this inappropriate comparison. When properly compared, the observed K_m values for FA are very similar in all published experiments. Thus, the K_m for palmitate is about 15 nmol/mg protein (80 nM free FA) in intact mitochondria (Gonzalez-Barroso et al., 1998), and about 10 nmol/mg lipid (21 nM free FA) in proteoliposomes (Table 4.1).

4.6 Is UCP1 a FA Channel or Carrier?

A minimum model of anion transport through UCP1 will include binding sites on both surfaces and a central binding site to facilitate transport through the bilayer. In fact, the "surface" binding sites are shielded from the aqueous medium and are therefore subsurface, as is evident from the fact that transport of alkylsulfonates is completely unaffected by hydrophilic sulfonates (Jezek and Garlid, 1990). The

TABLE 4.1

K_m Values for Fatty-Acid-Dependent, UCP-Mediated Proton Flux

Fatty acid	K_p	K_m (Total)	K_m (Memb)	K_m (Aqueous)
Lauric	5×10^3 [a]	8 μM	11.4 mM	2.3 μM
Oleic	3.6×10^5 [b]	5 mM	9.9 mM	28 nM
Palmitic	3.7×10^5 [b]	5.3 μM	10.5 mM	28 nM

K_m (Total) values refer to total FA in the assay, and were determined as by Garlid et al. (1996a). K_m (Memb) and K_m (Aqueous) were determined according to Equations 1 and 2, in the text.

[a] Simpson et al., 1974.

[b] Anel et al., 1993.

remarkable observation that any competitive inhibitor of FA or alkylsulfonate transport is also transported by UCP1 (Jezek and Garlid, 1990) also indicates that the binding sites are subsurface. They are probably located near the phospholipid acylglycerol linkages, which is also the equilibrium position of the FA carboxylic moiety (Hamilton and Cistola, 1986).

The existence of a single energy well located near the center of the membrane was deduced from flux-voltage analysis of non-ohmic Cl^- flux (Garlid, 1990). The FA protonophore model states that Cl^- cannot access the subsurface binding sites for FA, and that Cl^- is transported by virtue of thermal bombardment of the membrane. Thus, Cl^- uses only part of the physiological conductance pathway for FA anions (Garlid et al., 1996a). "Random" access to the central energy well in UCP1 is reflected in the very low affinity for Cl^- ($K_m \simeq 140$ mM) (Garlid et al., 1996a).

The fact that V_{max} values for alkylsulfonates increase with increasing chain length (Jezek and Garlid, 1990) places a further constraint on the transport pathway—the hydrophobic tail of FA must remain at all times in contact with the lipid bilayer core and must turn and reverse direction within this environment as the FA head group moves from one side to the other.

Within these constraints, the transport pathway in UCP1 may be an anion carrier/gated pore (West, 1997) or a hydrophobic, single-file, anion conductance pathway (Garlid, 1990). These alternatives cannot be distinguished at the present time. In either case, polar or cationic residues should reside in the subsurface region to serve as initial binding sites for the FA head group. Movement across the membrane would be facilitated by additional polar or cationic groups that are buried near the center of the membrane.

4.7 Location of the Fatty Acid Transport Pathway in UCPs

Mutations of the seven cysteines in UCP1 to serine had no effect on function or regulation of UCP1 (Murdza-Inglis et al., 1993, 1994); however, Gonzalez-Barroso et al. (1996) found that mutation of Cys^{304} to glycine increased the apparent affinity of UCP1 for palmitate about 2-fold (Gonzalez-Barroso et al., 1998). A 2-fold

change in affinity reflects a very small change in binding energy, about 0.38 kcal/mol. This is most likely a consequence of minor conformational changes in the mutated protein and not due to involvement of Cys^{304} in or near the transport site.

In contrast, mutation of histidines 145 and 147 had a dramatic effect (Bienengraeber et al., 1998). Single mutations reduced laurate-induced H^+ flux by 85–90%, and the double mutation nearly abolished H^+ transport. Loss of function after mutation can be difficult to interpret; however, a very nice aspect of this work was the demonstration that Cl^- transport and nucleotide binding were unaffected by the amino acid substitutions. The mutations were thus specific for H^+ transport (alkylsulfonate transport was not evaluated).

These findings, which strongly imply that H145 and H147 are located in the FA anion translocation pathway, are fully consistent with the FA protonophore model. In view of the preceding discussion, the fact that His mutations block FA transport without affecting Cl^- transport implies that these residues reside near the subsurface binding site for FA at the matrix lipid–water interface. We would predict further that one or both of these histidines protrudes partially into the membrane to be near the level of the acylglycerol lingages.

H145 and H147 are located in the matrix loop between transmembrane helices 3 and 4 of UCP1. As shown in Table 4.2, each of the UCPs contains 3–4 positive charges in the stretch corresponding to H145 and R152 in UCP1. These cationic residues may provide subsurface binding sites for hydrophobic anions and may also serve to anchor this segment to the membrane phospholipid head groups. To provide internal anion binding sites, the loop must protrude to a considerable extent into the membrane. In fact, this is in accord with the folding model of Klingenberg and Nelson (1994) in which a β-loop is inserted between each pair of transmembrane helices. The eight downstream residues between R152 and R161 in UCP1 are rich in hydrogen-bonding side chains (see Table 4.2), and these residues could form the central energy well of the anion conductance pathway.

Unlike the buffering model, which requires dissociable residues for H^+ transport (Bienengraeber et al., 1998), the FA protonophore model merely requires weak binding sites for anions, which may be provided by histidine, lysine, or

TABLE 4.2

Comparison of Amino Acid Sequences Among the Uncoupling Proteins

	135						140					145							150					155					160		
UCP1 134	E	V	V	K	V	R	L	Q	A	Q	S	H	L	H	G	I	-	-	K	P	R	Y	T	G	T	Y	N	A	Y	R	I
UCP2 138	D	V	V	K	V	R	F	Q	A	Q	A	R	A	G	G	G	-	-	R	Y	R	Q	S	-	T	V	N	A	Y	K	T
UCP3 138	D	V	V	K	V	R	F	Q	A	S	I	H	L	G	P	S	R	S	D	R	K	Y	S	G	T	M	D	A	Y	R	T
PUMP 140	D	L	V	K	V	R	L	Q	A	E	G	K	L	P	A	G	V	P	R	-	R	Y	S	G	A	L	N	A	Y	S	T

The sequences given [UCP1 (Aquila et al., 1985), UCP2 (Gimeno et al., 1997), UCP3 (Boss et al., 1997), and PUMP (Laloi et al., 1997)] are found in the matrix loop segment between the third and fourth transmembrane helices. PUMP has been analyzed by MALDI-mass spectroscopy (Jezek et al., unpublished data) and more than 30% of its sequence was found identical to the *St*UCP gene cloned from potato gene library (Laloi et al., 1997) The matched sequences included the matrix loop segment, confirming that FA-translocating PUMP contains no histidines in this region.

arginine. Similarly, the energy well sites may be provided by residues that are cations or H-bond donors. The sequences in Table 4.2 show that all UCPs contain such sites.

Additional experiments with the His mutants may help to distinguish between the two UCP transport models. The buffering model envisions a separate anion transport pathway in UCP1, and hence predicts that alkylsulfonate transport would be unaffected by the mutations. In the FA protonophore model, transport of Cl^- and short-chain sulfonates would be unaffected, because they do not use the surface binding sites. On the other hand, transport of long-chain sulfonates would be abolished by the His mutations, like FA. More precisely, the model predicts that the mutations would increase the K_m to levels exceeding the solubility of both long-chain FA and sulfonates.

4.8 Regulation of UCP1

There is considerable agreement about the nature of nucleotide regulation of UCP1. Purine nucleotide (PN) inhibition of UCP-mediated H^+ flux is purely allosteric, as confirmed by noncompetitive kinetics, by the lack of FA influence on the K_i for PN inhibition (Jezek et al., 1994), and by EPR studies with 5-doxyl-stearic acid (Jezek et al., 1995). These studies show that FA anion transport and nucleotide inhibition are distinct features of UCP involving two distinct binding domains.

The nucleotide binding pocket in UCP1 has been mapped by photoaffinity labeling and site-directed mutagenesis and is very extensive. Nucleoside phosphates interact with the three arginines that are located on helices 2, 4, and 6 (Modriansky et al., 1997), and the sugar base reacts with the matrix segment D233–E261 that connects helices 5 and 6. The latter interaction is presumed to confer nucleotide specificity (Winkler et al., 1997).

Nucleotide binding and inhibition take place in three steps (Modriansky et al., 1997). First, binding of the sugar base moiety and the binding of one β-phosphate group result in a loose-binding conformation of UCP1. In the second step, protonation of E190 makes R83 available for binding to the second charge on the β-

phosphate of diphosphates and the γ-phosphate of triphosphates. An unidentified histidine is thought to bind to the second charge on the γ-phosphate of triphosphates (Winkler et al., 1997). These events, which cause tight binding of PNs (Huang and Klingenberg, 1996), have been shown to be insufficient for inhibition (Modriansky et al., 1997). To reach the inhibited state, α-phosphate must bind to R276. This final step induces a conformational change that modifies the anion transport pathway, causing inhibition of transport (Modriansky et al., 1997).

It is noteworthy that the three phosphate binding arginines are conserved in UCP2, UCP3, and PUMP, suggesting that these proteins are also regulated by nucleotides. On the other hand, there are strong differences in the nucleotide-binding matrix loop between the fifth and sixth transmembrane domains, suggesting that nucleotide specifities may differ.

4.9 Summary

Two competing hypotheses describe the mechanism of uncoupling by UCP—the FA protonophore model and the H^+ buffering model. Both models employ the experimental observation that FA are obligatory for UCP1-mediated uncoupling. It may be possible to discriminate between the models when the transport functions of UCP1 and UCP2 are known. The FA protonophore model predicts that they will catalyze FA-dependent proton flux, whereas the buffering model predicts that they will not.

CHAPTER 5
TRANSPORT PROPERTIES AND REGULATION OF MITOCHONDRIAL UNCOUPLING PROTEINS 2 AND 3*

5.1 Introduction

Uncoupling protein 1 (UCP2) of brown adipose tissue (BAT) mitochondria occupies a special place in bioenergetics, because it is the exception that proves the rule of Mitchell's elegant chemiosmotic theory (Mitchell, 1961)—a protein designed to short circuit the redox proton pumps in order to generate heat and dissipate energy. UCP1 was identified from functional studies on BAT mitochondria (Nicholls and Locke, 1984) and was one of the first membrane proteins to be sequenced (Aquila et al., 1985).

For many years it was thought that UCP was expressed solely in mammalian BAT; however, it now turns out that Nature has engineered at least five uncoupling proteins. In 1995, a plant uncoupling protein was discovered and later sequenced (Vercesi et al., 1995; Laloi et al., 1997), and two years later, UCP2 and UCP3 were identified (Boss et al., 1997; Fleury et al., 1997; Gimeno et al., 1997; Vidal-Puig et al., 1997). UCP4 was recently described as a brain-specific UCP (Mao et al., 1999). UCP2 maps to regions of human chromosome 11 and mouse chromosome 7 that have been linked to hyperinsulinemia and obesity, and it is hypothesized that UCP2 is the peripheral target for energy dissipation in the regulation of body weight. UCP2 is

---

* This material has been published in this or similar form in the *Journal of Biological Chemistry* and is used here with permission of the American Society for Biochemistry and Molecular Biology:

Jabůrek, M., Vařecha, M., Gimeno, R. E., Dembski, M., Ježek, Zhang, M., Burn, P., Tartaglia, L. A., and Garlid, K. D. (1999) Transport function and regulation of mitochondrial uncoupling proteins 2 and 3. *J. Biol. Chem.* **273,** in press.

ubiquitously expressed in mammalian tissues, whereas UCP3 is expressed primarily in glycolytic skeletal muscle in humans and may account for the thermogenic effect of thyroid hormone (Gong et al., 1997). These aspects of this rapidly emerging area of research have been nicely reviewed by Boss et al. (1998).

Virtually nothing is known about the transport functions of UCP2 and UCP3, and their putative physiological functions have been deduced primarily from their striking sequence identities with UCP1 (Boss et al., 1998). To address this problem, we expressed human UCP2 and UCP3 in *E. coli*, where they accumulated in inclusion bodies. Following detergent extraction, we reconstituted the proteins into liposomes and measured H^+ and K^+ fluxes. Purified UCP2 and UCP3 both catalyzed electrophoretic flux of protons and alkylsulfonates, and proton flux exhibited an obligatory requirement for fatty acids. We also found that FA-dependent proton transport by UCP2 and UCP3 was inhibited by purine nucleotides, albeit with lower apparent affinities for nucleotides than those observed with UCP1. From these results, we conclude that UCP2 and UCP3 are functional uncoupling proteins and that their biophysical properties are consistent with a physiological role in energy dissipation.

5.2 Experimental Procedures

5.2.1 Expression of UCPs in *Saccharomyces cerevisiae*

UCPs were expressed in yeast as described previously (Murdza-Inglis et al., 1991). Briefly, the *Sac*I/*Sph*I fragments from the M13mp19 plasmid containing wild-type rat UCP1 cDNA were subcloned into a *Sac*I/*Sph*I-cut pCGS110 *E. coli/S. cerevisiae* shuttle vector. The *S. cerevisiae* strain JB516 (MATa, ura3, ade1, leu2, his4, gal^+) was transformed with the shuttle vector construct and plated on uracil-lacking selective plates. The resulting yeast transformants were grown at 30°C in selective medium, and overexpression of UCP1 was induced by addition of 0.2% galactose (Murdza-Inglis et al., 1991). Similar protocols were followed for UCP2 and UCP3.

5.2.2 Expression of UCP2 and UCP3 in *E. coli*

Human UCP2 and human UCP3 open reading frames were amplified by PCR and inserted into the *Nde*I and *Not*I sites of the pET21a vector (Novagen). From DNA sequencing, the constructs are predicted to encode proteins with an amino acid sequence identical to the wild-type UCP2 or UCP3 proteins (Boss et al., 1997; Fleury et al., 1997; Gimeno et al., 1997; Vidal-Puig et al., 1997). Plasmids were transformed into the bacterial strain BL21 (Novagen). Transformed cells were grown at 30°C to A_{600} = 0.6 and then induced with 1 mM IPTG at 30°C for 6 h. Cells from a 700-ml culture were lysed in a French press in 20 ml of lysis buffer (10 mM Tris, pH 7, 1 mM EDTA, 1 mM DTT). The lysate was centrifuged at 27,000 × *g* for 15 min, and the pellet was resuspended in 20 ml of lysis buffer and centrifuged at 1000 × *g* for 3 min. 1-ml aliquots of the supernatant were centrifuged at 14,000 × *g* for 15 min in a microcentrifuge, and the resulting pelleted inclusion bodies were stored frozen at -70°C.

5.2.3 Extraction of UCP2 and UCP3 from inclusion bodies

We modified published protocols (Fiermonte et al., 1993; Schroers et al., 1998) for solubilization of *E. coli* inclusion bodies. The pelleted inclusion bodies (~2 mg of protein) were suspended and washed three times in wash buffer [tetraethylammonium (TEA^+) salts of 0.15 M phosphate, 25 mM EDTA, 1 mM ATP, and 1 mM DTT, pH 7.8]. The final pellet was solubilized in 0.4 ml of 50 mM TEA–TES, pH 7.2, containing 1.5% sodium lauroylsarcosinate (SLS). The extract was supplemented with 10 mg/ml asolectin and 3% octylPOE (C_8E_5 detergent), then dialyzed for 15 h against 3 × 400 ml of extraction buffer (TEA^+ salts of 50 mM TES and 1 mM EDTA, pH 7.2) to remove SLS. In the first two dialysis periods (1 and 13 h), the extraction buffer was supplemented with 1 mM DTT and 0.03% sodium azide. These were removed from the final dialysis (1 h). Aliquots of the dialyzed extract, containing about 0.2 mg of protein, were stored at -20°C.

5.2.4 Reconstitution of uncoupling proteins into liposomes

Reconstitutions were carried out as previously described for UCP1 (Garlid et al., 1995). Egg yolk phosphatidylcholine (UCP1) or soybean phospholipids (UCP2 and UCP3) were supplemented with 2 mg/ml of cardiolipin, dried, and stored under nitrogen. Internal medium (TEA^+ salts of 30 mM TES, 80 mM SO_4, and 1 mM EDTA, pH 7.2) was added to give a final concentration of 40 mg of phospholipid/ml of proteoliposome stock. The mixture was vortexed and sonicated to clarity in a bath sonicator; detergent (10% C_8E_5), protein extract, and fluorescent probe were added. The final mixture (1.1 ml) was applied onto 2-ml of Bio-Bead SM-2 (Bio-Rad) column to remove the detergent. After incubation for 2 h, the column was centrifuged, and the resulting proteoliposomes were applied onto a new 2-ml Bio-Bead column, incubated for 30 min, and centrifuged. The formed vesicles (1 ml) were passed through a Sephadex G-25-300 column to remove external probe.

5.2.5 Fluorescence measurements of ion fluxes

Ion flux in proteoliposomes was measured using ion-specific fluorescent probes and an SLM Aminco 8000C spectrofluorometer. Measurements of H^+ fluxes were obtained from changes in SPQ fluorescence due to quenching by the anion of TES buffer (Orosz and Garlid, 1993). Measurements of K^+ fluxes, reflecting the movement of ionic charge across the membrane, were obtained from changes in PBFI fluorescence (Jezek et al., 1990a; Garlid et al., 1995). Internal and external media contained K^+ or TEA^+ salts of 30 mM TES buffer, 80 mM SO_4, and 1 mM EDTA, pH 7.2. TEA^+ internal medium and K^+ external medium were used for the experiments of Figs. 5.3 and 5.4 to measure electrophoretic H^+ efflux, while these cations were reversed for the experiments of Figs. 5.5 and 4.1 to measure nucleotide inhibition. Each proteoliposome preparation was individually calibrated for fluorescent probe response, and its internal volume was estimated from the volume of distribution of the fluorescent probe (Garlid et al., 1995).

5.2.6 Chemicals and reagents

PBFI and SPQ were purchased from Molecular Probes, Inc. Undecanesulfonate was purchased from Research Plus, Inc. Asolectin (45% L-α-phosphatidylcholine) was purchased from Avanti Polar-Lipids, Inc. Sulfuric acid was purchased from Fisher. Materials for UCP1 exression in yeast were from sources listed previously (Orosz and Garlid, 1993). All other chemicals were from Sigma. Purine nucleotides were adjusted to pH 7.2 with Tris base.

5.3 Results

5.3.1 Isolation and reconstitution of UCPs expressed in *E. coli*

The development of a functional yeast expression system allowed us to investigate the structure--function relationship of UCP1 using site-directed mutagenesis (Murdza-Inglis et al., 1994; Modriansky et al., 1997). Similarly, we attempted to use yeast expression for human UCP2 and UCP3 in order to study their function. Compared to UCP1, however, UCP2 and UCP3 expressed in lower quantities in yeast and were difficult to purify. Expression in *E. coli* yielded high amounts of UCP2 and UCP3, which accumulated in inclusion bodies. However, when the proteins were extracted using SLS detergent and reconstituted into liposomes, the proteins were found to be inactive (not shown). We obtained functionally active protein by supplementing the extract with asolectin and octylPOE and subjecting the extract to prolonged dialysis against SLS-free buffer. The dialysis may have reduced the SLS concentration, but this was not assayed. The proteoliposomes typically had an internal volume of 1.2 μl/mg lipid and contained 3–5 μg protein/mg lipid. To estimate the purity of reconstituted UCP2 and UCP3, the proteoliposomes were delipidated and subjected to SDS-PAGE with the results shown in Fig. 5.1.

5.3.2 Undecanesulfonate and fatty-acids induce electrophoretic fluxes in liposomes reconstituted with UCP2 and UCP3

The representative ion flux traces in Fig. 5.2 show that UCP2 catalyzes FA-dependent, electrophoretic proton flux. The traces in Fig. 5.2A follow H^+ movement across the membrane. It can be seen that FAs induce a strong H^+ flux

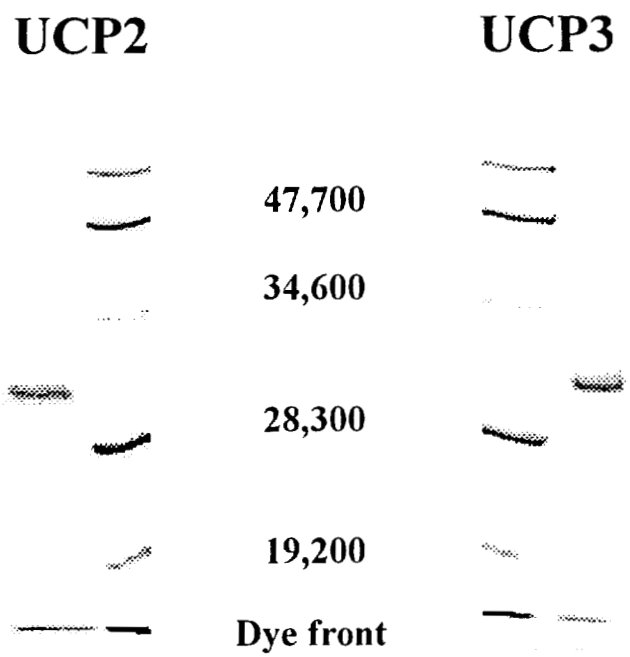

Figure 5.1 Purified, reconstituted UCP2 and UCP3. Coomassie-Blue-stained SDS-PAGE gels from proteoliposomes containing UCP2 and UCP3. The proteins were expressed in *E. coli*, extracted from inclusion bodies, and reconstituted into liposomes. 10 μg of delipidated proteins were loaded on each lane of the gel parallel to M_r standards.

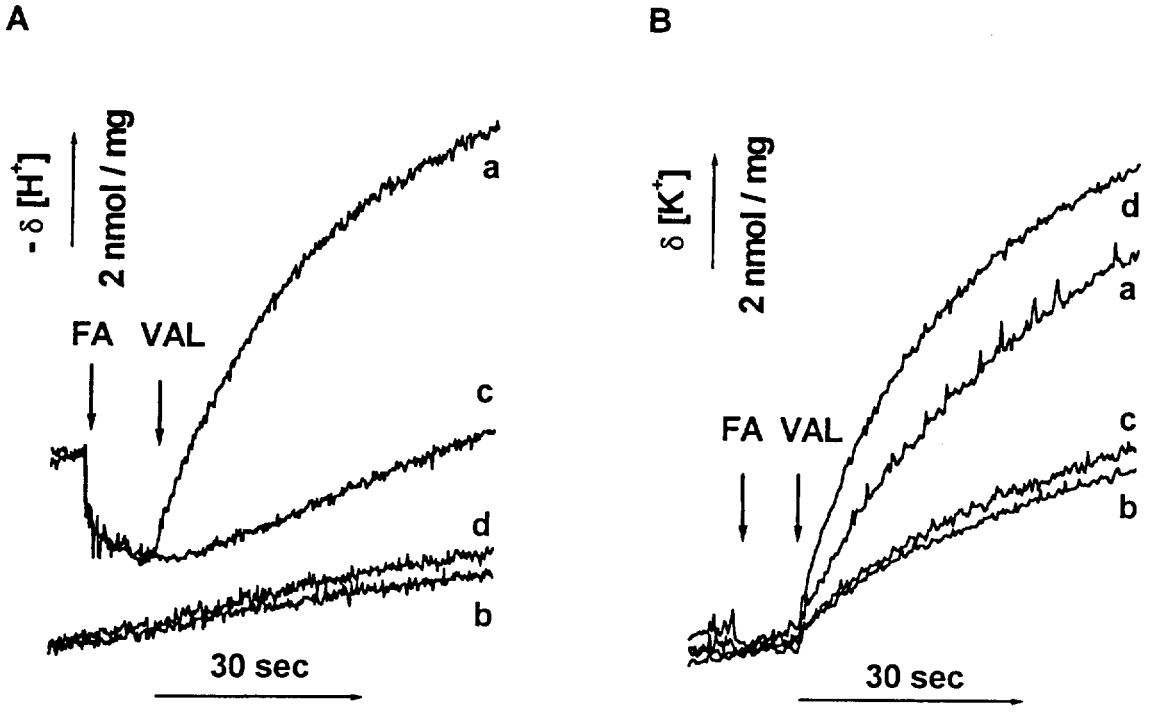

Figure 5.2 FA-dependent proton and undecanesulfonate transport via UCP2. **(A)** Traces follow changes in intraliposomal acid ($\delta[H^+]$), which were determined from quenching of SPQ fluorescence by the anion of TES buffer (Orosz and Garlid, 1993). *Trace a*, 40 μM palmitate and 0.1 μM valinomycin were added sequentially. *Trace b*, valinomycin was added without FA. *Trace c*, liposomes *without* UCP2; FA and valinomycin were added sequentially. *Trace d*, 40 μM undecanesulfonate and valinomycin were added sequentially. (Note that *traces a* and *c* are offset for clarity.) **(B)** Traces follow changes in total intraliposomal K^+ ($\delta[K^+]$), which were measured using PBFI fluorescence. Assay conditions and additions for each trace were identical to those described for **A**. Except for *trace c*, liposomes contained UCP2. H^+ efflux was driven by an inward K^+ gradient. These data are representative of more than 20 experiments on 10 different UCP2 reconstitutions.

(Fig. 5.2A, *trace a*) that is absent in the absence of FA (*trace b)* and does not occur in liposomes without protein (*trace c).* Undecanesulfonate, an analogue of laurate, does not support H^+ transport (*trace d*). The traces in Fig. 5.2B follow K^+ movement. It can be seen that charge movement across the membrane exactly matches FA-induced H^+ flux (*trace a*), confirming that the H^+ flux is electrophoretic. Undecanesulfonate induced a strong K^+ flux (*trace d)*, demonstrating that the sulfonate anion is transported by UCP2.

A rapid intraliposomal acidification ensues upon the addition of FA (Fig. 5.2A, *traces a* and *c*). This is due to flip-flop of the protonated FA and acid-base equilibration (Garlid et al., 1996a). It is an electroneutral process, as evidenced by the lack of a corresponding K^+ jump upon the addition of FA (Fig. 5.2B).

The representative ion flux traces in Fig. 5.3 were obtained with UCP3, and they are qualitatively identical in every detail with those of UCP2. These results are highly reproducible and are representative of more than 20 assays from 10 or more preparations of each UCP.

Preliminary results from a kinetic study of UCP2 and UCP3 (not shown) indicate that there may be quantitative differences in FA preference among the UCPs. The K_m values for FA are similar among all three UCPs (10–20 nmol of FA/mg of lipid), and the V_{max} values for palmitate are also similar (10–30 μmol/mg · min). However, the V_{max} for laurate is much lower in UCP2 than in UCP1 or UCP3, indicating a preference for long-chain FAs by UCP2.

5.3.3 Inhibition of UCPs by purine nucleotides

A second essential property of UCP1 is its inhibition of fatty acid-induced proton fluxes by purine nucleotides. To our surprise, we found striking differences in nucleotide sensitivity among the UCPs, as evidenced by the data in Fig. 5.4 comparing inhibition by 1 mM GDP, ATP, and GTP. To date, we have identified ATP as the most potent inhibitor of UCP2 (Fig. 5.5A) and UCP3 (Fig. 5.5B), although the apparent K_i values for ATP inhibition are considerably lower than that for UCP1 (Table 5.1). UCP2 and UCP3 are notably less sensitive to GDP or GTP, which are potent inhibitors of UCP1.

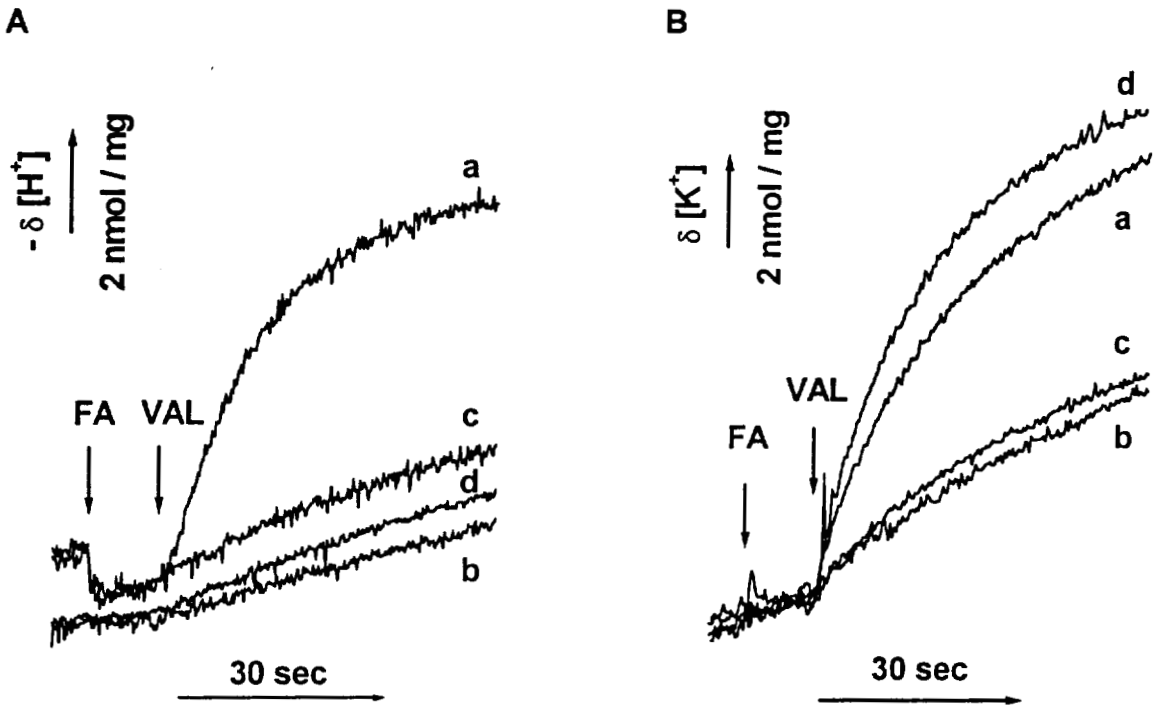

Figure 5.3 FA-dependent proton and undecanesulfonate transport via UCP3. The traces shown were obtained under assay conditions identical with those described in Fig. 5.2 for UCP2, except that 40 μM laurate was used instead of palmitate. **(A)** Traces follow changes in intraliposomal acid ($\delta[H^+]$). **(B)** Traces follow changes in total intraliposomal K^+ ($\delta[K^+]$). Except for *trace c*, liposomes contained UCP3. These data are representative of more than 20 experiments on 10 different UCP3 reconstitutions.

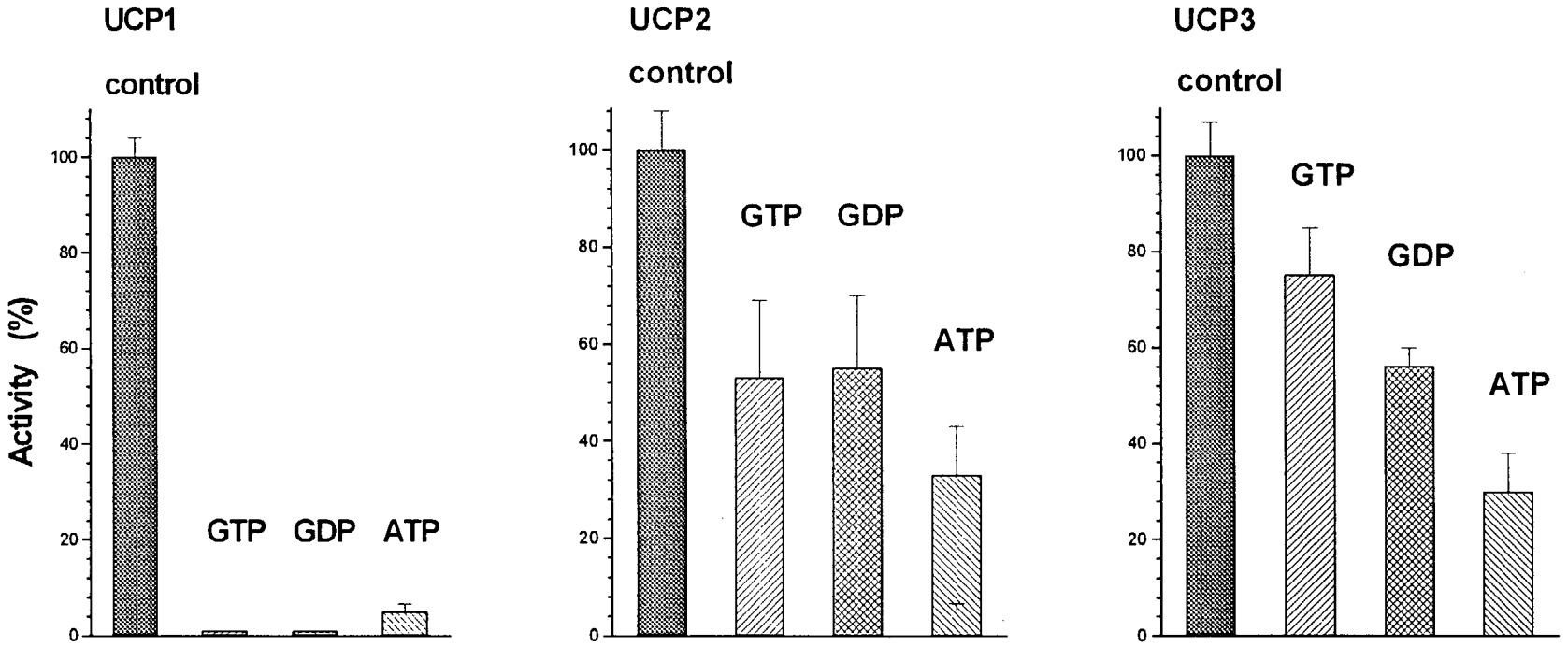

Figure 5.4 Sensitivities to nucleotide inhibition of UCP1, UCP2 and UCP3. The *bars* represent residual, FA-induced proton flux in the presence of 1 mM nucleotide. 100% inhibition was estimated by extrapolation of inhibitor concentration plots obtained with ATP, as in Fig. 5.5. 50 μM laurate was used for UCP1 and UCP3, and 50 μM palmitate was used for UCP2. H^+ influx was driven by an outward K^+ gradient in the presence of 30 nM valinomycin. Assay pH was 7.2.

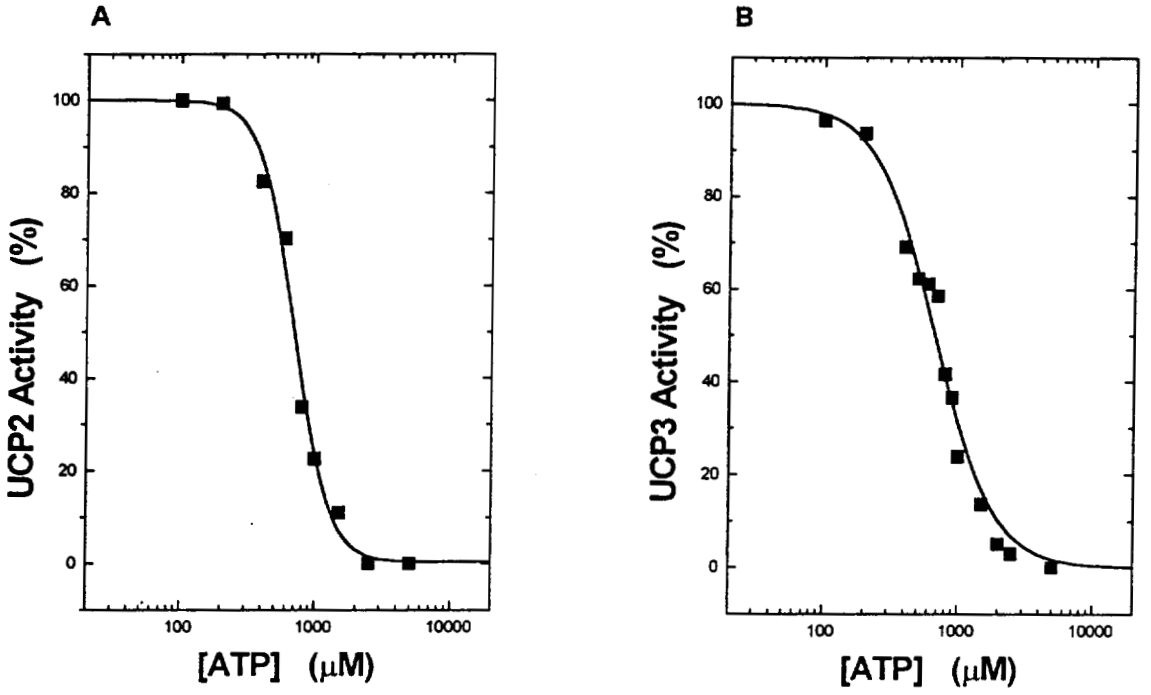

Figure 5.5 Concentration-dependence of nucleotide inhibition of UCP2 and UCP3. **(A)** ATP inhibition of UCP2-mediated H^+ influx, in the presence of 50 μM palmitate, pH 7.2. The K_i for ATP inhibition is 710 μM. **(B)** ATP inhibition of UCP3-mediated H^+ influx, in the presence of 50 μM laurate, pH 7.2. The K_i for ATP inhibition is 670 μM. The curves are representative of three independent preparations of UCP2 and UCP3.

TABLE 5.1

K_i Values for Nucleotide Inhibition of the Uncoupling Proteins

Nucleotide	UCP1	UCP2	UCP3
ATP	125 ± 5 μM	760 ± 50 μM	650 ± 36 μM
GTP	20 ± 3 μM	~1 mM	~1.7 mM
GDP	17 ± 2 μM	~1.2 mM	~1 mM

Experiments were carried out under identical assay conditions at pH 7.2 as described in the legend to Fig. 5.4.

5.4 Discussion

Electrophoretic proton flux is the *sine qua non* of an uncoupling function. The data in Figs. 5.3 and 5.4 show that UCP2 and UCP3 meet this primary criterion, thereby establishing them as uncoupling proteins in function as well as in name. Indeed, the transport properties of UCP2 and UCP3 are qualitatively *identical* with those of UCP1 with respect to transport of protons and alkylsulfonates (Jezek et al., 1994; Garlid et al., 1996a).

The finding that FAs are obligatory for proton flux mediated by UCP2 and UCP3, just as they are for UCP1 (Strieleman et al., 1985; Jezek et al., 1994) has important implications for the biophysical transport mechanism of UCPs, an issue that is not entirely resolved. We favor the FA protonophore model, shown in Fig. 4.1, in which UCPs contain a transport pathway for the anionic head groups of FAs and alkylsulfonates. The head group is driven from one membrane leaflet to the other by the electric field generated by electron transport. When the FA carboxylate reaches one side, it picks up a proton and rapidly flip-flops back to release the proton to the other side. The UCPs thus catalyze a protonophoretic cycle, leading to uncoupling of oxidative phosphorylation (Garlid et al., 1996a).

An alternative model by Klingenberg and coworkers (Klingenberg and Huang, 1999) proposes that UCP1 transports protons, that the transport pathway contains histidines, and that FAs function as non-stoichiometric cofactors to buffer intra-channel protons. In a major advance, Bienegraeber et al., (1998) demonstrated that substitution of two histidines (H145Q, H147N) in UCP1 caused selective loss of H^+ transport and concluded that these histidines constitute part of the proton conducting pathway. The authors go on to predict that UCP2, which contains neither histidine, will not conduct protons and that UCP3, which contains only one histidine, will conduct protons only weakly. In our view, the mutagenesis results are equally consistent with the FA protonophore model and suggest that the histidines in UCP1 form part of the surface binding site for the FA anion transport pathway. UCP2 and UCP3 possess ample basic residues in this region to fulfill this role (Garlid et al., 1998). Our interpretation therefore predicts that UCP2 and UCP3 will catalyze FA-

dependent proton transport, and our results thus provide independent support for the FA protonophore model (Fig. 4.1).

Transport of the head group of undecanesulfonate also supports the FA protonophore model. Undecanesulfonate is a close analogue of laurate and is a competitive inhibitor of laurate-induced H^+ transport in UCP1 (Jezek et al., 1994). The sulfonate group is transported across the membrane by all three UCPs; however, alkylsulfonates do not support H^+ transport. The reason for this failure is that sulfonates are very strong acids and, consequently, cannot deliver protons by electroneutral flip-flop across the bilayer (Garlid et al., 1996a). Thus, alkylsulfonates share the anion transport pathway in UCP1 with FAs, but they cannot complete the protonophoretic cycle. The fact that the anionic head group of alkylsulfonates is *transported across the membrane* is a serious problem for the buffering model, because there is no known physicochemical mechanism that would permit alkylsulfonate anion transport and prohibit FA anion transport.

Inhibition by purine nucleotides is also an essential property of UCP1. Since FAs have no effect on the K_i for nucleotide inhibition (Jezek et al., 1994), it is generally agreed that transport and inhibition take place on distinct domains. The nucleotide binding domain in UCP1 is very extensive and reasonably well characterized. The sugar-base moiety reacts with three residues located on the matrix segment that connects helices 5 and 6, an interaction that may confer selectivity among nucleotides (Winkler and Klingenberg, 1992; Mayinger and Klingenberg, 1992; Huang and Klingenberg, 1995). A glutamate, Glu^{190}, in the fourth transmembrane helix is the pH sensor for nucleotide binding (Winkler et al., 1997). Three arginines, located in the transmembrane helices 2, 4, and 6, are required for nucleotide inhibition and have been shown to bind the nucleoside phosphates (Modriansky et al., 1997). Site-directed mutagenesis studies have led to a three-stage binding-conformational change model for nucleotide binding and inhibition in UCP1 (Modriansky et al., 1997).

It is noteworthy that the seven residues involved in nucleotide inhibition are largely conserved in UCP2, UCP3, and plant uncoupling protein, suggesting not only that these proteins would be regulated by nucleotides but also that regulation would be

similar among the UCPs. Surprisingly, there are striking differences in nucleotide sensitivity among the UCPs, with UCP2 and UCP3 being only weakly sensitive to GDP, for example (Fig. 5.4, Table 5.1). Similarly, plant uncoupling protein was also only weakly sensitive to purine nucleotides (Jezek et al., 1996).

The physiological significance of variations in nucleotide inhibition is unclear, because it is not known how any of the UCPs are opened *in vivo*. In the case of UCP1, a common view is that uncoupling is initiated by dissociation of ATP (LaNoue et al., 1986). In our view, nucleotide debinding is an unlikely opening mechanism; to regulate important physiological processes, Nature normally relies on specific signalling pathways and not on the law of mass-action. Regulation may involve post-translational modification of the proteins; however, no such signaling pathway has yet been demonstrated in the opening of any of the UCPs.

A major value of studies such as these on isolated, reconstituted UCPs is that they permit direct comparison with similar studies obtained using UCP1. In this regard, our most noteworthy finding is that the three mammalian UCPs are qualitatively identical in mediating FA-dependent proton transport. Studies on whole cells and isolated mitochondria containing native UCP2 and UCP3 are urgently needed to advance the field. It is hoped that the biophysical approach described here will prove useful as a guide to studies on the native system.

LITERATURE CITED

Aguilar-Bryan, L., Nichols, C. G., Wechsler, S. W., Clement, J. P., IV, Boyd A. E., III, Gonzales, G., Herrera-Sosa, H., Nguy, K., Bryan, J., and Nelson, D. A. (1995) Cloning of the beta cell high-affinity sulfonylurea receptor: a regulator of insulin secretion. *Science* **268,** 423–426.

Anel, A., Richieri, G. V., and Kleinfeld, A. M. (1993) Membrane partition of fatty acids and inhibition of T cell function. *Biochemistry* **32,** 530–536.

Aquila, H., Link, T. A., and Klingenberg (1985) The uncoupling protein from brown fat mitochondria is related to the mitochondrial ADP/ATP carrier. Analysis of sequence homologies and of folding of the protein in the membrane. *EMBO J.* **4,** 2369–2376.

Astrup, A., Bulow, J., Madsen, J., and Christensen, N. J. (1985) Contribution of BAT and skeletal muscle to thermogenesis induced by ephedrine in man. *Am. J. Physiol.* **248,** E507–E515.

Astrup, A., Bulow, J., Christensen, N. J., Madsen, J., and Quaade, F. (1986) Facultative thermogenesis induced by carbohydrate: a skeletal muscle component mediated by ephinephrine. *Am. J. Physiol.* **250,** E226–E229.

Astrup, A., Simonsen, L., Bulow, J., Madsen, J., and Christensen, N. J. (1989) Ephinephrine mediates facultative carbohydrate-induced thermogenesis in human skeletal muscle. *Am. J. Physiol.* **257,** E340–E345.

Auchampach, J. A., Grover, G. J., and Gross, G. J. (1992) Blockage of ischaemic preconditioning in dogs by the novel ATP dependent potassium channel antagonist sodium 5-hydroxydecanoate. *Cardiovasc. Res.* **26,** 1054–1062.

Baysal, K., Brierley, G. P., Novgorodov, S., and Jung, D. W. (1991) Regulation of the mitochondrial Na^+/Ca^{2+} antiport by matrix pH. *Arch. Biochem. Biophys.* **291,** 383–389.

Baysal, K., Jung, D. W., Gunter, K. K., Gunter, T. E., and Brierley, G. P. (1994) Na^+-dependent Ca^{2+} efflux mechanism of heart mitochondria is not a passive $Ca^{2+}/2Na^+$ exchanger. *Am. J. Physiol.* **266,** C800–C808.

Beavis, A. D., Brannan, R. D., and Garlid, K. D. (1985) Swelling and contraction of the mitochondrial matrix. I. A structural interpretation of the relationship between light scattering and matrix volume. *J. Biol. Chem.* **260,** 13424–13433.

Beavis, A. D., Lu, Y., and Garlid, K. D. (1993) On the regulation of K^+ uniport in intact mitochondria by adenine nucleotides and nucleotide analogs. *J. Biol. Chem.* **268,** 997–1004.

Belyaeva, E. A., Szewczyk, A., Mikolajek, B., Nalecz, M. J., and Wojtczak, L. (1993) Demonstration of glibenclamide-sensitive K^+ fluxes in rat liver mitochondria. *Biochem. Mol. Biol. Int.* **31,** 493–500.

Bianco, A. C., and Silva, J. E. (1988) Cold exposure rapidly induces virtual saturation of brown adipose tissue nuclear T3 receptors. *Am. J. Physiol.* **255,** E496–E503.

Bienengraeber, M., Echtay, K. S., and Klingenberg, M. (1998) H^+ transport by uncoupling protein (UCP-1) is dependent on a histidine pair, absent in UCP-2 and UCP-3. *Biochemistry* **37,** 3–8.

Blinks, J. R., Wier, W. G., Hess, P., and Prendergast, F. G. (1982) Measurement of Ca^{2+} concentration in living cells. *Prog. Biophys. Mol. Biol.* **40,** 1–114.

Boss, O., Samec, S., Paoloni-Giacobino, A., Rossier, C., Dulloo, A., Seydoux, J., Muzzin, P., Giacobino, J.-P. (1997) Uncoupling protein-3: a new member of the mitochondrial carrier family with tissue-specific expression. *FEBS Lett.* **408,** 39–42.

Boss, O., Muzzin, P., Giaobino, J.-P. (1998) The uncoupling proteins, a review. *Eur. J. Endocrinol.* **139,** 1–9.

Bouillard, F., Ricquier, D., Thibault, J., and Weisenbach, J. (1985) Molecular approach to thermogenesis in brown adipose tissue: cDNA cloning of the mitochondrial uncoupling protein. *Proc. Nat. Acad. Sci. USA* **82,** 445–448.

Bouillard, F., Weissenbach, J., and Ricquier, D. (1986) Complete cDNA-derived amino acid sequence of rat brown fat uncoupling protein. *J. Biol. Chem.* **261,** 1487–1490.

Brand, M. D. (1985) The stoichiometry of the exchange catalysed by the mitochondrial calcium/sodium antiporter. *Biochem. J.* **229,** 161–166.

Brand, M. D. (1990) The proton leak across the mitochondrial inner membrane. *Biochim. Biophys. Acta* **1018,** 128–133.

Brand, M. D., Chien, L. F., Ainscow, E. K., Rolfe, D. F., and Porter R. K. (1994) The causes and functions of mitochondrial proton leak. *Biochim. Biophys. Acta* **1187,** 132–139.

Brierley, G. P., Baysal, K., and Jung, D. W. (1994) Cation transport systems in mitochondria: Na^+ and K^+ uniports and exchangers. *J. Bioenerg. Biomembr.* **26,** 519–526.

Cadrin, M., Tolszczuk, M., Guy, J., Pelletier, G., Freeman, K. B., and Bukowiecki, L. J. (1985) Immunohistochemical identification of the uncoupling protein in rat brown adipose tissue. *J. Histochem. Cytochem.* **33,** 150–154.

Cannon, B., and Nedergaard, J. (1985) The biochemistry of an inefficient tissue: brown adipose tissue. *Essays Biochem.* **20,** 110–164.

Cannon, B., Hedin, A., and Nedergaard, J. (1982) Exclusive occurence of thermogenin antigen in brown adipose tissue. *FEBS Lett.* **150,** 129–132.

Chiesi, M., Schwaller, R., and Eichenberger, K. (1987) Structural dependency of the inhibitory action of benzodiazepines and related compounds on the mitochondrial Na^+–Ca^{2+} exchanger. *Biochem. Pharmacol.* **37,** 4399–4403.

Chin, T. K., Spitzer, K. W., Philipson, K. D., and Bridge, J. H. (1993) The effect of exchange inhibitory peptide (XIP) on sodium–calcium exchange current in guinea pig ventricular cells. *Circ. Res.* **72,** 497–503.

Cinti, S., Zancarano, C., Sbarbati, A., Cicolini, M., Vogel, P., Ricquier, D., and Fakan, S. (1989) Immunoelectron microscopical identification of the uncoupling protein in brown adipose tissue mitochondria. *Biol. Cell* **67,** 359–362.

Coll, K. E., Joseph, S. K., Corkey, B. E., and Williamson, J. R. (1982) Determination of the matrix free Ca^{2+} concentration and kinetics of Ca^{2+} efflux in liver and heart mitochondria. *J. Biol. Chem.* **257,** 8696–8704.

Cox, D., and Matlib, M. (1993) A role forthe mitochondrial Na^+–Ca^{2+} exchanger in the regulation of oxidative phosphorylation in isolated heart mitochondria. *J. Biol. Chem.* **268,** 938–947.

Crompton, M., Capano, M., and Carafoli, E. (1976) Respiration-dependent efflux of magnesium ions from heart mitochondria. *Biochem. J.* **154,** 735–742.

Crompton, M., Kunzi, M., and Carafoli, E. (1977) The calcium-induced and sodium-induced effluxes of calcium from heart mitochondria. Evidence for a sodium–calcium carrier. *Eur. J. Biochem.* **79,** 549–558.

Crompton, M., Moser, R., Ludi, H., and Carafoli, E. (1978) The interrelations between the transport of sodium and calcium in mitochondria of various mammalian tissues. *Eur. J. Biochem.* **82,** 25-31.

Crompton, M., Heid, I., and Carafoli, E. (1980) The activation by potassium of the sodium-calcium carrier of cardiac mitochondria. *FEBS Lett.* **115,** 257-259.

Cunningham, S., Leslie, P., Hopwood, D., Illingworth, P., Jung, R. T., Nicholls, D. G. (1985) The characterization and energetic potential of brown adipose tissue in man. *Clin. Science* **69,** 343-348.

Debeer, L., Mannaerts, G., and De Schepper, P. J. (1974) Metabolic effects of hypoglycemic sulfonylureas. V. In vitro effects of sulfonylureas on mitochondrial adenosine triphosphatase activity. *Biochem. Pharmacol.* **23,** 251-258.

Denton, R. M., and McCormack, J. G. (1985) Ca^{2+} transport by mammalian mitochondria and its role in hormone stimulation. *Am. J. Physiol.* **249,** E543-E554.

Denton, R. M., and McCormack, J. G. (1990) Ca^{2+} as a second messenger within mitochondria of the heart and other tissues. *Annu. Rev. Physiol.* **52,** 451-466.

Denton, R. M., Randle, P. J., and Martin, B. R. (1972) Stimulation by calcium ions of pyruvate dehydrogenase phosphate phosphatase. *Biochem. J.* **128,** 161-163.

Denton, R. M., Richards, D. A., and Chin, J. G. (1978) Calcium ions and regulation of NAD+-linked isocitrate dehydrogenase from the mitochondria of rat heart and other tissues. *Biochem. J.* **176,** 899-906.

Fiermonte, G., Walker, J. E., and Palmieri, F. (1993) Abundant bacterial expression and reconstitution of an intrinsic membrane-transport protein from bovine mitochondria. *Biochem. J.* **294,** 293-299.

Fleury, C., Neverova, M., Collins, S., Raimbault, S., Champigny, O., Levi-Meyrueis, C., Bouillaud, F., Seldin, M. F., Surwit, R. S., Ricquier, D., and Warden, C. H. (1997) Uncoupling protein-2: a novel gene linked to obesity and hyperinsulinemia. *Nat. Genet.* **15,** 269-272.

Garlid, K. D. (1978) Unmasking the mitochondrial K^+/H^+ exchanger: swelling-induced K^+ loss. *Biochem. Biophys. Res. Commun.* **83,** 1450-1455.

Garlid, K. D. (1979) Unmasking the mitochondrial K^+/H^+ exchanger: tertraethylammonium induced K^+ loss. *Biochem. Biophys. Res. Commun.* **87,** 842-847.

Garlid, K. D. (1980) On the mechanism of regulation of the mitochondrial K^+/H^+ exchanger. *J. Biol. Chem.* **255,** 11273–11279.

Garlid, K. D. (1988) Sodium/proton antiporters in the mitochondrial inner membrane. *Adv. Exp. Med. Biol.* **232,** 37–46.

Garlid, K. D. (1990) New insights into mechanisms of anion uniport through the uncoupling protein of brown adipose tissue mitochondria. *Biochim. Biophys. Acta* **1018,** 151–154.

Garlid, K. D. (1996) Cation transport in mitochondria—the potassium cycle. *Biochim. Biophys. Acta* **1275,** 123–126.

Garlid, K. D. (1998) Physiology of mitochondria. In: *Cell Physiology Source Book,* 2nd Ed., pp. 111–118, Academic Press Inc., San Diego, CA.

Garlid, K. D., and Beavis, A. D. (1985) Swelling and contraction of the mitochondrial matrix. II. Quantitative application of the light scattering technique to solute transport across the inner membrane. *J. Biol. Chem.* **260,** 13434–13441.

Garlid, K. D., Diresta, D. J., Beavis, A. D., and Martin, W. H. (1986) On the mechanism by which dicyclohexylcarbodiimine (DCCD) and quinine inhibit K^+ transport in rat liver mitochondria. *J. Biol. Chem.* **261,** 1629–1536.

Garlid, K. D., Beavis, A. D., and Ratkje, S. K. (1989) On the nature of ion leaks in energy-transducing membranes. *Biochim. Biophys. Acta* **976,** 109–120.

Garlid, K. D., Shariat-Madar, Z., Nath, S., and Jezek, P. (1991) Reconstitution and partial purification of the Na^+-selectve Na^+/H^+ antiporter of beef heart mitochondria. *J. Biol. Chem.* **266,** 6518–6523.

Garlid, K. D., Sun, X., Paucek, P., and Woldegiorgis, G. (1995) Mitochondrial cation transport systems. *Methods Enzymol.* **260,** 331–348.

Garlid, K. D., Orosz, D. E., Modriansky, M., Vassanelli, S., and Jezek, P. (1996a) On the mechanism of fatty acid-induced proton transport by mitochondrial uncoupling protein. *J. Biol. Chem.* **271,** 2615–2620.

Garlid, K. D., Paucek, P., Yarov-Yarovoy, V., Sun, X., and Schindler, P. A. (1996b) The mitochondrial K_{ATP} channel as a receptor for potassium chAnnel openers. *J. Biol. Chem.* **271,** 8796–8799.

Garlid, K. D., Paucek, P., Yarov-Yarovoy, V., Murray, H. N., Darbenzio, R. B., D'Alonzo, A. J., Lodge, N. J., Smith, M. A., and Grover, G. J. (1997) Cardioprotective effect of diazoxide and its interaction with mitochondrial ATP-

sensitive K^+ channels. Possible mechanism of cardioprotection. *Circ. Res.* **81,** 1072–1082.

Garlid, K. D., Jaburek, M., and Jezek, P. (1998) The mechanism of proton transport mediated by mitochondrial uncoupling proteins. *FEBS Lett.* **438,** 10–14.

Gavin, C. E., Gunter, K. K., and Gunter, T. E. (1990) Manganese aned calcium efflux kinetics in brain mitochondria. Relevance to manganese toxicity. *Biochem. J.* **266,** 329–334.

Gavin, C. E., Gunter, K. K., and Gunter, T. E. (1991) Mn^{2+} transport across biological membranes may be monitored spectroscopically using the Ca^{2+} indicator dye antipyrylazo III. *Anal. Biochem.* **192,** 44–48.

Gimeno, R. E., Dembski, M., Weng, X., Deng, N., Shyjan, A. W., Gimeno, C. J., Iris, F., Ellis, S. J., Woolf, E. A., and Tartaglia, L. A. (1997) Cloning and characterization of an uncoupling protein homolog: a potential molecular mediator of human thermogenesis. *Diabetes* **46,** 900–906.

Gong, D.-W., He, Y., Karas, M., and Reitman, M. (1997) Uncoupling protein-3 is a mediator of thermogenesis regulated by thyroid hormone, beta3-adrenergic agonists, and leptin. *J. Biol. Chem.* **272,** 24129–24131.

Gonzalez-Barroso, M. M., Fleury, C., Arechaga, I., Zaragoza, P., Levi-Meyruesis, C., Raimbault, S., Ricquier, D., Bouillaud, F., and Rial, E. (1996) Activation of the uncoupling protein by fatty acids is modulated by mutations in the C-terminal region of the protein. *Eur. J. Biochem.* **239,** 445–450.

Gonzalez-Barroso, M. M., Fleury, C., Bouillaud, F., Nicholls, D. G., and Rial, E. (1998) The uncoupling protein UCP1 does not increase the proton conductance of the inner mitochondrial membrane by functioning as a fatty acid anion transporter. *J. Biol. Chem.* **273,** 15528–15532.

Gross, G. J., and Auchampach, J. A. (1992) Role of ATP dependent potassium channels in myocardial ischemia. *Cardiovasc. Res.* **26,** 1011–1016.

Grover, G. J. (1994) Protective effects of ATP-sensitive potassium-channel openers in experimental myocardial ischemia. *J. Cardiovasc. Pharmacol.* **24,** S18–S27.

Grover, G. J. (1997) Pharmacology of ATP-sensitive potassium channel (K_{ATP}) openers in models of myocardial ischemia and reperfusion. *Can. J. Physiol. Pharmacol.* **75,** 309–315.

Grover, G. J., McCullough, J. R., Henry, D. E., Conder, M. L., and Sleph, P. G. (1989) Anti-ischemic effects of the potassium channel activators pinacidil and

cromakalim and the reversal of these effects with the potassium channel blocker glyburide. *J. Pharmacol. Exp. Ther.* **251,** 98–104.

Grynkiewicz, G., Poenie, M., and Tsien, R. Y. (1985) A new generation of Ca^{2+} indicators with greatly improved fluorescence properties. *J. Biol. Chem.* **260,** 3440–3450.

Gunter, K. K., and Gunter, T. E. (1994) Transport of calcium by mitochondria. *J. Bioenerg. Biomembr.* **26,** 471–485.

Gunter, T. E. (1994) Cation transport in mitochondria. *J. Bioenerg. Biomembr.* **26,** 465–469.

Gunter, T. E., and Pfeifer, D. R. (1990) Mechanism by which mitochondria transport calcium. *Am. J. Physiol.* **258,** C755–C786.

Gunter, T. E., Gunter, K. K., Sheu, S. S., and Gavin, C. E. (1994) Mitochondrial calcium transport: physiological and pathological relevance. *Am. J. Physiol.* **267,** C313–C339.

Hajnóczky, G., Robb-Gaspers, L. D., Seitz, M. B., and Thomas, A. P. (1995) Decoding of cytosolic calcium oscillations in the mitochondria. *Cell* **82,** 415–424.

Halestrap, A. P. (1989) The regulation of the matrix volume of mammalian mitochondria in vivo and in vitro and its role in the control of mitochondrial metabolism. *Biochim. Biophys. Acta* **973,** 355–382.

Halestrap, A. P. (1994) Regulation of mitochondrial metabolism through changes in matrix volume. *Biochem. Soc. Trans.* **22,** 522–529.

Hamilton, J. A., and Cistola, D. P. (1986) Transfer of oleic acid between albumin and phospholipid vesicles. *Proc. Natl. Acad. Sci. U.S.A.* **83,** 82–86.

Hansen, E. S., and Knudsen, J. (1986) Parallel measurements of heat production and thermogenin content in brown fat cells during cold acclimation of rats. *Biosci. Rep.* **6,** 31–38.

Hansford, R. G. (1985) Relation between mitochondrial calcium transport and control of energy metabolism. *Rev. Physiol. Biochem. Pharmacol.* **102,** 1–72.

Hansford, R. G. (1991) Dehydrogenase activation by Ca^{2+} in cells and tissues. *J. Bioenerg. Biomembr.* **23,** 889–896.

Hansford, R. G., and Castro, F. (1982) Intramitochondrial and extramitochondrial free calcium ion concentration of suspensions of heart mitochondria with very low,

plausibly physiological, content of total calcium. *J. Bioenerg. Biomembr.* **14,** 361–376.

Harper, M. E., and Brand, M. D. (1993) The quantitative contributions of mitochondrial proton leak and ATP turnover reactions to the changed respiration rates of hepatacytes from rats of different thyroid status. *J. Biol. Chem.* **268,** 14850–14860.

Hayat, L. H., and Crompton, M. (1982) Evidence for the existence of regulatory sites for Ca^{2+} on the Na^{+}/Ca^{2+} carrier of cardiac mitochondria. *Biochem. J.* **202,** 509–518.

Hayat, L. H., and Crompton, M. (1985) Ca^{2+}-dependent inhibition by trifluoperazine of the Na^{+}–Ca^{2+} carrier in mitoplasts derived from heart mitochondria. *FEBS Lett.* **182,** 281–286.

Heaton, G. M., Wagenvoord, R. J., Kemp, A., Jr., and Nicholls, D. G. (1978) Brown-adipose tissue mitochondria: photoaffinity labeling of the regulatory site of energy dissipation. *Eur. J. Biochem.* **82,** 515–521.

Hide, E. J., and Thiemermann, C. (1996) Limitations of myocardial infarct size in the rabbit by ischaemic preconditioning is abolished by sodium 5-hydroxydecanoate. *Cardiovasc. Res.* **31,** 941–946.

Himms-Hagen, J. (1990) Brown adipose tissue thermogenesis: interdisciplinary studies. *FASEB J.* **4,** 2890–2898.

Huang, S.-G., and Klingenberg, M. (1995) Fluorescent nucleotide derivatives as specific probes for the uncoupling protein: thermodynamics and kinetics of binding and the control by pH. *Biochemistry* **34,** 349–360.

Huang, S.-G. and Klingenberg, M. (1996) Chloride channel properties of the uncoupling protein from brown adipose tissue mitochondria: a patch-clamp study. *Biochemistry* **35,** 7846–7854.

Inagaki, N., Gonoi, T., Clement, J. P., IV, Namba, N., Inazawa, J., Gonzalez, G., Aguilar-Bryan, L., Seino, S., and Bryan, J. (1995) Reconstitution od I_{KATP}: an inward rectifier subunit plus the sulfonylurea receptor. *Science* **270,** 1166–1170.

Inoue, I., Nagase, H., Kishi, K., and Higuti, T. (1991) ATP-sensitive K^{+} channel in the mitochondrial inner membrane. *Nature* **352,** 244–247.

Jacobsson, A., Stadler, U., Glotzer, M. A., and Kozak, L. P. (1985) Mitochondrial uncoupling protein from mouse brown fat. Molecular cloning, genetic mapping, and mRNA expression. *J. Biol. Chem.* **260,** 16250–16254.

Jezek, P., and Freisleben, H. J. (1994) Fatty acid binding site of the mitochondrial uncoupling protein. Demonstration of its existence by EPR spectroscopy of 5-DOXYL-stearic acid. *FEBS Lett.* **343,** 22–26.

Jezek, P., and Garlid, K. D. (1990) New substrates and competitive inhibitors of the Cl^- translocating pathway of the uncoupling protein of brown adipose tissue mitochondria. *J. Biol. Chem.* **265,** 19303–19311.

Jezek, P., Mahdi, F., and Garlid, K. D. (1990a) Reconstitution of beef heart and rat liver mitochondrial K^+/H^+ (Na^+/H^+) antiporter. Quantitation of K^+ transport with the novel fluorescent probe, PBFI. *J. Biol. Chem.* **265,** 10522–10526.

Jezek, P., Orozs, D. E., and Garlid, K. D. (1990b) Reconstitution of the uncoupling protein of brown adipose tissue mitochondria. *J. Biol. Chem.* **265,** 19296–19302.

Jezek, P., Orosz, D. E., Modriansky, M., and Garlid, K. D. (1994) Transport of anions and protons by the mitochondrial uncoupling protein and its regulation by nucleotides and fatty acids. *J. Biol. Chem.* **269,** 26184–26190.

Jezek, P., Bauer, M., and Trommer, W. E. (1995) EPR spectroscopy of 5-DOXYL-stearic acid bound to the mitochondrial uncoupling protein reveals its competitive displacement by alkylsulfonates in the channel and allosteric displacement by ATP. *FEBS Lett.* **361,** 303–307.

Jezek, P., Costa, A. D. T., and Vercesi, A. E. (1996) Evidence for anion-translocating plant uncoupling mitochondrial protein in potato mitochondria. *J. Biol. Chem.* **271,** 32743–32748.

Jezek P., Modrianský, M. and Garlid K. D. (1997a) Inactive fatty acids are unable to flip-flop across the lipid bilayer. *FEBS Lett.* **408,** 161–165.

Jezek, P., Modriansky, M., and Garlid K. D. (1997b) A structure-activity study of fatty acid interaction with mitochondrial uncoupling protein. *FEBS Lett.* **408,** 166–170.

Jou, M. J., Peng, T. I., and Sheu, S. S. (1996) Histamine induces oscillations of mitochondrial free Ca^{2+} concentration in single cultured rat brain astrocytes. *J. Physiol. (London)* **497,** 299–308.

Jung, D. W., Baysal, K., and Brierley, G. P. (1995) The sodium–calcium antiport of heart mitochondria is not electroneutral. *J. Biol. Chem.* **270,** 672–678.

Jurkowitz, M. S., Raltschuld, R. A., Brierley, G. P., and Cragoe, E. J., Jr. (1983) Inhibition of Na^+-dependent Ca^{2+} efflux from heart mitochondria by amiloride analogues. *FEBS Lett.* **162,** 262–265.

Kakar, S. S., Mahdi, F., Li, X., and Garlid, K. D. (1989) Reconstitution of the mitochondrial non-selective Na^+/H^+ (K^+/H^+) antiporter into proteoliposomes. *J. Biol. Chem.* **264,** 5846–5851.

Kamp, F., and Hamilton, J. A. (1992) pH gradients across phospholipid membranes caused by fast flip-flop of un-ionized fatty acids. *Proc. Natl. Acad. Sci. U.S.A.* **89,** 11367–11370.

Kamp, F. and Hamilton, J. A. (1993) Movement of fatty acids, fatty acid analogues, and bile acids across phospholipid bilayers. *Biochemistry* 32, 11074–11086.

Kaplan, R. S., and Pedersen, P. L. (1985) Determination of microgram quantities of protein in the absence of milligram levels of lipid with amido black 10B. *Anal. Biochem.* **150,** 97–104.

Klaus, S., Casteilla, L., Bouillaud, F., and Ricquier, D. (1991) The uncoupling protein UCP: a membraneous mitochondrial ion carrier exclusively expressed in brown adipose tissue. *Int. J. Biochem.* **23,** 791–801.

Kleiboeker, S. B., Milanick, M. A., and Hale, C. C. (1992) Interactions of the exchange inhibitory peptide with Na–Ca exchange in bovine cardiac sarcolemmal vesicles and ferret red cells. *J. Biol. Chem.* **267,** 17836–17841.

Klingenberg, M. (1990) Mechanism and evolution of the uncoupling protein of brown adipose tissue. *Trends Biochem. Sci.* **15,** 108–112.

Klingenberg, M., and Huang, S. G. (1999) Structure and function of the uncoupling protein from brown adipose tissue. *Biochim. Biophys. Acta* **1415,** 271–296.

Klingenberg, M., and Nelson, D. R. (1994) Structure–function relationships of the ADP/ATP carrier. *Biochim. Biophys. Acta* **1187,** 241–244.

Koyama, K., Chen, G., Wang, M. Y., Lee, Y., and Unger, R. H. (1997) Beta-cell function in normal rats made chronically hyperleptinemic by adenovirus-leptin gene therapy. *Diabetes* **48,** 1276–1280.

Laloi, M., Klein, M., Reismeier, J. W., Müller-Röber, B., Fleury, C., Bouillaud, F., and Ricquier, D. (1997) A plant cold-induced uncoupling protein. *Nature* **389,** 135–136.

LaNoue, K. F., Strzelecki, T., Strzelecka, D., and Koch, C. (1986) Regulation of the uncoupling protein in brown adipose tissue. *J. Biol. Chem.* **261,** 298–305.

Lean, M. E., James, W. P., Jennings, G., and Trayhurn, P. (1986) Brown adipose tissue uncoupling protein content in human infants, children, and adults. *Clin. Sci.* **71,** 291–297.

Lee, C. O., and Fozzard, H. A. (1975) Activities of potassium and sodium ions in rabbit heart muscle. *J. Gen. Physiol.* **65,** 695–708.

Li, W., Shariat-Madar, Z., Powers, M., Sun, X., Lane, R. D., and Garlid, K. D. (1992) Reconstitution, identification, purification, and immunological characterization of the 110-kDa Na^+/Ca^{2+} antiporter from beef heart mitochondria. *J. Biol. Chem.* **267,** 17983–17989.

Li, X. Q., Hegazy, M. G., Mahdi, F., Jezek, P., Lane, R. D., and Garlid, K. D. (1990) Purification of a reconstitutively active K^+/H^+ antiporter from rat liver mitochondria. *J. Biol. Chem.* **265,** 15316–15322.

Li, Z., Nicoll, D. A., Collins, A., Hilgemann, D. W., Filoteo, A. G., Penninston, J. T., Weiss, J. N., Tomich, J. M., and Philipson, K. D. (1991) Identification of a peptide inhibitor of the cardiac sarcolemmal Na^+–Ca^{2+} exchanger. *J. Biol. Chem.* **266,** 1014–1020.

Lin, C., and Klingenberg, M. (1982) Characteristics of the isolated purine nucleotide binding protein from brown fat mitochondria. *Biochemistry* **21,** 2950–2956.

Liu, Y., Sato, T., O'Rourke, B., and Marban, E. (1998) Mitochondrial ATP-dependent potassium channels: novel effectors of cardioprotection? *Circulation* **97,** 2464–2469.

Mao, W., Yu, X. X., Zhong, A., Li, W., Brush, J., Sherwood, S. W., Adams, S. H., and Pan, G. (1999) UCP4, a novel brain-specific mitochondrial protein that reduces membrane potential in mammalian cells. *FEBS Lett.* **433,** 326–330.

Martin, W. H., Beavis, A. D., and Garlid, K. D. (1984) Identification of an 82,000-dalton protein responsible for K^+/H^+ antiport in rat liver mitochondria. *J. Biol. Chem.* **259,** 2062–2065.

Matlib, M. A., Rouslin, W., Vaghy, P. L., and Schwartz, A. (1984) Isolation of cardiac muscle mitochondria: an update. In *Methods in Pharmacology*, Vol. 5 (Schartz, A., ed.), Plenum Press, New York, pp. 25–37.

Mayinger, P., and Klingenberg, M. (1992) Labeling of two different regions of the nucleotide binding site of the uncoupling protein from brown adipose tissue mitochondria with two ATP anologs. *Biochemistry* **31,** 10536–10543.

McCormack, J. G., and Denton, R. M. (1979) The effects of calcium ions and adenine nucleotides on the activity of pig heart 2-oxoglutarate dehydrogenase complex. *Biochem. J.* **180,** 533-544.

McCormack, J. G., Browne, H. M., and Dawes, N. J. (1989) Studies on mitochondrial Ca^{2+}-transport and matrix Ca^{2+} using fura-2 loaded rat heart mitochondria. *Biochim. Biophys. Acta* **973,** 420–427.

McCullough, J. R., Normandin, D., Conder, M. L., Sleph, P. G., Dzwonczyk, S., and Grover, G. J. (1991) Specific block of the anti-ischemic actions of cromakalim by sodium 5-hydroxydecanoate. *Circ. Res.* **69,** 949–958.

McEnery, M. W., Hullihen, J., and Pedersen, P. L. (1989) F_0 "proton channel" of rat liver mitochondria. Rapid purification of a functional complex and a study of its interaction with the unique probe diethylstilbestrol. *J. Biol. Chem.* **264,** 12029–12036.

McGuinness, O. P., and Cherrington, A. D. (1990) Effect of glyburide on hepatic glucose metabolism. *Am. J. Med.* **89,** 26S-37S.

Mironova, G. D., Baumann, M., Kolomytkin, O., Krasichkova, Z., Berdimuratov, A., Sirota, T., Virtanen, I., and Saris, N. E. (1994) Purification of the channel componenent of the mitochondrial calcium uniporter and its reconstitution into planar lipid bilayers. *J. Bioenerg. Biomembr.* **26,** 231–238.

Mitchell, P. (1961) Coupling of phosphorylation to electron and hydrogen transfer by a chemiosmotic type of mechanism. *Nature* **191,** 144–148.

Mitchell, P. (1966) Chemiosmotic coupling in oxidative and photosynthetic phosphorylation. *Biol. Rev. Camb. Philos. Soc.* **41,** 445–502.

Mitchell, P., and Moyle, J. (1969) Estimation of membrane potential and pH difference across the cristae membrane of rat liver mitochondria. *Eur. J. Biochem.* **7,** 471–484.

Modriansky, M., Murdza-Inglis, D. L., Patel, H. V., Freeman, K. B., and Garlid, K. D. (1997) Identification by site-directed mutagenesis of three arginines in uncoupling protein that are essential for nucleotide binding and inhibition. *J. Biol. Chem.* **272,** 24759–24762.

Mory, G., Bouillaud, F., Combes-George, M., and Ricquier, D. (1984) Noradrenaline controls tha concentration of the uncoupling proteinin brown adipose tissue. *FEBS Lett.* **166,** 393–396.

Murdza-Inglis, D. L., Patel, H. V., Freeman, K. B., Jezek, P., Orosz, D. E., and Garlid K. D. (1991) Functional reconstotution of rat uncoupling protein following its high level expression in yeast. *J. Biol. Chem.* **260,** 11871–11875.

Murdza-Inglis, D. L., Patel, H. V., Freeman, K. B., Orosz, D. E., Modriansky, M. and Garlid, K. D. (1993) Functional analysis of rat uncoupling protein site directed mutants. *FASEB J.* **7,** A1108.

Murdza-Inglis, D. L., Modriansky, M., Patel, H. V., Woldegiorgis, G., Freeman, K. B., and Garlid, K. D. (1994) A single mutation in uncoupling protein of rat brown adipose tissue mitochondria abolishes GDP sensitivity of H^+ transport. *J. Biol. Chem.* **269,** 7435–7438.

Murphy, A. N., and Fiskum, G. (1988) Ca^{2+}-transport-mediated regulation of metabolism in hepatoma mitochondria. *Ann. N. Y. Acad. Sci.* **551,** 253–255.

Muzzin, P., Revelli, J. P., Ricquier, D., Meier, M. K., Assimacopoulos-Jeannet, F., and Giacobino, J. P. (1989) The novel thermogenic beta-adrenergic agonist Ro 16-8714 increases the interscapular brown-fat beta-receptor-adenylate cyclase and the uncoupling-protein mRNA level in obese (*fa/fa*) Zucker rats. *Biochem. J.* **261,** 721–724.

Nedergaard, J., and Cannon, B. (1992) The uncoupling protein thermogenin and mitochondrial thermogensis. In: *New Comprehensive Biochemistry—Molecular Mechanisms in Bioenergetics* (Ernster, L., ed.) **23,** 385–420, Elsevier Science Publishers B.V., Amsterdam.

Négre-Salvayre, A., Hirtz, C., Carrera, G., Cazenave, R., Troly, M., Salvayre, R., Pénicaud, L., and Caisteila, L. (1997) A role for uncoupling protein-2 as a regulator of mitochondrial hydrogen peroxide generation. *FASEB J.* **11,** 809–815.

Nicchitta, C. V., and Williamson, J. R. (1984) Spermine. A regulator of mitochondrial calcium cycling. *J. Biol. Chem.* **259,** 12978–12983.

Nicholls, D. G. (1974) Hamster brown adipose tissue mitochondria. The chloride permeability of the inner membrane under respiring conditions, the influence of purine nucleotides. *Eur. J. Biochem.* **49,** 585–593.

Nicholls, D. G. (1977) The effective proton conductance of the inner membrane of mitochondria from brown adipose tissue. Dependency on proton electrochemical potential gradient. *Eur. J. Biochem.* **77,** 349–356.

Nicholls, D. G. (1979) Brown adipose tissue mitochondria. *Biochem. Biophys. Acta* **549,** 1–29.

Nicholls, D. G., and Locke, R. M. (1984) Thermogenic mechanisms in brown fat. *Physiol. Rev.* **64,** 1–64.

Nicholls, D. G., Grav, H. J., and Lindberg, O. (1972) Mitochondria from hamster brown-adipose tissue. Regulation of respiration in vitro by variations in volume of the matrix compartment. *Eur. J. Biochem.* **31,** 526–533.

Nilsson, T., Schultz, V., Berggren, P. O., Corkey, B. E., and Tornheim, K. (1996) Temporal patterns of changes in ATP/ADP ratio, glucose 6-phosphate and cytoplasmic free Ca^{2+} in glucose-stimulated pancreatic beta-cells. *Biochem. J.* **314,** 91–94.

Nobes, C. D., Brown, G. C., Olive, P. N., and Brand, M. D. (1990) Non-ohmic proton conductance of the mitochondrial inner membrane in hepatocytes. *J. Biol. Chem.* **265,** 12903–12909.

Noma, A. (1983) ATP-regulated K^+ channels in cardiac muscle. *Nature* **305,** 147–148.

Orosz, D. E., and Garlid, K. D. (1993) A sensitive new fluorescence assay for measuring proton transport across liposomal membranes. *Anal. Biochem.* **210,** 1–15.

Paucek, P., Mironova, G., Mahdi, F., Beavis, A. D., Woldegiorgis, G., and Garlid, K. D. (1992) Reconstitution and partial purification of the glibenclamide-sensitive, ATP-dependent K^+ channel from rat liver and beef heart mitochondria. *J. Biol. Chem.* **267,** 26062–26069.

Paucek, P., Yarov-Yarovoy, V., Sun, X., and Garlid, K. D. (1996) Inhibition of the mitochondrial K_{ATP} channel by long-chain acyl-CoA esters and activation by guanine nucleotides. *J. Biol. Chem.* **271,** 32084–32088.

Paucek, P., Yarov-Yarovoy, V., and Garlid, K. D. (1997) Sulfonylurea receptor of the mitochondrial K_{ATP} channel. *Biophys. J.* **72,** A39.

Paucek, P., Bajgar, R., Yarov-Yarovoy, V., and Garlid, K. D. (1999) Regulatory sites of mitoKATP are on mitoSUR. *Biophys. J.* **76,** A328.

Pedersen, P. L., Greenawalt, J. W., Reynafarje, B., Hullihen, J., Decker, G. L., Soper, J. W., and Bustamente, E. (1978) Preparation and characterization of mitochondria and submitochondrial particles of rat liver and liver-derived tissues. *Methods Cell. Biol.* **20,** 411–481.

Porter, R. K., and Brand, M. D. (1993) Body mass dependence on H^+ leak in mitochondria and its relevance to metabolic rate. *Nature* **362,** 628–630.

Quast, U., and Cook, N. S. (1989) *In vitro* and *in vivo* comparison of two K^+ channel openers, diazoxide and cromakalim, and their inhibition by glybenclamide. *J. Pharmacol. Exp. Ther.* **250,** 261-271.

Rafael, J., Fesser, W., and Nicholls, D. G. (1986) Cold adaptation in guinea pig at level of isolated brown adipocyte. *Am. J. Physiol.* **250,** C228-C235.

Rehnmark, S., Nechad, M., Herron, D., Cannon, B., and Nedergaard, J. (1990) α- and β-adrenergic induction of the expression of the uncoupling protein thermogenin in brown adipocytes differentiated in culture. *J. Biol. Chem.* **265,** 16464-16471.

Ricquier, D., Bouillaud, F., Toumelin, P., Mory, G., Bazin, R., Arch, J., and Penicaud, L. (1986) Expression of uncoupling protein mRNA in thermogenic or weakly thermogenic brown adipose tissue. Evidence for a rapid beta-adrenoreceptor-mediated and transcriptionally regulated step during activation of thermogenesis. *J. Biol. Chem.* **261,** 13905-13910.

Ricquier, D., Casteilla, L., and Bouillaud, F. (1991) Molecular studies of the uncoupling protein. *FASEB J.* **5,** 2237-2242.

Ridley, R. G., Patel, H. V., Gerber, G. E., Morton, R. C., and Freeman, K. B. (1986) Complete nucleotide and derived amino acid sequence of cDNA encoding the mitochondrial uncoupling protein of rat brown adipose tissue: lack of a mitochondrial targeting presequence. *Nucleic Acids Res.* **14,** 4025-4035.

Rizzuto, R., Bernardi, P., Favaron, M., and Azzone, G. F. (1987) Pathways for Ca^{2+} efflux in heart and liver mitochondria. *Biochem. J.* **246,** 271-277.

Rizzuto, R., Simpson, A. W., Brini, M., and Pozzan, T. (1992) Rapid changes of mitochondrial Ca^{2+} revealed by specifically targeted recombinant aequorin. *Nature* **358,** 325-327.

Rizzuto, R., Bastianutto, C., Brini, M., Murgia, M., and Pozzan, T. (1994) Mitochondrial Ca^{2+} homeostasis in intact cells. *J. Cell Biol.* **126,** 1183-1194.

Rolfe, D. F., and Brand, M. D. (1996) Contribution of mitochondrial proton leak to skeletal muscle respiration and to standard metabolic rate. *Am. J. Physiol.* **271,** C1380-C1389.

Rolfe, D. F., and Brand, M. D. (1997) The physiological significance of mitochondrial proton leak in animal cells and tissues. *Biosci. Rep.* **17,** 9-16.

Rothwell, N. J., and Stock, M. J. (1979) A role for brown adipose tissue in diet induced thermogenesis. *Nature* **281,** 31-35.

Rottenberg, H., and Marbach, M. (1991) Alcohol stimulates Na^+/Ca^{2+} exchange in brain mitochondria. *Life Sci.* **48,** 987–994.

Rutter, G. A., and Denton, R. M. (1988) Regulation of NAD+-linked isocitrate dehydrogenase and 2-oxoglutarate dehydrogenase by Ca2+ ions within toluene-permeabilized rat heart mitochondria. Interactions with regulation by adenine nucleotides and NADH/NAD+ ratios. *Biochem. J.* **252,** 181-189.

Rutter, G. A., and Denton, R. M. (1989) The binding of Ca2+ ions to pig heart NAD+-isocitrate dehydrogenase and the 2-oxoglutarate dehydrogenase complex. *Biochem. J.* **263,** 453-462.

Rutter, G. A., Burnett, P., Rizzuto, R., Brini, M., Murgia, M., Pozzan, T., Tavaré, J. M., and Denton, R. M. (1996) Subcelluar imaging of intramitochondrial Ca^{2+} with recombinant targeted aequorin: significance for the regulation of pyruvate dehydrogenase activity. *Proc. Natl. Acad. Sci. U.S.A.* **93,** 5489–5494.

Saris, N. E., Sirota, T. V., Virtanen, I., Niva, K., Penttila, T., Dolgachova, L. P., and Mironova, G. D. (1993) Inhibition of the mitochondrial calcium uniporter by antibodies against a 40-kDa glycoproteinT. *J. Bioenerg. Biomembr.* **25,** 307–312.

Sato, T., O'Rourke, B., and Marban, E. (1998) Modulation of mitochondrial ATP-dependent K^+ channels by protein kinase C. *Circ. Res.* **83,** 110–104.

Savontaus, E., Raasmaja, A., Rouru, J., Koulu, M., Pesonen, U., Virtanen, R., Savola, J. M., and Huupponen, R. (1997) Anti-obesity effect of MPV-1743 A III, a novel imidazoline derivative, in genetic obesity. *Eur. J. Pharmacol.* **328,** 207–215.

Schellenberg, G. D., Anderson, L., Cragoe, E. J., Jr., and Swanson, P. D. (1985) Inhibition of synaptosomal membrane N^+–Ca^{2+} exchange transport by amiloride and amiloride analogues. *Mol. Pharmacol.* **27,** 537–543.

Schnetkamp, P. P. M., and Szerencsei, R. T. (1991) Effect of potassium ions and membrane potential on the Na-Ca-K exchanger in isolated intact bovine rod outer segments. *J. Biol. Chem.* **266,** 189–197.

Schoenmakers, T. J. M., Visser, G. J., Flik, G., and Theuvenet, A. P. R. (1992) CHELATOR: an improved method for computing metal ion concentration in physiological solutions. *BioTechniques* **12,** 870–879.

Schroers, A., Burkovski, A., Wohlrab, H., and Kramer R. (1998) The phosphate carrier from yeast mitochondria. Dimerization is a prerequisite for function. *J. Biol. Chem.* **273,** 14269–14276.

Schultz, J. E. J., Qian, Y. Z., Gross, G. J., and Kukreja, R. C. (1997) The ischemia-selective K_{ATP} channel antagonist, 5-hydroxydecanoate, blocks ischemic preconditioning in the rat heart. *J. Mol. Cell. Cardiol.* **29,** 1055–1060.

Shannon, T. R., Hale, C. C., and Milanick, M. A. (1994) Interaction of cardiac Na–Ca exchanger and exchenge inhibitory peptide with membrane phospholipids. *Am. J. Physiol.* **266,** C1350–C1356.

Shariat-Madar, Z., and Garlid, K. D. (1993) Antibodies raised against the 59 kDa Na^+/H^+ antiporter from beef heart mitochondria inhibit Na^+ flux in a reconstituted system. *Biophys. J.* **64,** A14.

Silva, J. E. (1988) Full expression of uncoupling protein gene requires the concurrence of norepinephrine and triiodothyronine. *Mol. Endocrinol.* **2,** 706–713.

Silva, J. E., and Rabelo, R. (1997) Regulation of the uncoupling protein gene expression. *Eur. J. Endocrinol.* **136,** 251–264.

Simonsen, L., Stallknecht, B., and Bulow, J. (1993) Contribution of skeletal muscle and adipose tissue to adrenaline induced thermogenesis in man. *Int. J. Obes. Rel. Metab. Dis.* **17** (Suppl. 3), S47–S51.

Simpson, R. B., Ashbrook, J. D., Santos, E. C. and Spector, A. A. (1974) Partition of fatty acids. *J. Lipid Res.* **15,** 415–422.

Skulachev, V. P. (1991) Fatty acid circuit as a physiological mechanism of uncoupling of oxidative phosphorylation. *FEBS Lett.* **294,** 158–162.

Skulachev, V. P. (1996) Role of uncoupled and non-coupled oxidations in maintenance of safely low levels of oxygen and its one-electron reductants. *Q. Rev. Physiol.* **29,** 169–202.

Skulachev, V. P. (1998) Uncoupling: new approaches to an old problem of bioenergetics. *Biochim. Biophys. Acta* **1363,** 100–124.

Soejima, A., Inoue, K., Takai, D., Kaneko, M., Ishihara, H., Oka, Y., and Hayashi, J. I. (1996) Mitochondrial DNA is required for regulation of glucose-stimulated insulin secretion in a mouse pancreatic beta cell line, MIN6. *J. Biol. Chem.* **271,** 26194–26199.

Somogyi, J., Vér, Á., Trója, G., Végh, E., Bühler, C., Hatfaludi, F., Csermely, P., and Popovic, S. (1995) Interference of the sulphonylurea antidiabeticum gliquidone with mitochondrial bioenergetics in the rat under in vitro conditions. *Acta Physiol. Hung.* **83,** 229–312.

Sordahl, L. A., LaBelle, E. F., and Rex, K. A. (1984) Amiloride and diltiazem inhibition of microsomal and mitochondrial Na^+ and Ca^{2+} transport. *Am. J. Physiol.* **246,** C172-C176.

Sparagna, G. C., Gunter, K. K., Sheu, S. S., and Gunter, T. E. (1995) Mitochondrial calcium uptake from physiological-type pulses of calcium. A description of the rapid uptake mode. *J. Biol. Chem.* **270,** 27510-27515.

Strieleman, P. J., Schalinske, K. L., and Shrago, E. (1985) Fatty acid activation of the reconstituted brown adipose tissue mitochondria uncoupling protein. *J. Biol. Chem.* **260,** 13402-13405.

Suzuki, M., Kotake, K., Fujikura, K., Suzuki, T., Gonoi, T., Seino, S., and Takata, K. (1997) Kir6.1: a possible subunit of ATP-sensitive K+ channels in mitochondria. *Biochem Biophys. Res. Commun.* **241,** 693-697.

Szewczyk, A., Mikolajek, B., Pikula, S., and Nalecz, M. J. (1993) Potassium channel openers induce mitochondrial matrix volume changes via activation of ATP-sensitive K^+ channel. *Pol. J. Pharmacol.* **45,** 437-443.

Szewczyk, A., Pikula, S., Wojcik, G., and Nalecz, M. J. (1996) Glibenclamide inhibits mitochondrial K^+ and Na^+ uniports induced by magnesium depletion. *Int. J. Biochem. Cell Biol.* **28,** 863-871.

Szewczyk, A., Wojcik, G., Lobanov, N. A., and Nalecz, M. J. (1997) The mitochondrial sulfonylurea receptor: identification and characterization. *Biochem. Biophys. Res. Commun.* **230,** 611-615.

Thomas, A. P., Robb-Gaspers, L. D., Rooney, T. A., Hajnoczky, G., Renard-Rooney, D. C., and Lin, C. (1995) Spatial organization of oscillating calcium signals in liver. *Biochem. Soc. Trans.* **23,** 642-648.

Vaghy, P. L., Johnson, J. D., Matlib, M. A., Wang, T., and Schwartz, A. (1982) Selective inhibition of Na^+-induced Ca^{2+} release from heart mitochondria by diltiazem and certain other Ca^{2+} antagonist drugs. *J. Biol. Chem.* **257,** 6000-6002.

Van Echteld, C. J. A., Kirkels, J. H., Eijgelshoven, M. H. J., van der Meer, P., and Ruigrok, T. J. C. (1991) Intracellular sodium during ischemia and calcium-free perfusion: a 23Na NMR study. *J. Mol. Cell. Cardiol.* **23,** 297-307.

Vercesi, A. E., Martins, I. S., Silva, M. A. P., and Leite, H. M. F. (1995) PUMPing plants. *Nature* **375,** 24.

Vidal-Puig, A., Solanes, G., Grujic, D., Flier, J. S., and Lowell, B. B. (1997) UCP3: An uncoupling protein homologue expressed preferentially and abundantly in skeletal muscle and brown adipose tissue. *Biochem. Biophys. Res. Commun.* **235,** 79–82.

West, I. C. (1997) Ligand conduction and the gated-pore mechanism of the transmembrane transport. *Biochim. Biophys. Acta* **1331,** 213–234.

Wingrove, D. E., and Gunter, T. E. (1986) Kinetics of mitochondrial calcium transport. II. A kinetic description of the sodium-dependent calcium efflux mechanism of liver mitochondria and inhibition by ruthenium red and by tetraphenylphosphonium. *J. Biol. Chem.* **261,** 15166–15171.

Winkler, E., and Klingenberg, M. (1992) Photoaffinity labeling of the nucleotide-binding site of the uncoupling protein from hamster brown adipose tissue. *Eur. J. Biochem.* **203,** 295–304.

Winkler, E., and Klingenberg, M. (1994) Effect of fatty acids on H^+ transport activity of the reconstituted uncoupling protein. *J. Biol. Chem.* **269,** 2508–2515.

Winkler, E., Wachler, E., and Klingenberg, M. (1997) Indentification of the pH-sensor for nucleotide binding in the uncoupling protein from brown adipose tissue. *Biochemistry* **36,** 148–155.

Wolkowicz, P. E., Michael, L. H., Lewis, R. M., McMillin-Wood, J. (1983) Sodium-calcium exchenge in dog heart mitochondria: effects of ischemia and verapamil. *Am. J. Physiol.* **244,** H644–H651.

Zhou, Y.-T., Shimabukuro, M., Koyama, K., Lee, Y., Wang, M.-Y., Trieu, F., Newgard, C., and Unger, R. H. (1997) Induction by leptin of uncoupling protein-2 and enzymes of fatty acid oxidation. *Proc. Natl. Acad. Sci. U.S.A.* **94,** 6386–6390.

BIOGRAPHICAL SKETCH

Martin Jaburek was born in Slavicin, Czech Republic, on April 13, 1969. He attended Palacky University in Olomouc, Czech Republic, and in 1992 earned a Magister degree in Biophysics and Chemical physics. On August 1992, Martin joined the laboratory of Dr. Keith D. Garlid in the Department of Pharmacology at the Medical College of Ohio, Toledo, OH. In 1993, Martin continued his work in Dr. Garlid's laboratory after its move to the Department of Biochemistry and Molecular Biology at the Oregon Graduate Institute of Science and Technology, Portland, OR, from which he received his Ph.D.

List of Publications

Yarov-Yarovoy, V., Paucek, P., Jaburek, M., and Garlid, K. D. (1997) The nucleotide regulatory sites on the mitochondrial K_{ATP} channel face the cytosol. *Biochem. Biophys. Acta* **1321,** 128–136.

Jaburek, M., Yarov-Yarovoy, V., Paucek, P., and Garlid, K. D. (1998) State-dependent inhibition of the mitochondrial K_{ATP} channel by glyburide and 5-hydroxydecanoate. *J. Biol. Chem.* **273,** 13578–13582.

Garlid, K. D., Jaburek, M., and Jezek, P. (1998) The mechanism of proton transport mediated by mitochondrial uncoupling proteins. *FEBS Lett.* **438,** 10–14.

Jabůrek, M., Vařecha, M., Gimeno, R. E., Dembski, M., Ježek, Zhang, M., Burn, P., Tartaglia, L. A., and Garlid, K. D. (1999) Transport function and regulation of mitochondrial uncoupling proteins 2 and 3. *J. Biol. Chem.* **273,** in press.

List of Abstracts

Jaburek M., and Garlid, K. D. (1995) Effect of membrane potential on activity of reconstituted mitochondrial Na^+/Ca^{2+} antiporter. *Biophys. J.* **68,** A413.

Garlid, K. D., Jaburek, M., Yarov-Yarovoy, V., and Paucek, P. (1997) Sulfonylurea receptor—K^+ channel coupling in the mitochondrial K_{ATP} channel. *Biophys. J.* **72,** A39.

Garlid, K. D., Jaburek, M., Yarov-Yarovoy, V., and Paucek, P. (1997) Sulfonylurea receptor—K^+ channel coupling in the mitochondrial K_{ATP} channel. *Biophys. J.* **72,** A39.

Jaburek, M., Paucek, P., and Garlid, K. D. (1998) MitoK_{ATP} regulates steady-state matrix volume. *Biophys. J.* **74,** A383.

Garlid, K. D., Jaburek, M., Varecha, M., Gimeno, R. E., and Tartaglia, L. A. (1999) Transport function and regulation of uncoupling proteins 2 and 3. *Biophys. J.* **76,** A1.